



UiT Norges arktiske universitet

Faculty of Science and Technology  
Department of Geosciences

## **Ice-sheet Dynamics and Postglacial Sedimentary Processes of Coastal Søre Sunnmøre, Southwest Norway**

-

**Steven Ossim**

*GEO-3900 Master's Thesis in Geology  
May 2020*





## Abstract

Submarine glacial landforms have been identified and mapped in order to reconstruct ice sheet dynamics and to describe postglacial sedimentary processes of coastal Søre Sunnmøre in southwestern Norway which lies between 62 and 62.5°N. Landform identification has been accomplished through analysis of high-resolution multibeam echosounder (MBES) bathymetric data, backscatter data, LiDAR data, video recordings, and seismic data using ArcGIS (geographical information system).

The submarine landscape architecture of coastal Søre Sunnmøre has been largely shaped by glacial-interglacial cycles. The majority of present-day glacial landforms and deposits are a result of growth and decay cycles of the Fennoscandian Ice Sheet during the late Weichselian glaciation of the Pleistocene. A simplified model describing ice sheet dynamics from maximum glacial conditions until final deglaciation is proposed based on evidence including glacial lineations, glacial troughs, morainal banks, and De Geer moraines. Søre Sunnmøre's dissected and discontinuous distribution of high elevation alpine environments has resulted in a unique glacial dynamics narrative which differs from other localities of southwestern Norway.

Sedimentary processes active during final deglaciation up until the present have continued to rework glacially deposited sediment and alter glacial landforms. Fluvial systems and terrestrial mass wasting events continue to supply sediment to marine environments. The occurrence of slope failures, potentially triggered by postglacial isostatic rebound, is indicated by evidence such as submarine rock avalanche deposits and slide scars.



## Acknowledgements

First and foremost a big tusen takk to my supervisor Sigrid Elvenes for sharing her expertise with me, for always providing thorough and thoughtful explanations, and for her yoga iPhone app recommendations.

Tusen takk/danke schön to my supervisor Matthias Forwick for always having an open door, a smile and a joke, and some constructive feedback.

Thanks to Jochen Knies, the NGU, and CAGE for inviting me to Svalbard to join the research cruise onboard the Kronprins Haakon.

Thanks to Julie Brigham-Grette, Ross Powell, and the NSF for my first trip to Svalbard all those years ago which inspired me to pursue a masters at UiT.

Thanks to my parents and siblings for always supporting me and encouraging me especially in these years abroad.

Thanks to the creators of Bixit Havrekjeks for always making havrekjeks.

Thanks to Jørgen Berg for always saying "prosit" when I sneezed.

Og til slutt, takk til alle vennene mine og klassekameratene som hjalp meg til å føle hjemme her i Norge. Dere vil alltid ha en sofa å sove på i USA.

These past two years have been a truly unforgettable experience and I wouldn't want to change a thing.



# Contents

Abstract .....	i
Acknowledgements .....	iii
1 Introduction.....	1
1.1 Motivation .....	1
1.2 Aim and Approach .....	2
1.3 Goals .....	2
1.4 Introduction to the Study of Glacial Dynamics along Glaciated Continental Margins.....	2
1.4.1 Behavior and Dynamics of Glaciers .....	3
1.4.2 Glacial Environments, Thermal Regimes, and Sediment Transport.....	4
1.5 Glaciations of the Quaternary .....	6
1.5.1 Weichselian Glaciation .....	8
1.6 Glacial Landforms and Deposits .....	9
1.6.1 Fjords and Sounds .....	11
1.6.2 Moraines.....	12
1.7 Postglacial Processes .....	12
2 Background.....	13
2.1 Study Area and Geographic Setting.....	13
2.2 Bedrock Geology of Søre Sunnmøre .....	16
2.3 Seabed Sediments of Søre Sunnmøre Map.....	17
2.4 Glacial History of Søre Sunnmøre.....	18
2.4.1 Ålesund Interstadial.....	18
2.4.2 Late Weichselian.....	19
2.4.3 The Younger Dryas in Søre Sunnmøre.....	20
2.4.4 Final Deglaciation .....	22
2.5 Sediment Distribution .....	22
2.6 Cave Deposits .....	23
2.7 Postglacial Mass Wasting .....	24
2.8 Storegga Slide Tsunami .....	24
2.9 Sea Level Change .....	25
3 Material and Methodology	
3.1 Bathymetric Data .....	27
3.2 Backscatter Data.....	29
3.3 LiDAR Data.....	30

3.4 Seismic Data .....	31
3.5 Video Recordings.....	32
3.6 DATED-1 Database.....	32
3.7 ArcGIS Pro 10.5 and ArcMap 10.5 .....	33
4 Results .....	34
4.1 Submarine Glacial Landforms.....	36
4.1.2 Infilled Glacial Troughs - interpretation .....	37
4.1.3 Deep Areas at Fjord Heads Bounded by Pronounced Ridges- description .....	38
4.1.4 Overdeepened Fjord Basins and Sills- interpretation .....	39
4.1.5 Curved Transverse Ridges- description .....	40
4.1.6 Moraine Banks- interpretation.....	42
4.1.7 Sequences of Multiple Regularly Spaced Ridges- description.....	42
4.1.8 Feature Interpretation- De Geer Moraines .....	44
4.1.9 Streamlined Linear Ridge Bedforms- description.....	44
4.1.10 Glacial Lineations- interpretation.....	45
4.1.11 Streamlined Knoll Features- description .....	46
4.1.12 Crag-and-Tail Structures- interpretation.....	46
4.1.13 Elongated Jagged Ridges- description .....	47
4.1.14 Eskers- interpretation.....	47
4.1.15 Smoothed bedrock- description.....	47
4.1.16 Glacially smoothed bedrock- interpretation .....	47
4.2 Non-Glacial/Postglacial Landforms and Deposits .....	49
4.2.1 Fan-shaped Deposits- description .....	49
4.2.2 Delta Fan Deposits- interpretation.....	49
4.2.3 Irregular Depression- description.....	49
4.2.4 Ripple Scour Depression- interpretation.....	51
4.2.5 Boulder Fields- description.....	51
4.2.6 Rock Avalanches- interpretation .....	52
4.2.7 Depressions- description .....	52
4.2.8 Submarine Slide Scars- interpretation.....	53
4.2.9 Lobe-Shaped Deposits- description.....	53
4.2.10 Stacked Debris Flows- interpretation .....	54
4.2.11 Multiple Circular Depressions within Glacial Trough- description .....	54
4.2.12 Pockmarks- interpretation .....	55
4.2.13 Circular Depression- description .....	55



4.2.14 Unknown- interpretation .....	56
4.2.15 Feature Description- Smoothed ridges .....	57
4.2.16 Feature Interpretation- Unknown.....	57
5 Discussion .....	58
5.1 Glacial Trough Network.....	58
5.2 Extent of Glaciation and Topographic Constraints.....	58
5.2.1 Maximum Flow Style Conditions of the Late Weichselian .....	60
5.3 Thermal Regimes .....	61
5.4 Younger Dryas .....	62
5.4.1 Younger Dryas Re-advances in other areas of Southwest Norway .....	64
5.5 Final Deglaciation .....	64
5.5.2 Implications of De Geer Moraines.....	65
5.5.3 Rate of Retreat .....	66
5.5.4 Timing of Deglaciation.....	67
5.5.6 Deglaciation Comparison with other Regions of Southwestern Norway.....	68
5.6 Formation and Preservation Potential of Landforms.....	69
5.7 Ages of Landforms .....	70
5.8 Postglacial Sedimentation Processes .....	72
5.8.1 Fjord Infill.....	72
5.9 Bottom Currents.....	74
5.10 Postglacial Mass Wasting .....	74
5.11 Further Studies .....	75
6 Summary and Conclusions .....	76
References.....	viii

# 1 Introduction

## 1.1 Motivation

In order to be able to quantify and predict the potential effects climate change can have on our planet and civilizations, it is crucial that we research glaciers and their behavior as they respond to climatic variations. Glaciers are considered to be one of the most critical indicators of climate change (Yde and Paasche, 2010). This includes glaciers which are still in existence as well as glaciers that have melted long ago. To understand the behavior of past glaciers, we must identify and analyze the landforms and deposits which they leave behind. Due to a decreased exposure to erosional forces, glacial landforms and deposits are often better preserved in submarine environments, such as the seafloor of a fjord, than they are in terrestrial environments (Boulton et al., 1996). This makes submarine environments invaluable natural laboratories for studying glacial dynamics of ice sheets which have appeared and disappeared throughout geologic time.

Studying currently active glaciers in the high Arctic and elsewhere can provide valuable information regarding the current state of Earth's climate as well as the insight necessary to understand past glaciations. As stated by the father of geology, James Hutton, "the present is the key to the past". Research of past glaciations is accomplished through the examination of glacial sedimentary deposits, erosional features, and landforms.

The main purpose of this thesis will be to identify submarine glacial landforms and deposits found in the fjords, sounds, and inner continental shelf of coastal Søre Sunnmøre (English: Southern Sunnmøre). Glacial landforms will be used to reconstruct a glacial dynamics narrative detailing glacial processes that have shaped Søre Sunnmøre. Generally speaking, research efforts have neglected this area. Little focus has been placed on this specific area in the 21<sup>st</sup> century, with most Søre Sunnmøre specific literature having been generated in papers published in the 1970's, 80's and 90's (e.g. Mangerud 1979; Reite, 1983; Svendsen and Mangerud, 1990). Submarine landforms will be identified primarily using bathymetric and backscatter data collected by a high-resolution multibeam echosounder (MBES). This data has been made publically available by the Norwegian Hydrographic Service (Sjødivisjonen i Kartverket, NHS) and the Geological Survey of Norway (Norges Geologiske Undersøkelse, NGU). For reasons primarily pertaining to national security, high-resolution data covering such a large area of the Norwegian coast is not typically made available in this way. Additionally, datasets span multiple municipalities and have been combined to form a single

continuous dataset which allows for geologic evaluation. Such projects involving cooperation between multiple municipalities have rarely been undertaken.

## **1.2 Aim and Approach**

Due to the data's recent acquisition a detailed and systematic mapping of these features has yet to be conducted. In addition to swath bathymetry data, backscatter data, seismic profiles, video transects, and LiDAR data will also be used in mapping and describing landforms within the study area.

Results gathered will be used to discuss the dynamics of the Fennoscandian Ice Sheet in Søre Sunnmøre during the late Weichselian glaciation of the Quaternary. Local climate and geology will be investigated to inform the glacial dynamics narrative. Active Holocene postglacial sedimentary and geomorphologic processes will also be discussed.

## **1.3 Goals**

The primary goal of this thesis is to identify glacial and non-glacial landforms in order to reconstruct glacial dynamics and to discuss postglacial sedimentary processes of coastal Søre Sunnmøre.

Secondary goals are as follows:

- To analyse seafloor competency using backscatter data in order to describe sediment types present along the seafloor within Søre Sunnmøre
- To discuss slope stabilities, mass wasting events, and other geomorphologic processes currently active in Søre Sunnmøre
- To provide possible explanations regarding how the local climate and geology of Søre Sunnmøre uniquely influenced the dynamics of the Fennoscandian Ice Sheet

## **1.4 Introduction to the Study of Glacial Dynamics along Glaciated Continental Margins**

The morphology of a glaciated continental margin is shaped over time by glacial-interglacial cycles (Dahlgren and Vorren, 2003). Ice sheets and ice streams cut deep troughs as they erode, often forming glacial lineations as debris entrained within the ice scours the substrate. The topography of

a landscape is altered as moraines are deposited along the edges of an ice flow which provide evidence for the location of the maximum extent reached by the ice. Sediment is carried from the inner continent to the continental margin and creates fan deposits on the continental slope. The immense erosional and depositional capabilities of moving ice can have a tremendous impact on landscape architecture (Figure 1).

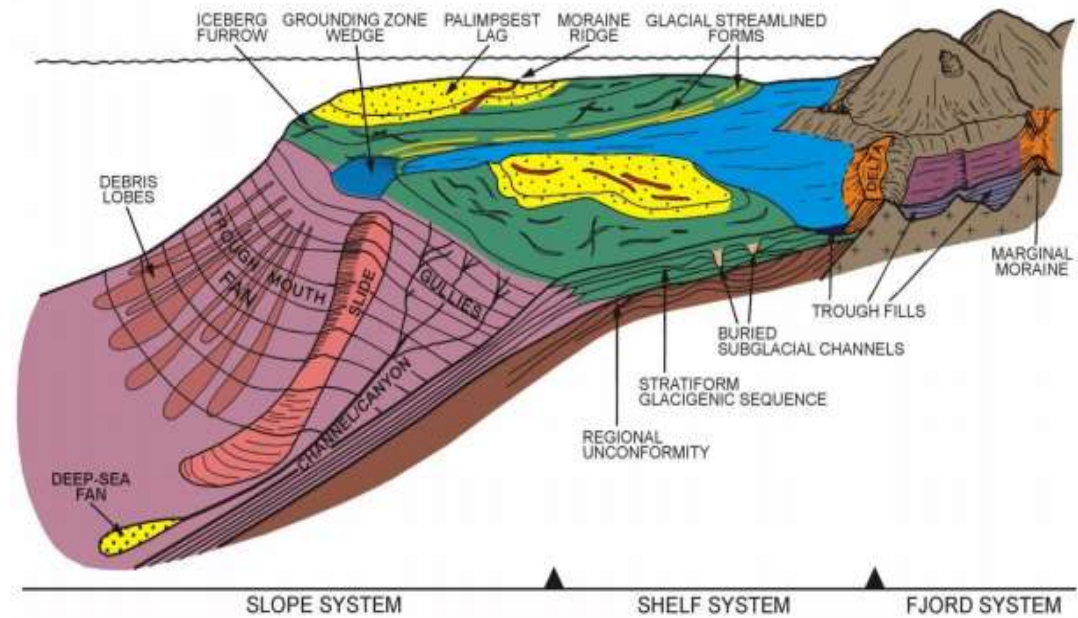


Figure 1. Conceptual model showing glacial morphological elements common of glaciated continental margins (From Dahlgren and Vorren, 2003).

### 1.4.1 Behavior and Dynamics of Glaciers

It is important to study multiple glacial systems in order to formulate accurate information regarding glacial responses to past climatic variations. As stated by Yde and Paasche (2010) "Glaciers come in many forms, and their sensitivity to climate change depends partly on the physics governing the individual glacier implying that a response can be fast or slow, straight forward or complex, which in sum suggest that not all glaciers are equally suitable for reconstructing past and present climate conditions".

The behavior of a glacier is ultimately the result of a complex system of responses to climatic variations which occur on scales ranging from local to global phenomena (Yde and Paasche, 2010). There are almost limitless interactions between inputs from geochemical, geologic, geomorphologic, and atmospheric conditions. Each of these inputs play an important role in determining the dynamic movements of a glacier (Bush, 2018).

### 1.4.2 Glacial Environments, Thermal Regimes, and Sediment Transport

One important aspect of a glacier is what is known as its equilibrium-line altitude (ELA). This is an imaginary line marking the zone of a glacier at which annual accumulation and ablation is at an equilibrium (Knight, 1999). Glaciers also have a grounding line, which is the zone where glacial ice ceases to be in direct contact with a terrestrial substrate. If the grounding line of a glacier is proximal to a shoreline it is known as a tidewater glacier, or a glacier which terminates in the sea making floating ice susceptible to calving as gravity and other stresses cause ice to break off into the sea (Knight, 1999).

Glacial deposits can be quite confounding in terms of the complex depositional processes and post-depositional reworking that occur. Deposits often reflect the multiple ways in which material is able to travel from source to sink through heterogeneous glacial systems which drive sediment transportation (Benn and Evans, 2011).

Glaciers can deposit material which originates from valley sides, from the subglacial bed, or from nunataks (rock "islands" in the middle of an ice flow) (Boulton, 1978). Once the glacier has incorporated material, it can be transported on top of the ice (supraglacially), within the ice itself (englacially), or beneath the ice (subglacially) (Figure 2).

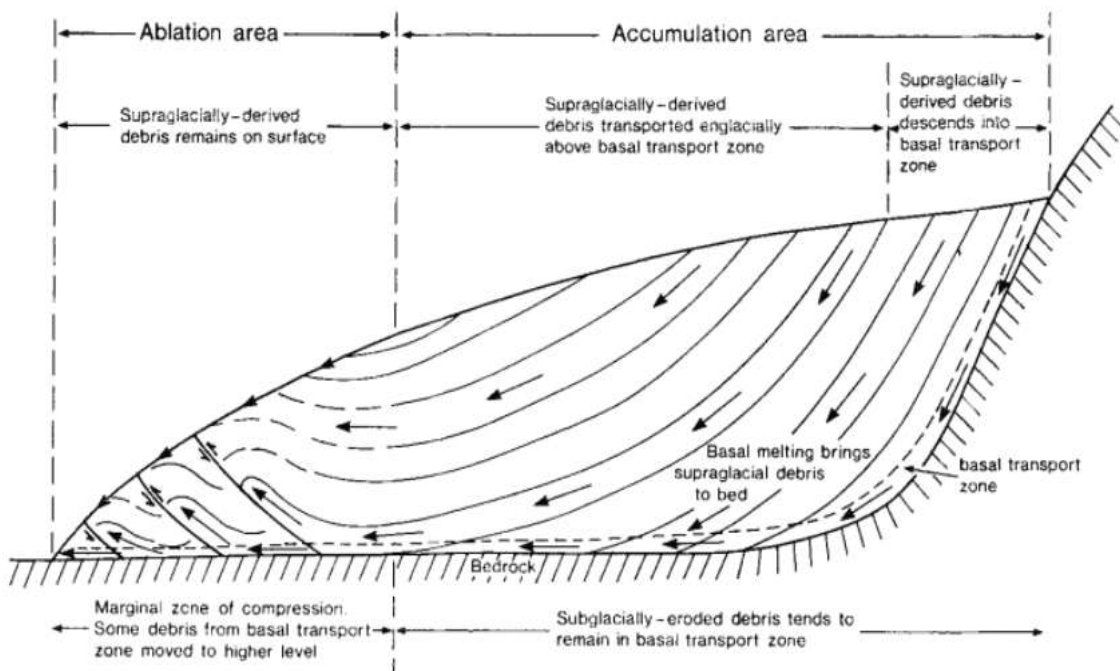


Figure 2. Diagram showing the various glacial environments and how they transport material throughout both the accumulation (creation) and ablation (destruction) zones of a glacier (From Boulton, 1978).

In the supraglacial environment, material is derived from gravitational processes such as rock falls and avalanches, or from erosional processes occurring along the sides of a glacier such as glacial abrasion or glacial plucking. Debris can then travel downward through the glacier where it is transported englacially or can eventually reach the subglacial basal transport zone. The subglacial environment is often the most difficult glacial environment to study as it is inaccessible, at least directly, due to thick layers of ice above. The subglacial environment is also the area of a glacier in which the majority of active sediment transportation takes place. Factors such as grain size, angularity of the sediment, and mineral composition are often indicative of the sediment's origin as well as the transport mechanism which led to its deposition (Boulton, 1978).

The proglacial environment is considered to be the area immediately beyond the ice margin. It is here in the proglacial environment where glaciers have their greatest influencing power on landscape architecture (Carrivick and Heckmann, 2017). Glaciers erode landscapes, flatten topography, and transport material as they advance. They then deposit debris and expose previously ice-covered landscapes to other processes of erosion and deposition that continue to rework sedimentary structures and further shape landscape architecture (Benn and Evans, 2011). Most erosion takes place during ice advance while most deposition occurs during retreat. However, deposition can sometimes occur during glacial advance and erosion can occur during retreat. Sedimentary processes active during glacial advance and retreat act as an effective sorting agent, resulting in fine-grained silts and clays being deposited in fjord basins, while coarser sands and gravels are deposited primarily in either sills, moraines, or at fjord heads (Aarseth, 1997).

In glaciers of sufficient thickness, pressure-induced melting can occur in the basal zone as the immense weight of the ice lowers the temperature at which melting can occur (Benn and Evans, 2011). Glaciers can be warm-based, where basal sliding is allowed as friction between ice and the substrate is reduced, or cold-based, where the ice is frozen to the subglacial bed and no basal sliding occurs. The commonly held assumption that cold-based glaciers are not capable of eroding, entraining, and transporting sediment is likely an over-simplification of a more complex reality (Waller, 2001). The rigidity of the subglacial bed is also influential in determining the primary mode of locomotion for a glacier (Figure 3).

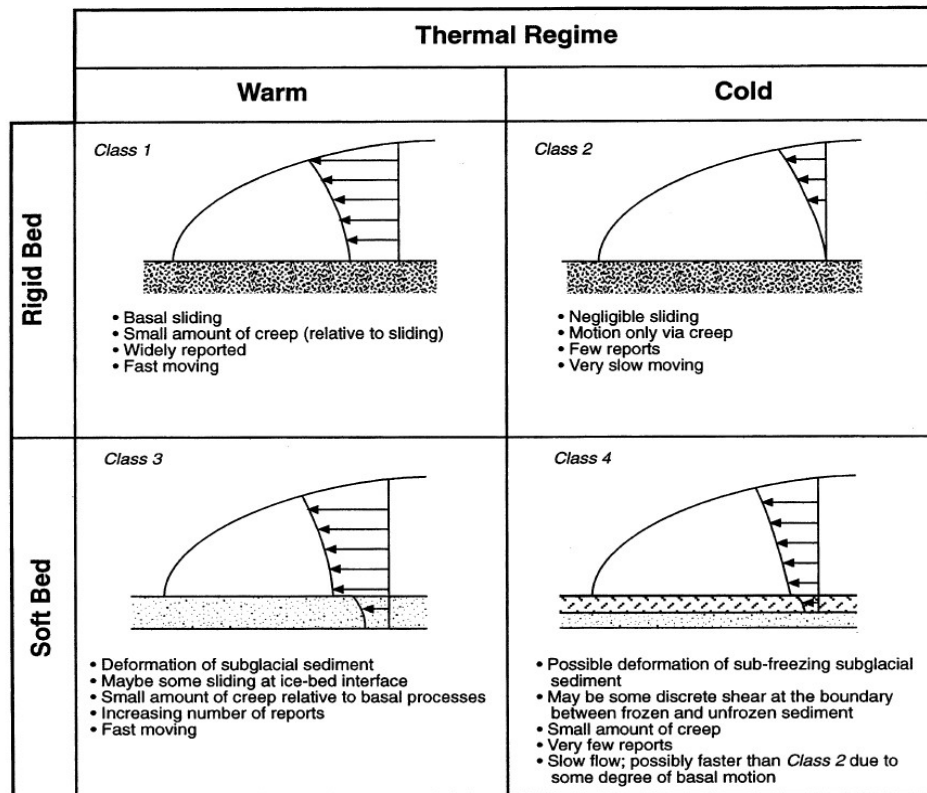


Figure 3. Locomotive behavior of a glacier as controlled by substrate integrity and its thermal regime (From Waller, 2001).

## 1.5 Glaciations of the Quaternary

The Quaternary period consists of two epochs; the Pleistocene (2.6 Mya -11.7 ka BP) and the Holocene (11.7 ka BP-present). Throughout the Pleistocene, continental scale ice sheets and extensive networks of glaciers have developed which influenced landscape architectures throughout the northern hemisphere. The duration and cyclicity of glacial-interglacial periods has varied (Hjelstuen et al., 2005).

Analyses of seismic stratigraphies along the continental shelf and slope have revealed that the Norwegian continental margin has been significantly influenced by cycles of ice growth and decay (Ottesen et al., 2006). The first time an ice sheet margin reached the outer edge of the continental shelf of Norway occurred 1.1 Mya. Since then ice has fluctuated back and forth reaching the shelf margin at least 6 times (Figure 4).

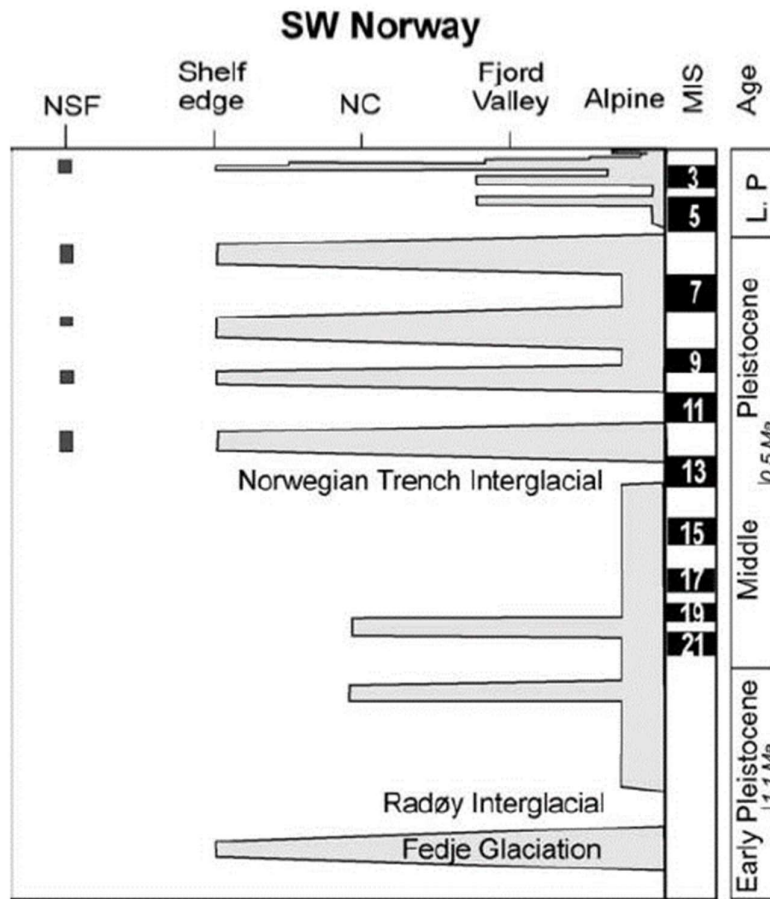


Figure 4. Timeline of glaciations in SW Norway throughout the Pleistocene. Ice has reached the shelf edge a total of six times. Norway became completely ice free at least four times during the Pleistocene. MIS, Marine Isotope Stage; NC, Norwegian Channel; NSF, North Sea Fan (From Hjelstuen et al., 2005).

Between glaciations, fluvial and gravity driven geomorphological processes have dominated (Rye et al., 1987). Climate variations which controlled glacial-interglacial cycles throughout the Pleistocene have been primarily driven by Milankovitch cycles. A complete glacial-interglacial cycle during the early Pleistocene took an average of 41 ka to run its course. However, cycles of the late Pleistocene have taken much longer or approximately 100 ka each. This is thought to have allowed for the formation of more extensive glacial networks and subsequently greater shaping of landscapes during the late Pleistocene when compared with more ancient glaciations (Catt et al., 2006).



### 1.5.1 Weichselian Glaciation

The most recent major glaciation of the Pleistocene is a period known as the Weichselian glaciation that began 115 ka BP and ended with the beginning of the Holocene 11.7 ka BP (Fredin, 2002). The Fennoscandian Ice Sheet is the main body of ice associated with the Weichselian glaciation of Northern Europe (Larsen, 2016). The ice sheet likely originated from small ice fields and ice caps throughout the Scandinavian mountains. Moisture from the Atlantic Ocean, coupled with the high altitude alpine setting, allowed for massive ice complexes to develop. A modern analogue for this phenomenon is the present day ice fields and glaciers of the Andean Patagonia in South America (Fredin, 2002).

During the middle Weichselian a major interstadial, or warming period, known as the Ålesund Interstadial resulted in melting and retreat of the Fennoscandian Ice Sheet from 34-28 ka BP (Mangerud, 2010). Following the Ålesund Interstadial, the maximum extent of glaciation during the late Weichselian was reached when the Fennoscandian Ice Sheet coalesced with other major ice sheets in the Barents Sea and British Islands. This combined mass of ice has come to be known as the Eurasian Ice Sheet Complex and spanned from Ireland to Novaya Zemlya (Russia). The Eurasian Ice Sheet Complex reached its maximum extent of the late Weichselian (Figure 5) at approximately 20 ka BP, in what is known as the Last Glacial Maximum (LGM) (Patton et al., 2017).

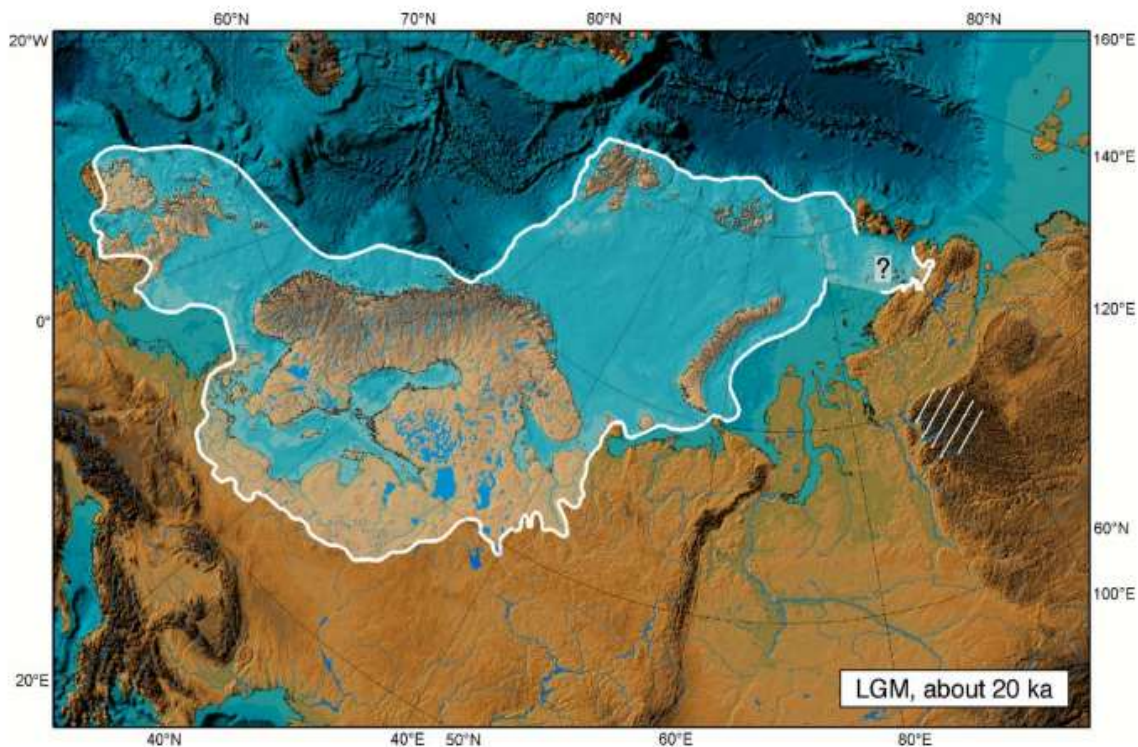


Figure 5. The maximum extent of the Fennoscandian Ice Sheet reached during the LGM approximately 20 ka BP (From Svendsen et al., 2004).

Following the LGM, a warming period known as the Bølling-Allerød chronozone lasted from 14.7-12.9 ka BP that again resulted in a major melting and retreat of the Fennoscandian Ice Sheet (Aarseth, 1997). The exact magnitude of this retreat remains poorly understood. After the Bølling-Allerød chronozone, a cooling period known as the Younger Dryas resulted in re-advances of many parts of the ice complex between 12.9-11.7 ka BP before final deglaciation and transition into the Holocene (Rasmussen et al., 2006).

The DATED-1 database (Hughes et al., 2016) presents time-slice reconstructions of the Eurasian Ice Sheet Complex at 1,000 year intervals between 25-10 ka BP, with four select time periods between 25-40 ka BP also included. The authors produced ice margin reconstructions by compiling all known published (and some unpublished) numerical dates which constrain glacial advances, retreats, and ice-free periods throughout the mid to late Weichselian. The time-slice reconstructions presented by DATED-1 will be referred to throughout this thesis (see section 3.7 for further explanation).

## 1.6 Glacial Landforms and Deposits

Glaciers produce a wide variety of landforms and deposits. Landforms can be erosional or depositional, marine or terrestrial, form cumulatively or non-cumulatively, and range from small

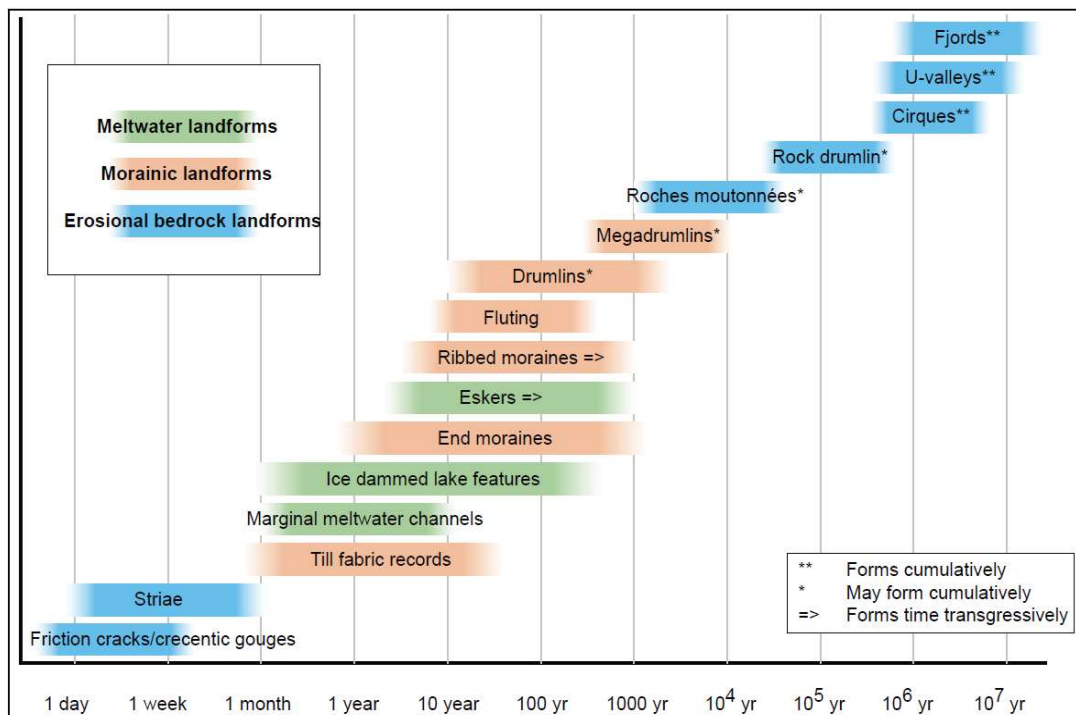


Figure 6. Various glacial landforms and the required time for their formation. Landforms can be created either cumulatively or transgressively. (From Fredin et al., 2013).

local-scale to large regional-scale (Fredin et al., 2013). The amount of time required for the formation of glacial landforms can vary from days to millions of years (Figure 6).

One common erosional landform found in many previously glaciated regions are glacial lineations. Glacial lineations are formed as debris which has been entrained at the base of a glacier is dragged across a substrate (Fredin et al., 2013). The resulting scours in bedrock or other substrate material that are left behind indicate flow direction, due to the fact that they form parallel to the movement of the ice. Glacial lineations are most often found in sets containing multiple straight and parallel scours. Scours can range from 10's to 1000's of meters in length, and typically have length to width ratios of at least 10:1 (Easterbrook, 1999). If a glacial striation measures at least 10km in length and has a length to width ratio greater than 15:1 it becomes what is known as a Mega Scale Glacial Lineation (MSGL) (Figure 7). MSGL's and glacial lineations are indicative of fast moving ice flows occurring on a regional scale (Spagnolo et al., 2014).

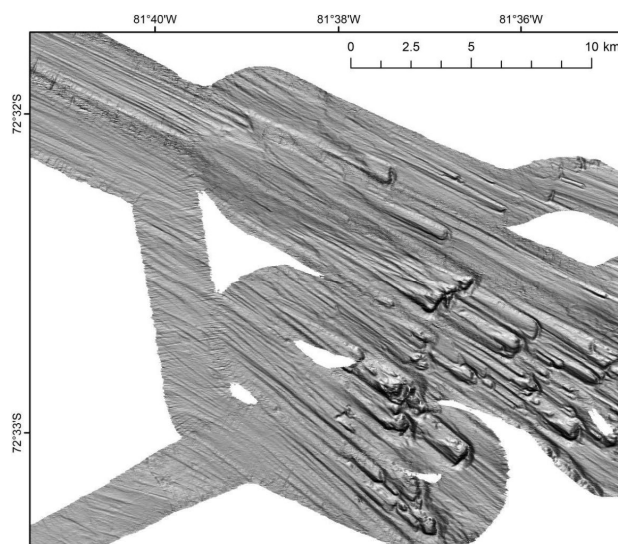


Figure 7. MSGL's found in Antarctica as represented in bathymetric data (From Cofaigh et al., 2014).

Additional erosional features include roche moutonees, rock drumlins, and crag-and-tail features which are bedrock knolls that have been subjected to reshaping and polishing via glacial abrasion. These can also often be used to indicate ice flow direction as they become elongated parallel to the direction of ice flow. Glacial cirques are large amphitheatre shaped bowls that can form on mountainsides or saddles between peaks which are caused by glacial erosion and scouring. Cirques allow for the accumulation of snow, thus serving as starting points for the formation of new glaciers. Sediment infilled glacial troughs, otherwise known as U-shaped valleys due to their cross sectional "U" shape, form by glacial erosion over hundreds of thousands of years spanning multiple glaciations (Fredin et al., 2013).

### 1.6.1 Fjords and Sounds

Norway's famous fjords are glacial troughs which have been cut deep into bedrock fracture zones or former fluvial valleys below modern sea-level. The difference between a fjord and a sound is that fjords are closed (bounded by land) at one end, while sounds are completely open at both ends (Gehrels, 2006). Fjords and sounds serve as both an interface and a buffer between terrestrial continents and oceanic marine environments and can often continue beyond the coast far out onto the continental shelf. One key difference between an inland fjord and one that continues out onto the continental shelf is that overdeepening at the head of inland fjords can result in the formation of deep basins with sills, or ridges at the fjord mouth that partially segregate fresh water within a fjord from more saline water further out at sea (Fredin et al., 2013) (Figure 8).

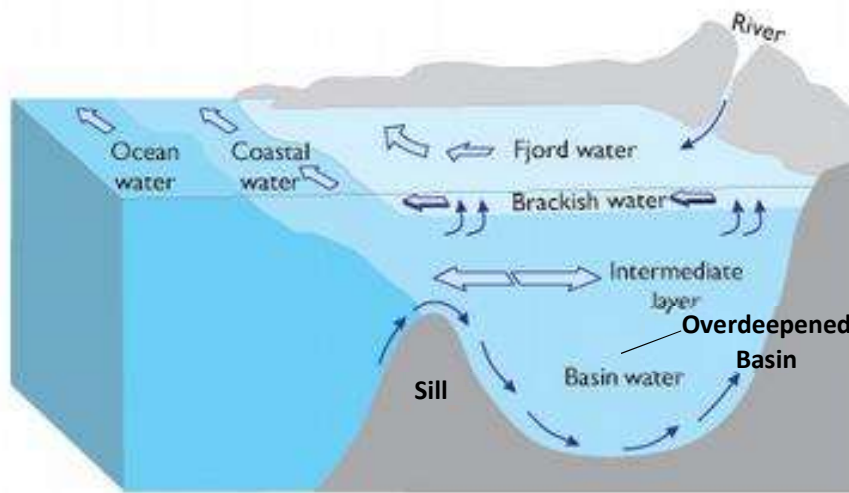


Figure 8. Diagram showing how the sill influences the exchange of water between the fjord and the outer sea. The sill can be made of eroded bedrock or a depositional feature of coarse grained material deposited at the glacial terminus (Modified from Aksnes et al., 2019).

Sills can be made of bedrock or coarse-grained material such as morainic material. If a glacial terminus is proximal to a sill, it will remain unstable and undergo frequent oscillations between advance and retreat as the glacier seeks to stabilize and become grounded (Meier and Post, 1987). Once the glacial terminus has retreated to shallow enough water, calving activity will diminish, and the glacier will become relatively stable (Aarseth, 1997). Fjords also serve as effective sediment traps during periods of deglaciation or interglacial and interstadial phases (Syvitski et al., 1988).

## 1.6.2 Moraines

A common depositional glacial landform that is crucial for reconstructing glacial dynamics, are ridges of sediment deposited by the glacier known as moraines. Moraines can be defined as glacially deposited accumulations of unconsolidated debris (Benn and Evans, 1998). Several varieties of moraines exist. Moraines deposited in the periglacial environment are known as end moraines or a terminal moraines as they reflect the shape of the glacier's terminus and mark the glacier's maximum extent (Figure 9). Debris is able to accumulate and be deposited as long as the terminus of the glacier remains stationary (Benn and Evans, 1998).

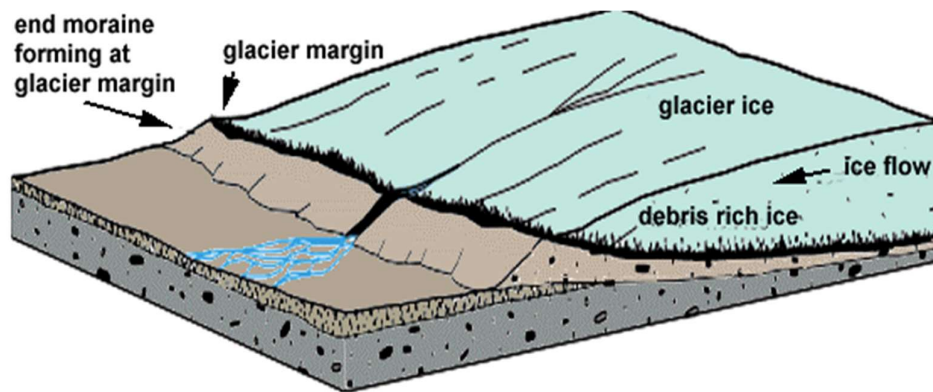


Figure 9. An end moraine forms at the glacier's margin as debris rich ice deposits material while the terminus remains stationary (From Hansel, 2003).

Other varieties of moraines include lateral moraines which are parallel ridges of debris deposited along the sides of a glacier. Recessional moraines are deposited during temporary stand-stills in a glacier's terminus as it retreats (Boulton, 1986). Moraines can also form annually due to seasonal variations at regularly spaced intervals forming what are known as De Geer moraines (Larsen et al., 1991). Some moraines even form beneath the glacier, creating Rogen moraines (Möller, 2006). Active processes such as glaciotectonism can create push or thrust moraines, which are composed of reworked proglacial sediment (Bennett, 2001). Moraines can be indicative of several aspects of glacial locomotion (i.e. advances, retreats, and standstills), thus making them vital landforms in the field of glacial dynamic reconstruction (Fredin et al., 2013).

## 1.7 Postglacial Processes

During and after final deglaciation, landscape development in southwestern Norway has continued through fluvial, gravitational, and coastal processes (Ballantyne, 2002). Coastal areas have experienced postglacial landform development conditioned by the former presence of ice sheets, as

postglacial isostatic rebound drives shoreline displacement (Augustinus, 1996). This combines with other modern erosional processes, such as wave action, to rework sediment and modify glacial landforms (Beylich et al., 2010; Burki et al., 2010). Perched glaciomarine deltas are common in Norway, as glaciofluvial systems continue to transport material into the sea well after deglaciation (Eilertsen et al., 2005).

Gravitational processes produce rock slides, rock avalanches, and rock falls which are commonplace in coastal Norway (Ballantyne, 2002). Glaciation has impacted slope stability through three primary modes; (1) Glacial erosion leading to increased slope relief and steepening of valleys, causing increased tensional stresses and overburdening of rock mass; (2) Melting ice resulting in debuitressing of the landscape as gravitational stresses decrease; (3) Disappearance of the ice sheet leading to isostatic rebound and other seismic activity, thus acting as a potential trigger for rock slope failures (Blikra, 1999).

## 2 Background

### 2.1 Study Area and Geographic Setting

Søre Sunnmøre lies along the coast of southwestern Norway between 62 and 62.5°N, with Nordfjord to the south and the town of Ålesund to the north. Consistent with much of the Norwegian coast, a number of fjords and sounds have been created in the coastal regions of Søre Sunnmøre as a result of repeated glacial-interglacial cycles (Mangerud, 1979). The study area primarily consists of 900 sq. km worth of MBES bathymetric data mostly contained in a dataset named "Batymetri Søre Sunnmøre 2017" (Figure 10).

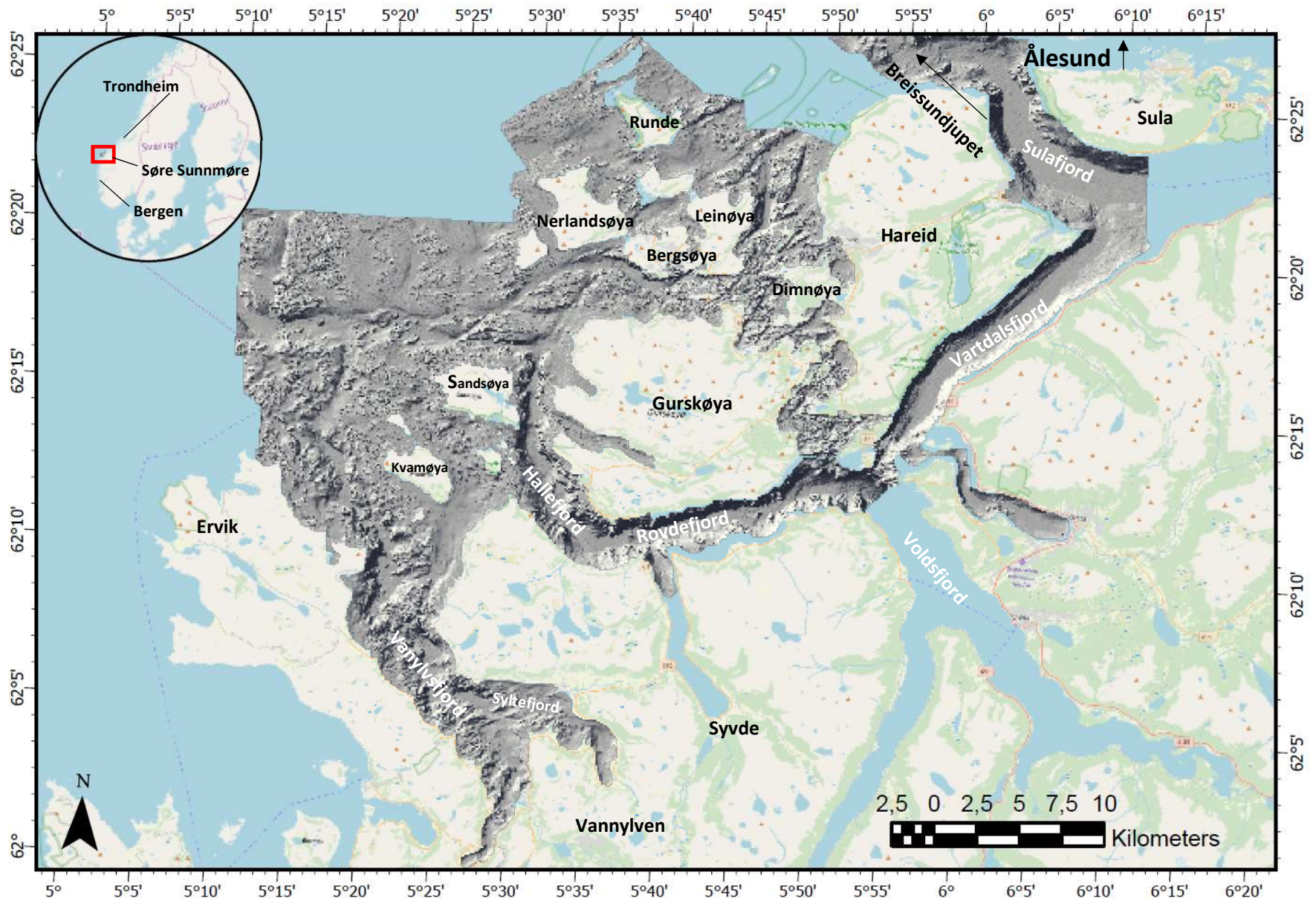


Figure 10. Overview of the study area and “Batymetri Søre Sunnmøre 2017” dataset . The location of Søre Sunnmøre within Norway is shown in the top left of the figure (red box).

Søre Sunnmøre lies roughly halfway between the major Norwegian cities of Trondheim and Bergen, or just south of the town of Ålesund.

Søre Sunnmøre is situated east of the Norwegian Channel (Figure 11), which acted as a conduit for rapid ice flows during glacial cycles (Ottesen et al., 2005). This was determined by examining MSGL's within glacial troughs spanning the entire Norwegian shelf from the North Sea (57°N) to Svalbard (80°N). Breisunddjupet is the longest glacial trough in Søre Sunnmøre and is found in the northernmost portion of the dataset.

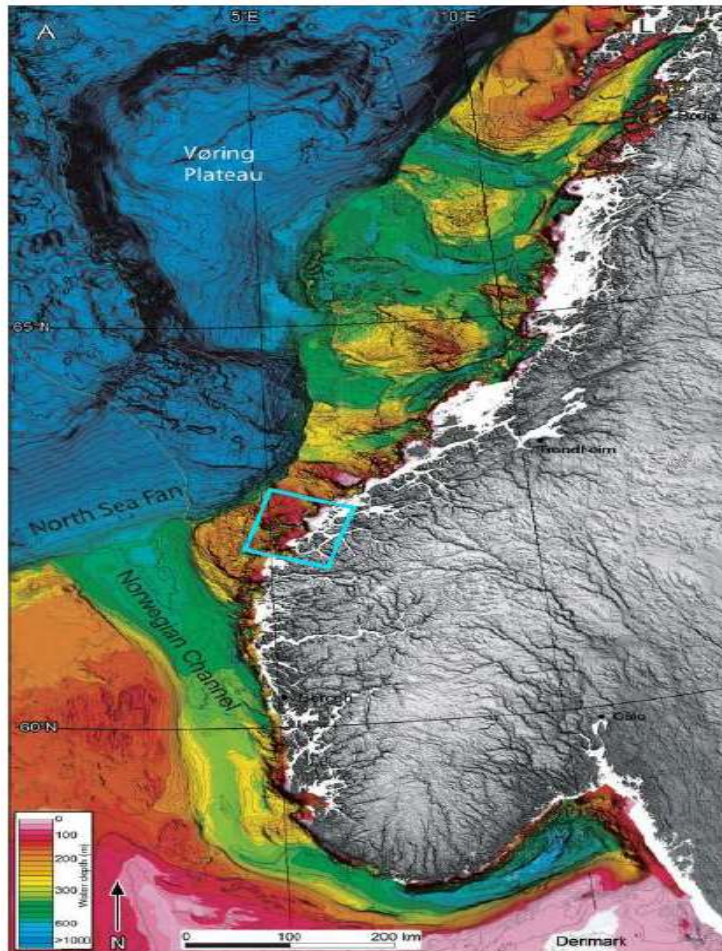


Figure 11. Overview map showing Søre Sunnmøre (blue box) position relative to the Norwegian Channel (Modified from Ottesen et al., 2005).

Coastal Søre Sunnmøre lies within the strandflat which runs nearly the entire length of the Norwegian coast from Rogaland to Troms. The strandflat is made of bedrock plane which was exhumed, weathered, and peneplaned by freeze-thaw cycles combined with wave action throughout the late Triassic to early Jurassic. The strandflat was further modified and leveled by erosion during the Pleistocene (Olesen et al., 2012).



## 2.2 Bedrock Geology of Søre Sunnmøre

Bedrock in Søre Sunnmøre comprises the northwestern-most portion of the Western Gneiss Region (WGR) that extends throughout the southern Scandinavian Peninsula and contains Precambrian gneisses of either granitic or granodioritic composition (Lidmar-Bergström, Ollier, & Sulebak, 2000). Within these gneisses exist two zones which contain either crystalline limestone or lime-silicate gneisses rich in amphibole, diopside, and garnet. The occurrence of diopside-amphibolites suggests that portions of the WGR are of a metasedimentary origin. Metamorphism likely occurred as a result of the Gothian and Caledonian orogeny (400 Mya) which sank bedrock deep enough to experience gneissic grade metamorphism (Holdhus, 1971). Caledonian structures are oriented ENE-WSW in inland Søre Sunnmøre, and shift to a more NE-SW orientation in coastal/offshore environments (Krohn-Nydal, 2019).

Søre Sunnmøre lies within a subdivision of the WGR known as the Fjordane complex (Figure 12) which is dominated by migmatite rocks (Young, 2017). The Fjordane complex is comprised of a shallow, east plunging syncline containing superimposed folds and is bordered to the north by the Sandane shear zone (Krohn-Nydal, 2019).

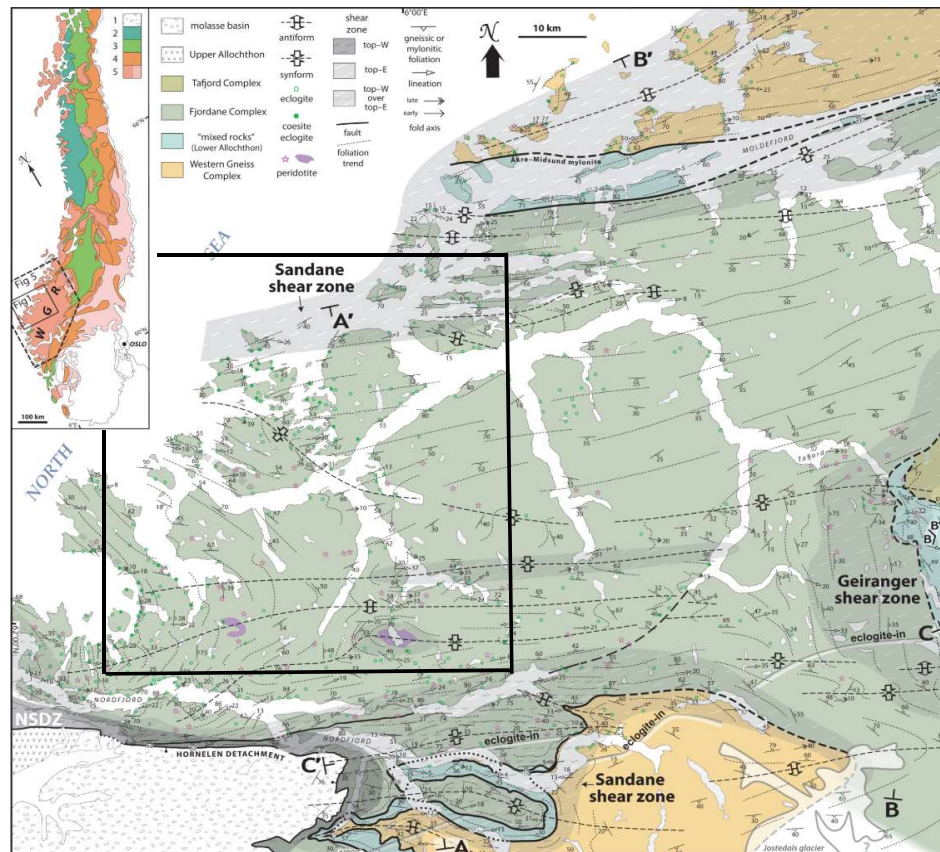


Figure 12. Structural map of the WGR. Study area marked by black box (Modified from Young, 2017).

Orientation of fjords in Søre Sunnmøre follow structural elements such as fluvial valleys or bedrock fracture zones (Aarseth, 1997). Topographic relief is consistent with much of the rest of the Norwegian coast. The highest point in the region is the peak of Kvitægga standing at 1,699m asl.

## 2.3 Seabed Sediments of Søre Sunnmøre Map

Elvenes et al. (2019) presents a detailed map of the seafloor titled "Seabed Sediments of Søre Sunnmøre, Norway" which shows the distribution of sediment within coastal Søre Sunnmøre (Figure 13). The map also includes other information such as the location of sediment accumulation basins and the diggability of specific areas. The map was created using bathymetric and backscatter data as well as additional groundtruthing measures in the form of video and sediment sample analysis.

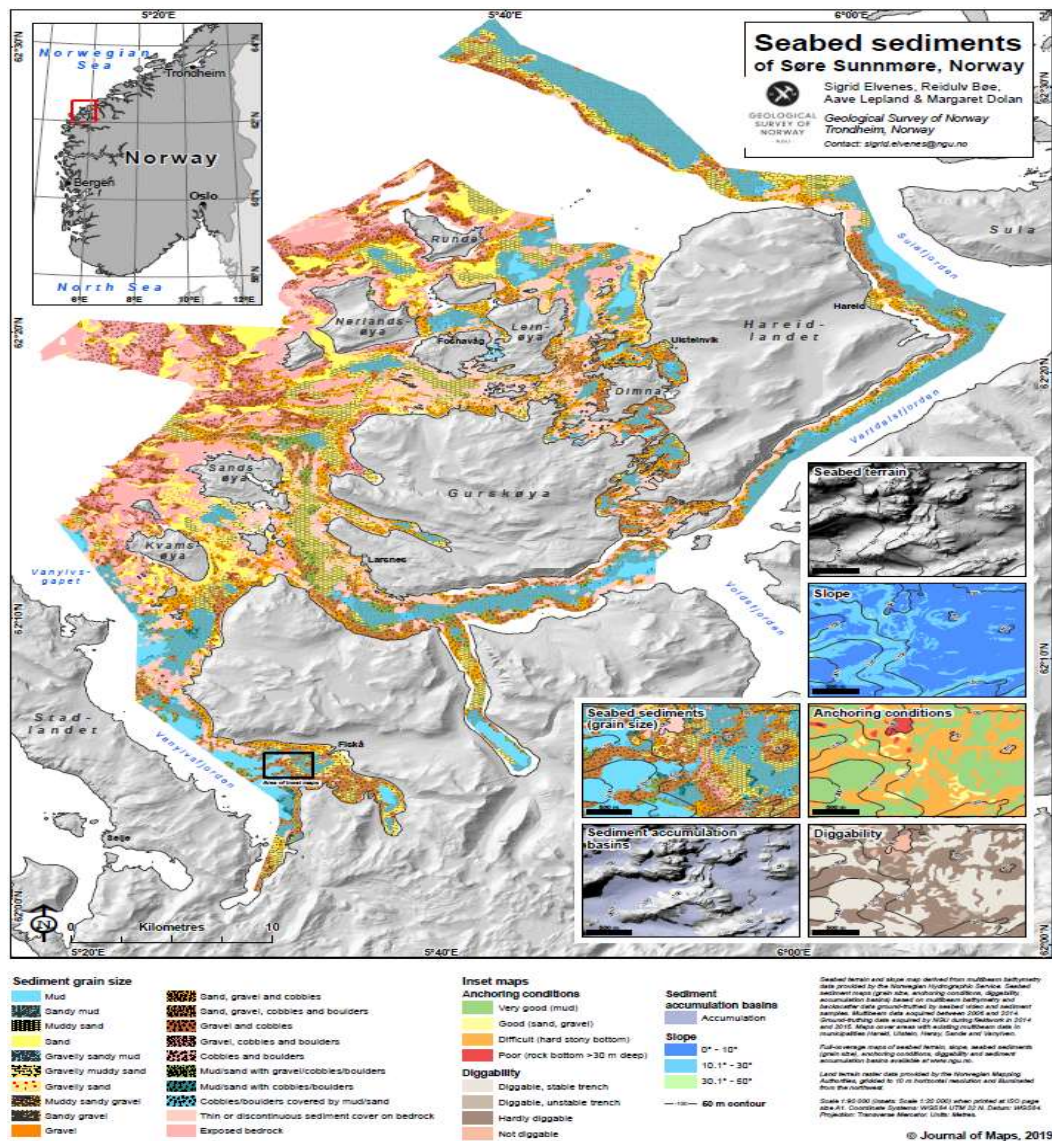


Figure 13. Sediment types found throughout Søre Sunnmøre (From Elvenes et al (2019)).

## 2.4 Glacial History of Søre Sunnmøre

It has been suggested by Mangerud (1979; 2008) and Reite (1983) that the glacial history of Søre Sunnmøre is somewhat anomalous when compared to other areas of southwestern Norway and that glaciers haven't reached Søre Sunnmøre as often as they have other coastal areas of Norway. It is possible that mountainous areas shielded Søre Sunnmøre from advancing ice by glacial diffluence, or the rerouting of ice flow by structural elements, and that glacial development was limited (Aarseth, 1997). An overview of glacial cycles in the study area (Figure 14) was created using sediment cores taken from caves (Olahola and Skjonghelleren) within the Søre Sunnmøre (Chapter 2.5).

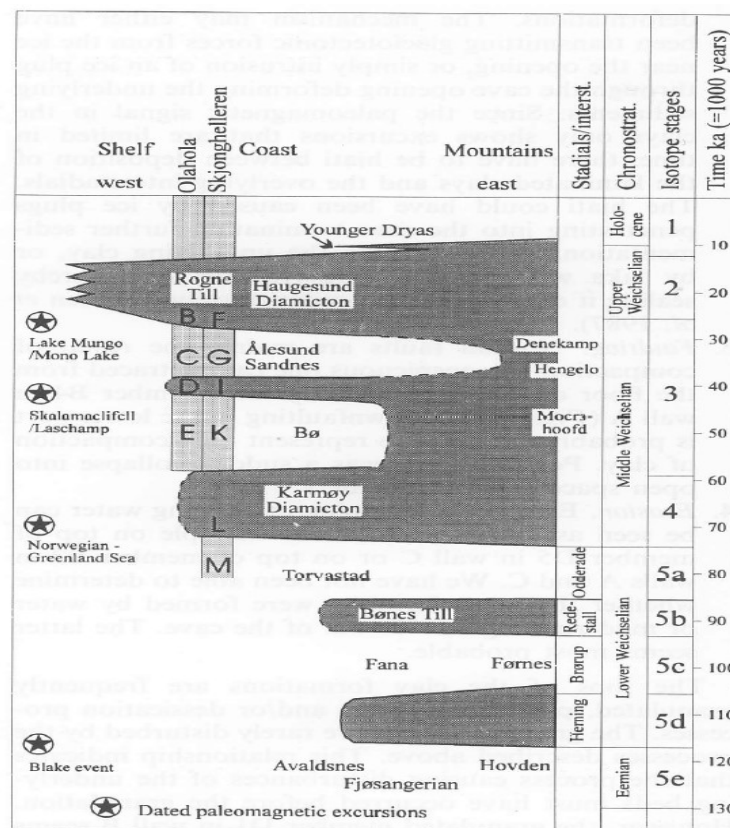


Figure 14. Timeline of glaciations throughout the Weichselian with relation to both Olahola and Skjonghelleren. Note the Younger Dryas re-advance does not reach the caves (From Valen, 1995).

### 2.4.1 Ålesund Interstadial

A warming period known as the Ålesund Interstadial resulted in a major retreat of the entire Fennoscandian Ice Sheet during the middle Weichselian (Mangerud et al., 1979). The Ålesund Interstadial is named as such due to its initial discovery near the town of Ålesund. Carbon-14 dating

provided ages between 38-28 ka BP for marine mollusk shells found along coastal areas of Søre Sunnmøre, implying that large swaths of the coast of Søre Sunnmøre were completely ice free during this timeframe of the middle Weichselian. Further dating later narrowed down this timeframe to 34-28 ka BP (Mangerud, 2010). The formation of marine caves, which are now above sea level, has been dated to pre-Ålesund Interstadial. Most of these caves have since been overrun by glacial ice, thus implying significant isostatic depression prior to the Ålesund interstadial when the caves were formed (Mangerud, 1979).

### **2.4.2 Late Weichselian**

Following the Ålesund Interstadial ice began to re-advance to its maximum extent of the late Weichselian. This most recent maximum reach of the Fennoscandian Ice Sheet, as well as other ice sheets around the world such as the Laurentide Ice Sheet of North America, has come to be known as the Last Glacial Maximum (LGM) (Cohen et al., 2013). Sediment coring data has indicated that the Fennoscandian Ice Sheet terminated at the mouth of the Norwegian Channel in three separate phases during the LGM between 30 and 19 ka BP (Nygård et al., 2007).

Early research by Manguerud (1979) originally suggested that the extent of glaciation in Søre Sunnmøre during the LGM was limited to sporadic cirque glaciers which only briefly, if at all, advanced to low-lying coastal areas of the region. This original theory, which prevailed for decades, was supported by arguments such as those made by Løwe & Løwe (1963) who state that much of the flora and fauna of Søre Sunnmøre survived the LGM, implying that the most recent maximum extent of glacial coverage in Søre Sunnmøre was not reached during the LGM, but rather sometime in the middle Weichselian.

However, more recent data (Valen et al., 1996; Olsen et al., 2013; Koren et al., 2008; Mangerud et al., 2010), which has been compiled in the DATED-1 database (Hughes et al., 2016), refuted the theory that any localities of Søre Sunnmøre were ice free for any period during the LGM and it is now accepted that the Fennoscandian Ice Sheet fully covered the entire area during the LGM.

Following the LGM the Bølling-Allerød chronozone occurred which was a non-localized warming period between 14.7-12.9 ka BP that resulted in major retreats of the Fennoscandian Ice Sheet (Rasmussen et al., 2006). The magnitude of ice retreat resulting from the Bølling-Allerød chronozone remains poorly quantified (Aarseth, 1997).

### 2.4.3 The Younger Dryas in Søre Sunnmøre

The Younger Dryas is a well-studied cooling period between 12.9-11.7 ka BP that resulted in re-advances of the Fennoscandian Ice Sheet in many localities throughout Northern Europe (Rasmussen et al., 2006). However, the Younger Dryas re-advance was of a rather inconsistent nature between regions and is not likely to have resulted in the re-glaciation of low-lying coastal areas in Søre Sunnmøre (Mangerud, 1979). Glacial activity in Søre Sunnmøre during the Younger Dryas was likely limited to high alpine and cirque glaciers. End moraines within cirques are much more common in Søre Sunnmøre than surrounding areas (Figure 15). If the ages of cirque moraines are assumed to be Younger Dryas, then the much higher concentration of cirque moraines in Søre Sunnmøre compared to other areas implies that ice was present but that re-glaciation in was limited to only high elevation areas (Reite, 1983). The ice margin of the Younger Dryas re-advance reached the Norwegian coast north of Trøndelag and south of Nordfjord (Hughes et al., 2016)

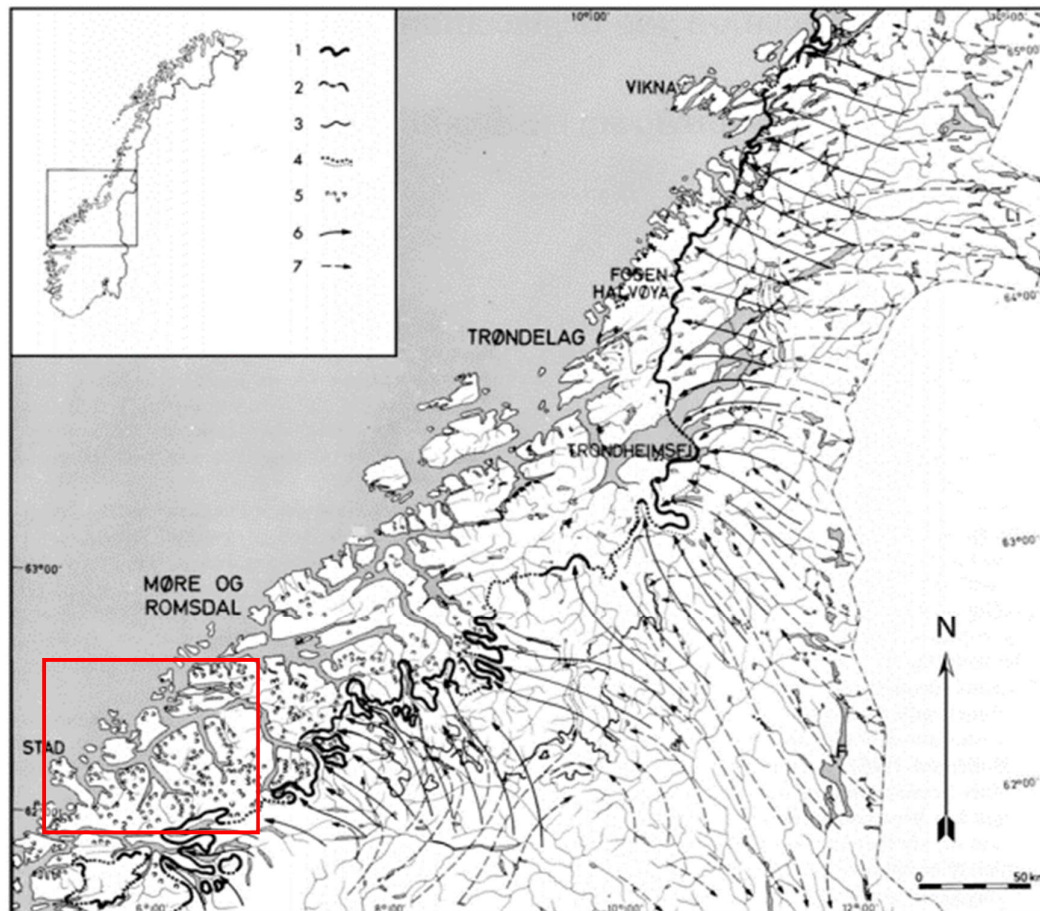


Figure 15. Younger Dryas ice margin in Central Norway. Symbols are as follows; 1.)Terminal moraines 2.)Younger Dryas ice margin 3.)Preboreal ice margin 4.)Assumed ice margins 5.) Cirque moraines from the Younger Dryas 6.) Ice flow direction during the Younger Dryas 7.) Preboreal ice movment. Notice that the density of cirque moraines within Søre Sunnmøre (red box) is far greater than surrounding areas (Modified from Sollid & Sørbel, 1978)

Preservation of morainic material is poor throughout much of southwestern Norway (Aarseth et al., 1997). This makes the use of marine records the best way of reconstructing the extent of the Younger Dryas re-advance. Reflection seismic profiling for this purpose was first performed by Giskeødegaard (1983). Recent advances in seismic technology has produced more detailed profiles that revealed minor oscillations of the ice margin during the Younger Dryas (Aarseth et al., 1997). The DATED-1 database was used to create an updated regional map showing the approximate position of the Fennoscandian Ice Sheet margin during the Younger Dryas (Figure 16).

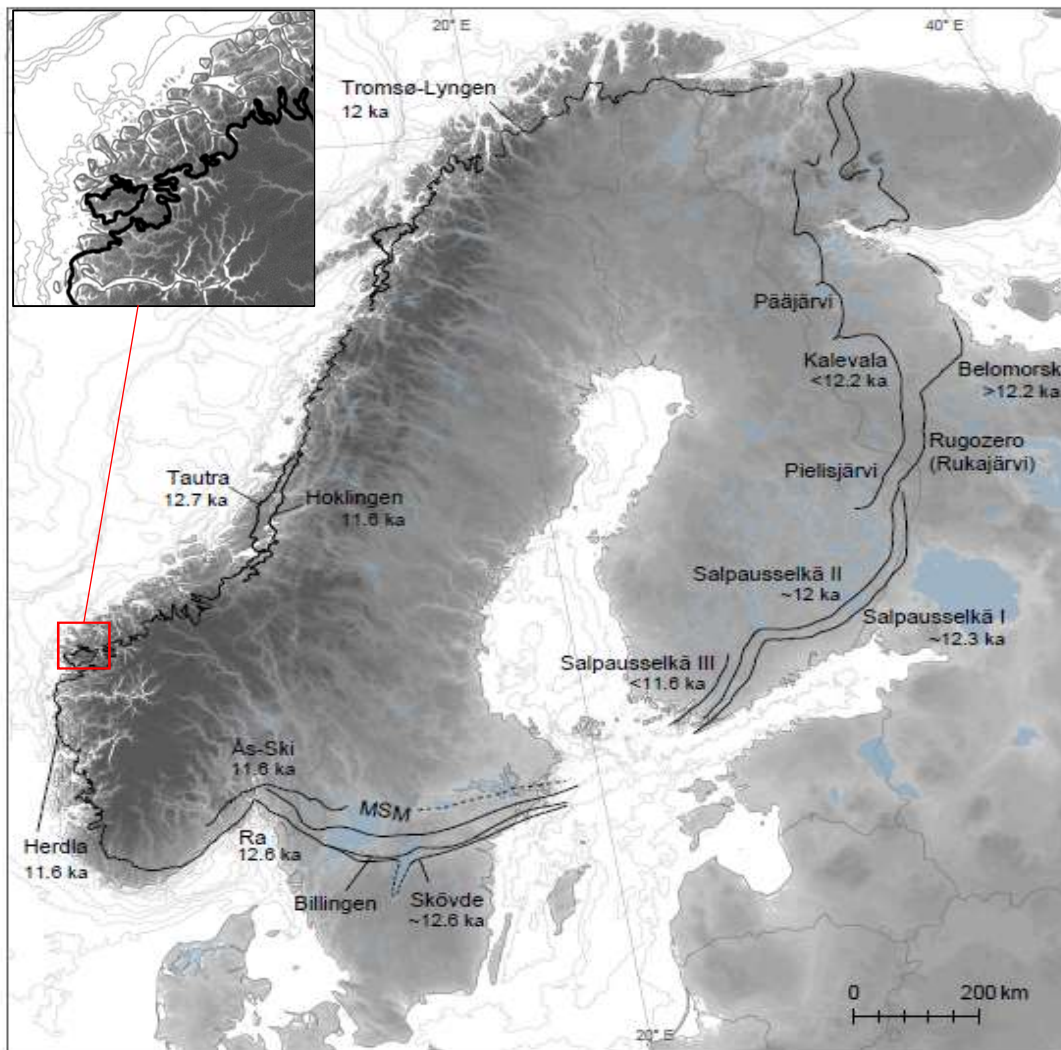


Figure 16. Terminal moraine positions mapping the extent of the Fennoscandian Ice Sheet during the Younger Dryas (Modified from Hughes et al., 2016). Study area is shown by the inset map (top left).

## 2.4.4 Final Deglaciation

Final deglaciation of the Norwegian Channel occurred approximately 15 ka BP, and the outermost coast of southwestern Norway most likely became ice free within the time interval of 14-12.6 ka BP (Mangerud, 1977; Andersen, 1979; Anundsen, 1985; Andersen et al., 1987; Paus, 1990).

In Søre Sunnmøre coastal areas specifically, Carbon-14 dating provides a minimum age of deglaciation of 12,060+/- 160 yr BP (Mangerud, 1979; 2010). However, unglaciated high shorelines originally described by Reite (1983) could indicate that deglaciation of coastal areas in Søre Sunnmøre was complete well before this. Glacial erosion in low-lying coastal areas during previous ice advances had overdeepened fjords such that calving activity was accelerated by the unstable bedrock profiles, thus accelerating deglaciation (Aarseth, 1997). Using the updated DATED-1 database (Hughes et al., 2016), final deglaciation in Søre Sunnmøre has been dated between 15-14.5 ka BP.

## 2.5 Sediment Distribution

The majority of sediment found in marine environments of Søre Sunnmøre was deposited during the deglaciation of the Fennoscandian Ice sheet or later (Aarseth, 1997). Only a small portion (10% or less) is older than late Weichselian. This is due to both glacial and glaciofluvial erosional processes that periodically empty fjord basins by transporting sediment to the continental shelf and slope during glacial periods (Aarseth, 1997). A generalized diagram which shows a sequence containing five different sedimentary units in a typical western Norway fjord is shown below (Figure 17).

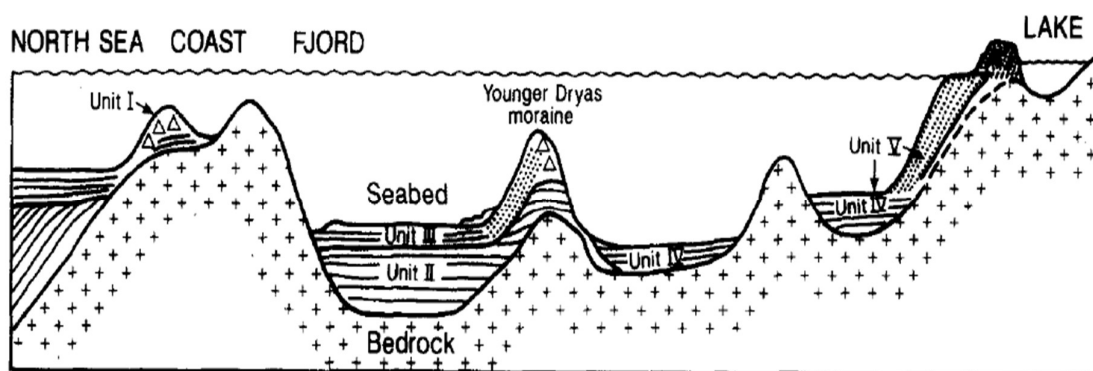


Figure 17. Unit I- Older than late Weichselian

Unit II- Deposited by glacial oscillations during the Bølling-Allerød Chronozone (14-11 ka BP)

Unit III- Superimposed sediment deposited during the Younger Dryas (11-10.3 ka BP)

Unit IV- Sediment deposited during the Preboreal chronozone (10-9 ka BP)

Unit V- Top 3-6m of sediment deposited (<9 ka BP)

From Aarseth (1997).

## 2.6 Cave Deposits

Glacial deposits have been found inside marine wave-cut caves that have survived multiple glaciations. When analysed these deposits provide useful evidence for determining the ages of glacial cycles (Larsen, 1987; Valen, 1995; Valen, 1996). Three caves have been studied in the Søre Sunnmøre area which include Hamnsundhelleren, Skjonghelleren, and Olahola (Figure 18).

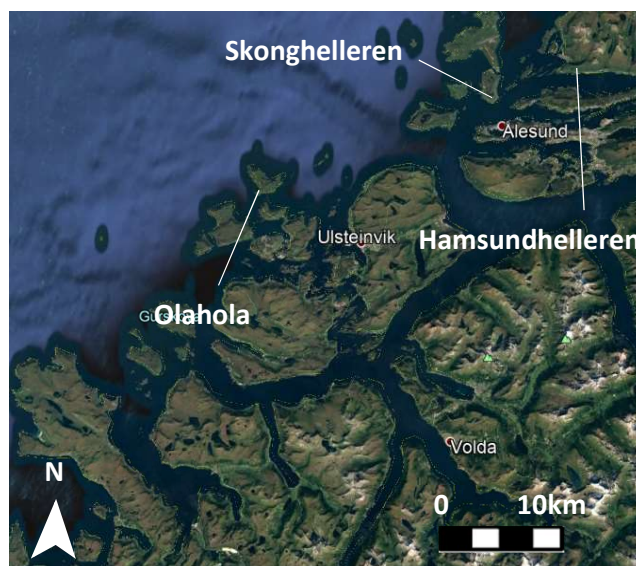


Figure 18. A map of Sunnmøre displaying the location of the three caves that have been explored for glacial deposits. Only Olahola lies directly in the study area while Skonghelleren and Hamnsundhelleren lie approximately 10 km north of the study area. Figure created using Google Earth.

The caves functioned as sediment traps during both ice-free and glacial periods. During ice-free periods, animal bones (particularly bird) and weathered boulders falling from the roof of the cave accumulated. When the area was ice-covered, the entrance to the cave was blocked and fine-grained sediment accumulated through suspension settling in ice-dammed lakes found inside the caves. Sediments in caves are ideal for dating due to their high rates of sedimentation and minimal post-depositional disturbances (Larsen et al., 1987).

In all caves, three beds of fine-grained laminated glacial clays were found alternating with beds of blocky interglacial sediments. This implies that the caves survived a minimum of three glaciations since their formation. Radiocarbon dates of bone fragments found in the lowermost blocky interglacial bed provided dates around 30 ka BP which likely represent the Ålesund Interstadial. The coarse-grained, blocky bed above the uppermost glaciolacustrine bed contained bone material which was dated to between 12-10 ka BP, likely representing the earliest deposits following final deglaciation.



## 2.7 Postglacial Mass Wasting

Following deglaciation gravity-driven mass wasting processes resulting in rockfalls, debrisflows, and snow avalanches have played a large role in the developing the present-day landscape architecture of Søre Sunnmøre (Aarseth, 1997). Postglacial sedimentary systems in southwestern Norway consist of alluvial fans and steep colluvial fans that combine to form aprons or bajadas. These systems develop along the steep slopes of valley sides and fjord margins. Coarse-grained sediment continues to be derived from weathered gneissic bedrock (Blikra, 1999).

Unstable rock slopes along the Norwegian coast have been identified in a 2014 report from NGU (Oppikofer et al., 2014). This report serves as a risk assessment for potential rock slope failures and their consequences. Unstable rock slopes have been identified in several localities throughout Søre Sunnmøre (Figure 19). Isostatic rebound induced trembling could be a potential cause for rock slope failures which have already occurred.

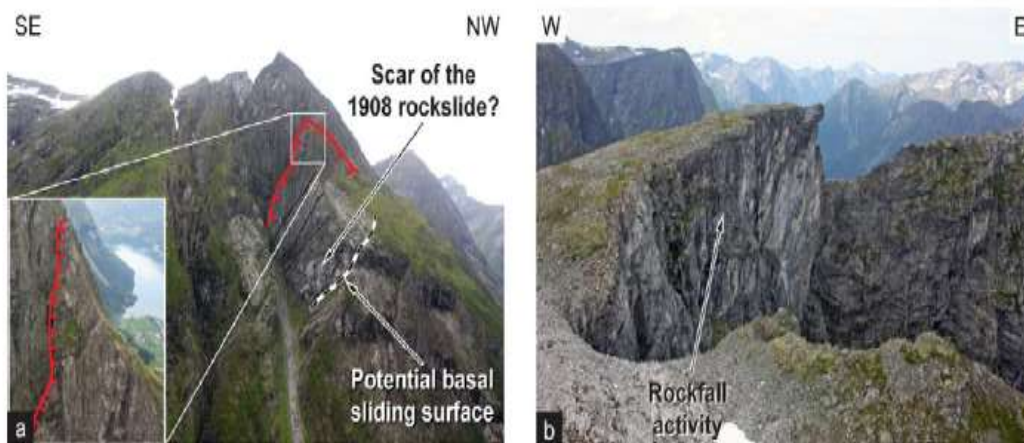


Figure 19. Unstable rock slopes found in Ørsta municipality. Similar rockfall activity and potential slide surfaces have been identified in dozens of other localities throughout Søre Sunnmøre (From Oppikofer et al., 2014).

## 2.8 Storegga Slide Tsunami

Roughly 7.2 ka BP ago a tsunami struck the coast of Norway as a result of the Storegga slide (Bondevik, 1997). The tsunami affected almost the entire coast of Norway as well as the Shetland Islands, Scotland, and other localities. It was determined through coring and stratigraphic analysis of several coastal lakes that maximum run-up of the tsunami wave first impacted coastal Søre Sunnmøre, due to its proximity to the submarine slide which caused the tsunami. In all cores

collected throughout Søre Sunnmøre, the tsunami facies sequence was found to overlay lacustrine gyttja or marine sediments which have been dated to Younger Dryas age. The estimated run-up in Søre Sunnmøre was between the interval of 9-13m above sea level or 10-11m above high tide (Bondevik, 1997). A bathymetric map of the Norwegian Sea and North Sea (Figure 20) shows the location of the slide scar and Søre Sunnmøre's proximity to the slide, as well as the heights of the tsunami's run-up.



Figure 20. Bathymetric map of the Norwegian Sea and North Sea showing the areal extent of the Storegga submarine slide and estimated wave run-ups (above high tide)

## 2.9 Sea Level Change

Svendsen and Mangerud (1990) conducted stratigraphic analysis of emerged lake basins on the island of Leinøy in order to establish a relative sea level curve for Søre Sunnmøre (Figure 21).

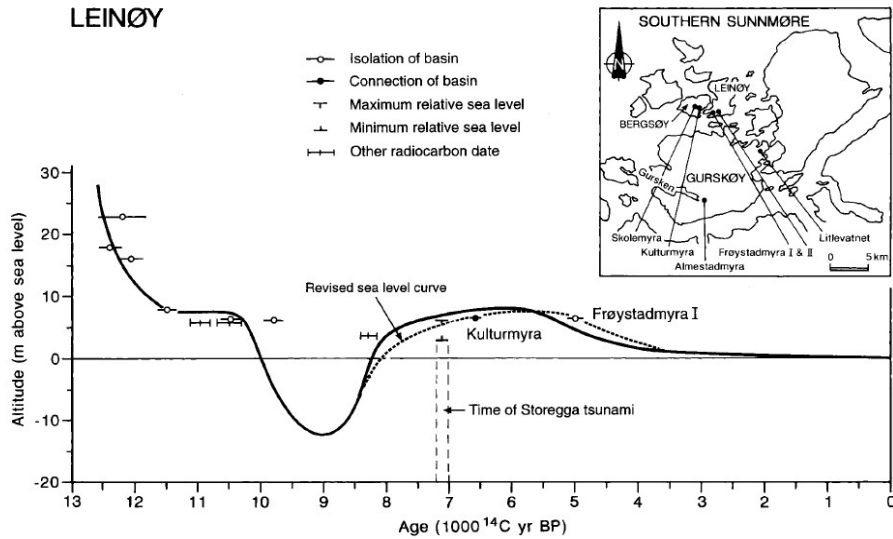


Figure 21. Sea level curve as established by measuring lake basins on the island of Leinøy (From Svendsen and Mangerud, 1990).

Rapid sea level regression between 12.5-11.5 ka BP was followed by a levelling out for the latter half of the Younger Dryas. This stillstand in sea level indicates that local isostatic forces and global eustatic processes cancelled each other out for a time span of roughly 1000 years. Leinøy lies roughly 80 km west of the extent of the Younger Dryas re-advance, thus postglacial isostatic uplift following the Younger Dryas is not considered to be a likely contributing factor to relative sea level fall. This would also suggest that eustatic sea level changes were also minor.

Rapid transgression from 9-8 ka BP indicates a sea level rise of at least 20m, suggesting a significant increase in the rate of eustatic rise during the early Holocene (Svendsen and Mangerud, 1990). Bondevik (1997) asserts that the eustatic rise of global sea level was faster than isostatic uplift, which resulted in shorelines deposited at 9 ka BP being crossed by younger shorelines. This eustatic sea level rise is known as the Tapes transgression and likely ended 6ka BP (Bondevik, 1997). Furthermore, the Tapes transgression is evidenced in Søre Sunnmøre by distinct beach ridges on islands throughout the region (Svendsen and Mangerud, 1990).

# 3 Material and Methodology

## 3.1 Bathymetric Data

Identification of glacial landforms and other features in the study area was possible primarily through the use of high-resolution multi-beam echosounder (MBES) data. A MBES utilizes sound waves to map the bathymetry of the seabed by recording the amount of time necessary for the sound wave to reflect off of the seafloor and return to a receiver onboard the data collection vessel. MBES is unique from other sonar based data collection methods, such as seismic reflection profiling, because it uses a technique called beamforming which makes it able to extract directional information from the signal returning to the receiver, thereby producing a swath of depth readings from each individual ping (Theberge and Cherkis, 2013) (Figure 22).

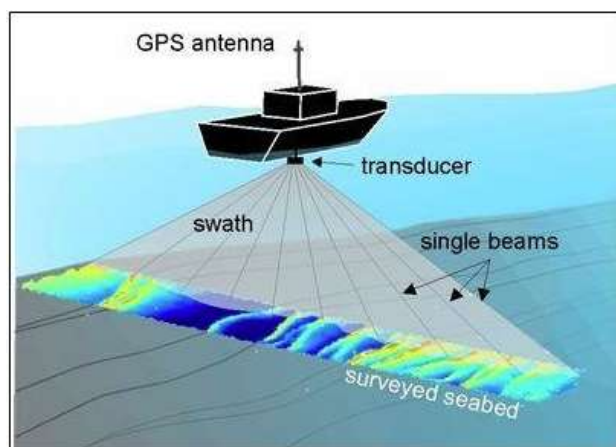


Figure 22. Bathymetric readings being recorded by a MBES (From Sitorus, 2015)

The primary dataset, “Batymetri Søre Sunnmøre 2017”, is comprised of 38 bathymetric surveys conducted by the Norwegian Hydrographic Service (NHS) between the years 2006 and 2012 covering nearshore marine areas of Søre Sunnmøre between five municipalities including Hareid, Ulstein, Herøy, Sande and Vanylven. Data was collected using different MBES systems (Table 1). The depth range covered by this dataset is 0.2-636m below the water surface. The dataset was downloaded from Kvartverket through hoydedata.no and gridded to a 5 x 5m isometric grid in ArcGIS (see section 3.7).

Table 1. MBES data acquisition specifications as collected by the NHS. Table taken from Elvenes et al. (2019) where the same bathymetric data was used to create a Seabed Sediment map of Søre Sunnmøre (Figure 13).

MBES system	Frequency	Recommended maximum operating depth*	Acquisition depths in study area	Year of data acquisition	Number of surveys	Total area covered	Backscatter available
EM 710	40–100 kHz	2800 m	7–636 m	2012	4	241 km <sup>2</sup>	Yes
EM 1002	95 kHz	1000 m	13–307 m	2007	2	71 km <sup>2</sup>	Yes
EM 3000	300 kHz	200 m	0.8–63 m	2006	1	2 km <sup>2</sup>	No
EM 3002D	300 kHz	200 m	0.8–221 m	2007	9	143 km <sup>2</sup>	Yes
EM 3002D	300 kHz	200 m	0.2–207 m	2008	11	172 km <sup>2</sup>	For 10 surveys (129 km <sup>2</sup> )
EM 3002D	300 kHz	200 m	0.8–76 m	2009	2	1 km <sup>2</sup>	Yes
EM 3002D	300 kHz	200 m	0.9–310 m	2012	9	206 km <sup>2</sup>	Yes

MBES data was initially published at a resolution of 25cm. This resolution is likely artificially high especially for deeper portions of the study area and could potentially distort the resulting image at depth.

Noise and artefacts are found within the MBES data which could not be processed out. Side lobe interference has resulted from slope fluctuations which are perpendicular to the path of the collection vessel that manifest as a succession of concave arcs (Moustier and Kleinrock, 1986) (Figure 23). Other potential sources for noise and artefacts in the data include imperfect tide corrections, and input from external sounds (i.e. waves, animals, boat engines). These artefacts were identified and ignored while interpreting the MBES data, and only features belonging to a plausible narrative of glacial dynamics have been considered in this thesis.

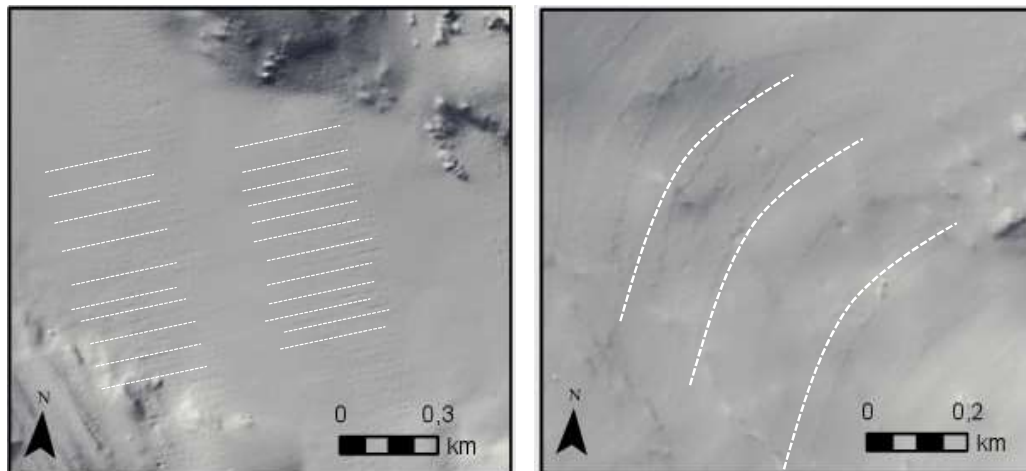


Figure 23. Two examples of artefacts found within the MBES data (marked with white dotted lines). On the left the artefacts appear as two sets of parallel thin grooves within a glacial trough, potentially caused by interference from an external sound source. The right image shows concentric arcuate bars, also found within a glacial trough, resulting from side lobe interference.

### 3.2 Backscatter Data

Backscatter data, which measures the reflectivity of the seabed, was collected contemporaneously to MBES data. Backscatter data can be useful in determining grain size and hardness of sediment on the seabed, as grain size and hardness both alter acoustic impedance and are strongly correlated with reflectivity. Soft sediment will tend to absorb the signal while harder material will reflect it. Additionally, backscatter data can inform to the surficial roughness of the seafloor or the presence of heterogeneities such as trapped fluid and organic material (Bellec et al., 2017). Crucial to the accurate analysis of backscatter data is the assumption that values increase with grain size, as shown below by a Kernel Density Estimation (KDE) plot (Figure 24).

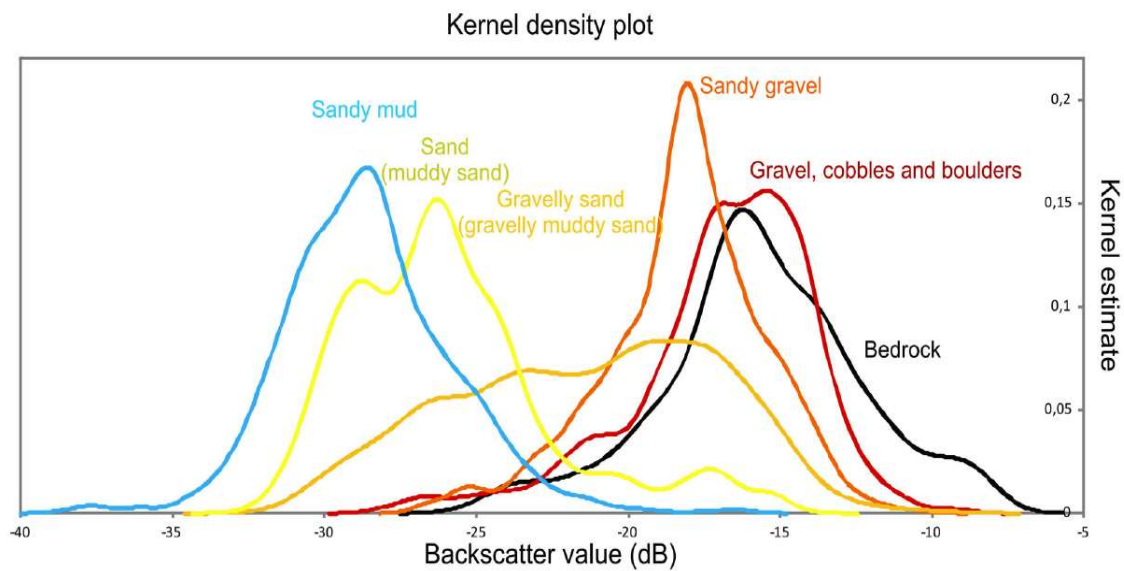


Figure 24. Kernel Density Estimation Plot showing backscatter data correlation to kernel size, and ultimate interpretation of sediment type present at each location (From Bellec et al., 2017). Kernel density plots are closely related to histograms and are used to estimate the probability of the occurrence of any given variable (Hastie, 2001).

Methods used in backscatter data collection and interpretation have limitations. Several studies have suggested that backscatter data cannot be taken as absolute. Ferrini & Flood (2006) found that the mathematical correlation between grain size, roughness, and backscatter intensity varied significantly from site to site, suggesting that backscatter data cannot be used alone in interpreting seabed characteristics.

Many features such as moraines are not easily visible in a typical hillshaded bathymetric representation, but can more easily be identified using backscatter data especially if the moraine is partially buried. Depending on the frequency used, backscatter signals will penetrate typically between 10-30cm into the sediment drape covering the moraine ridges (Beyer, 2006). Due to the sharp contrast in hardness between the coarse-grained morainic ridges and the softer mud surrounding the ridges, moraines are often more easily detected using backscatter than MBES data (Figure 25).

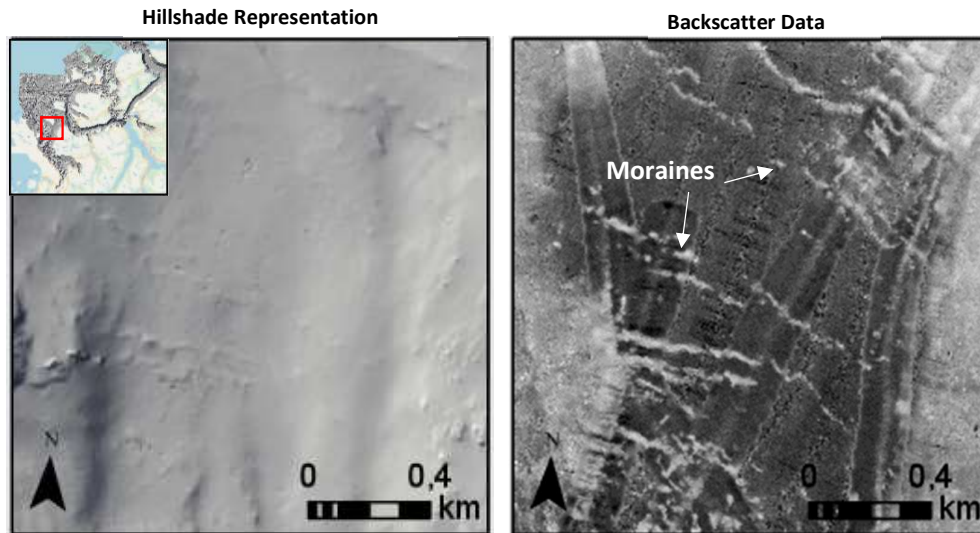


Figure 25. Hillshaded MBES data vs. Backscatter data

### 3.3 LiDAR Data

While the primary focus of this thesis is on submarine landforms, wherever submarine landforms appeared to transition into terrestrial environments, LiDAR (light detection and ranging) data was used to analyze the characteristics of landforms in their terrestrial environment. LiDAR data was collected aerially by plane (flight company Terratec AS) as commissioned by The Norwegian Mapping Authority (NMA) (Norwegian: Kartverket) between the years 2010-2019. LiDAR surveys were downloaded through hoydedata.no and integrated into ArcGIS.

Most LiDAR surveys employ a red laser beam which is shot toward the earth and the return time to a receiver onboard the plane is measured, thus giving a highly accurate elevation measurement (Figure 26).

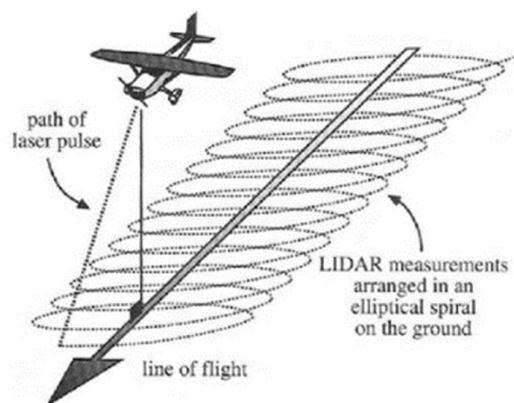


Figure 26. LiDAR data is collected by the emission and reception of laser pulses from an aircraft. Measurements are arranged in overlapping ellipses in order to measure topography (From Engelkemeir and Kahn, 2007).

The NMA began a surveying campaign known as the Green Laser Søre Sunnmøre (GLaSS) in 2017 (dataset titled: NDH Sunnmøre dybde data 2017) in which data collection was performed using a green laser, rather than a red laser, in order to record nearshore depth measurements in the land-sea transition zone (Dolan et al., 2018). Green laser LiDAR data is limited to shallow depths (maximum 5m) and its results can be significantly impacted by signal attenuation due to water column characteristics such as vegetation, color, and turbidity (Dolan et al., 2018).

### 3.4 Seismic Data

Select seismic lines were examined which cover several fjords and sounds of coastal Søre Sunnmøre (Figure 27). Seismic data was made available through MAREANO (Marine Area Database for Norwegian Coastal and Marine Areas) which is a collaboration between NGU and Kartverket. Seismic data was collected using a sparker sonar source at various frequencies. Seismic lines were uploaded and examined using the Petrel (2019) seismic interpretation software.



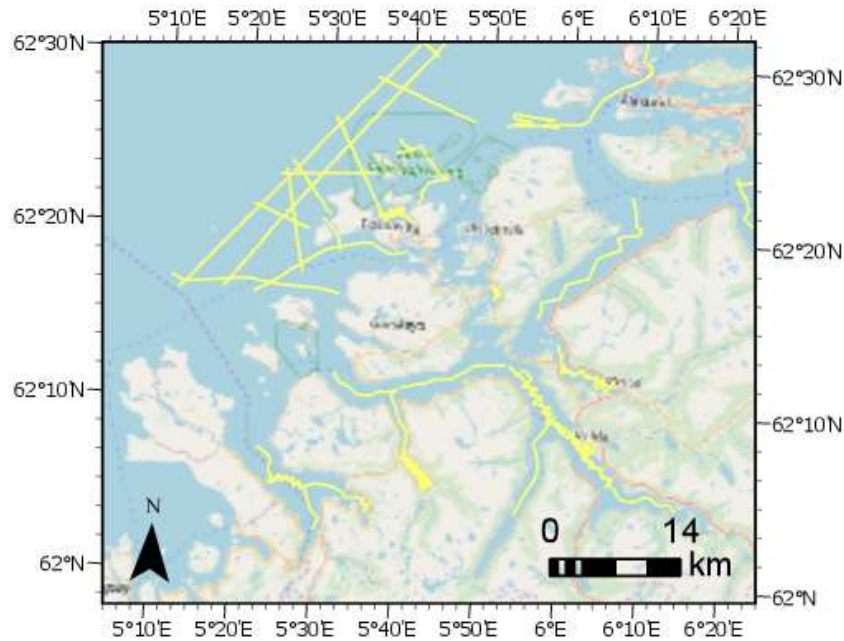


Figure 27. Seismic lines (yellow lines) contained in Søre Sunnmøre made available for analysis by MAREANO.

### 3.5 Video Recordings

During two field seasons in the years 2014 and 2015, NGU collected 219 video transects throughout coastal Søre Sunnmøre using a boat-towed camera and a mounted transponder to position the camera. Wherever video transects were seen to crossover features or landforms of interest, the corresponding video recording was reviewed for visual confirmation.

### 3.6 DATED-1 Database

Time slice reconstructions of growth and decay cycles of the Fennoscandian Ice Sheet presented by the DATED-1 database (Hughes et al., 2016) were used to corroborate landform identifications. Time slice reconstructions were created at 1,000 yr intervals between 25-10 ka BP. Additional time slices were created at select time intervals between 40-25 ka BP. Reconstructions were created by compiling all known existing dates presented within published (and some unpublished) articles (Table 2). Ages used in the creation of time slice reconstructions were produced using various dating techniques including Carbon-14, Optically-Stimulated Luminescence (OSL), and cosmogenic nuclide dating. In total, 189 samples were dated in the Søre Sunnmøre area. Each sample is also placed in geological context and is assigned a value which corresponds to a glacial advance, retreat, or ice free period.

Table 2. Summary of sample locations, organic material used (including bulk sediments), and authors used for DATED-1 (Hughes et al., 2016). All samples in Søre Sunnmøre were dated using Carbon-14 methods. Each age was assigned a quality value of 1-3 based on the credibility of the sample, and was weighted accordingly. Source references which are not mentioned elsewhere in this thesis are not included in the references section.

Site	Material	Source Reference
Kulturmyra, Leinøy	Shell and Terrestrial Plant Fragments	Svendsen & Mangerud 1990; Bondevik et al. 1999; 2006
Frøystadmyra	Bulk Sediment	Svendsen & Mangerud 1990
Dimnamyr	Leaves and Bark (Salix or Betula nana)	Koren et al. 2008
Litlevatn	Bulk Sediment	Svendsen & Mangerud 1990
Voldafjorden	Shell Fragments	Grøsfjeld et al. 1999
Dyb, Godøy	Shell Fragments	Landvik & Mangerud 1985; Mangerud et al. 2010
Hamnsundhelleren	Bone Fragments	Valen et al. 1996; Mangerud et al. 2010
Vikebukta, Vigra	Shell Fragments	Landvik & Hamborg 1987
Hjørungavåg	Marine shells	Mangerud, unpublished
Skjonghelleren	Bone Fragments (bird, fox, seal)	Mangerud et al. 2010; Mangerud et al. 1981
Liaaen	Shell Fragments (mya truncata)	Mangerud et al. 1981
Gjøundet, Vigra	Unidentified fragments	Greve 1984
Volsdalsberga	Marine shells: Mya truncata	Mangerud, unpublished
Ullaholmen	Mya truncata	Mangerud et al. 1981
Sauedalsmyra	Bulk sediment	Lie et al. 1983; Kristiansen et al. 1988
Torvlømyra	Bulk sediment	Lie et al. 1983; Kristiansen et al. 1988
Gjølvatnet	Marine shells: Chlamys islandica	Mangerud, unpublished
Eidsvik	Shell Fragments	Mangerud et al. 1981
Hamnsundhelleren	Bone Fragments (Plautus alle, bird)	Valen et al. 1996; Mangerud et al. 2010
Longva	Mainly Mya truncata	Mangerud et al. 1981; Mangerud et al. 2010
Lerstadvatn	Bulk seds.	Lie et al. 1983; Kristiansen et al. 1988
Gamlemsveten	Bulk plant remains	Mangerud et al. 1981; Nesje et al. 1987
Hildre	Marine shell (Mya truncata, Arctica islandica)	Mangerud, unpublished
Hildrestrand	Mainly Mya truncata	Mangerud et al. 1981
Vegsundet	Marine shells (Chlamys islandica)	Mangerud, unpublished
Sjøløkavik, Ålesund	Small, poorly preserved and unidentified fragments from sea	Henningsen & Hovden 1984; Mangerud et al. 2010
Rogneholmen	Marine shell: Mya truncata	Mangerud, unpublished
Kaldvatn	Marine shells	Sollid & Reite 1983
Vikane	Marine shells	Larsen et al. 1988
Ertvågøya	Shell	Follestad 1992

### 3.7 ArcGIS Pro 10.5 and ArcMap 10.5

All above datasets were loaded into both ArcGIS Pro 10.5 and ArcMap 10.5. The majority of analysis was conducted within ArcGIS Pro 10.5, while ArcMap 10.5 was used for spatial analysis of landforms such as the creation of cross-sectional profiles. After downloading bathymetric and LiDAR data from hoydedata.no, datasets were gridded into a 5 x 5 m isometric grid before being further processed using various geoprocessing tools within ArcGIS such as data mosaicking and resampling functions. Hillshades created using artificial lighting from multiple angles allowed for improved recognition of submarine features. Additionally, the geoprocessing tool "Slope Rasters" provided slope angle measurements which aided in identification and analysis of submarine landforms. All data was oriented using the 1989 UTM Zone 32N coordinate system.

## 4 Results

Several glacial and non-glacial landforms can be identified using available datasets. Some landforms are easily distinguishable, while other landforms have undergone partial erosion or burial and appear more subtly in their bathymetric representation. The first portion of this results section will focus strictly on glacial landforms while non-glacial and postglacial landforms will be identified in later sections. Only glacial landforms which have been identified to be most prominent and characteristic of the study area will be identified and interpreted. Figures 28 and 29 below show a general overview of glacial features in the area. Subsequent figures within the results section will include more zoomed in representations of individual features.

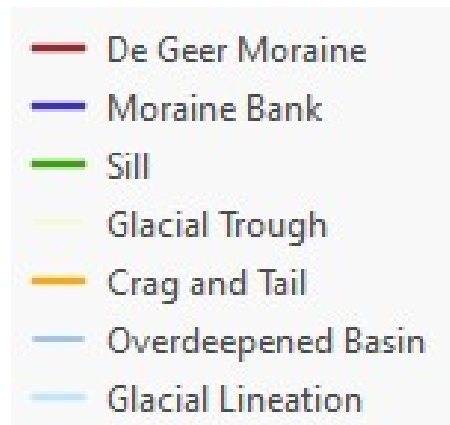
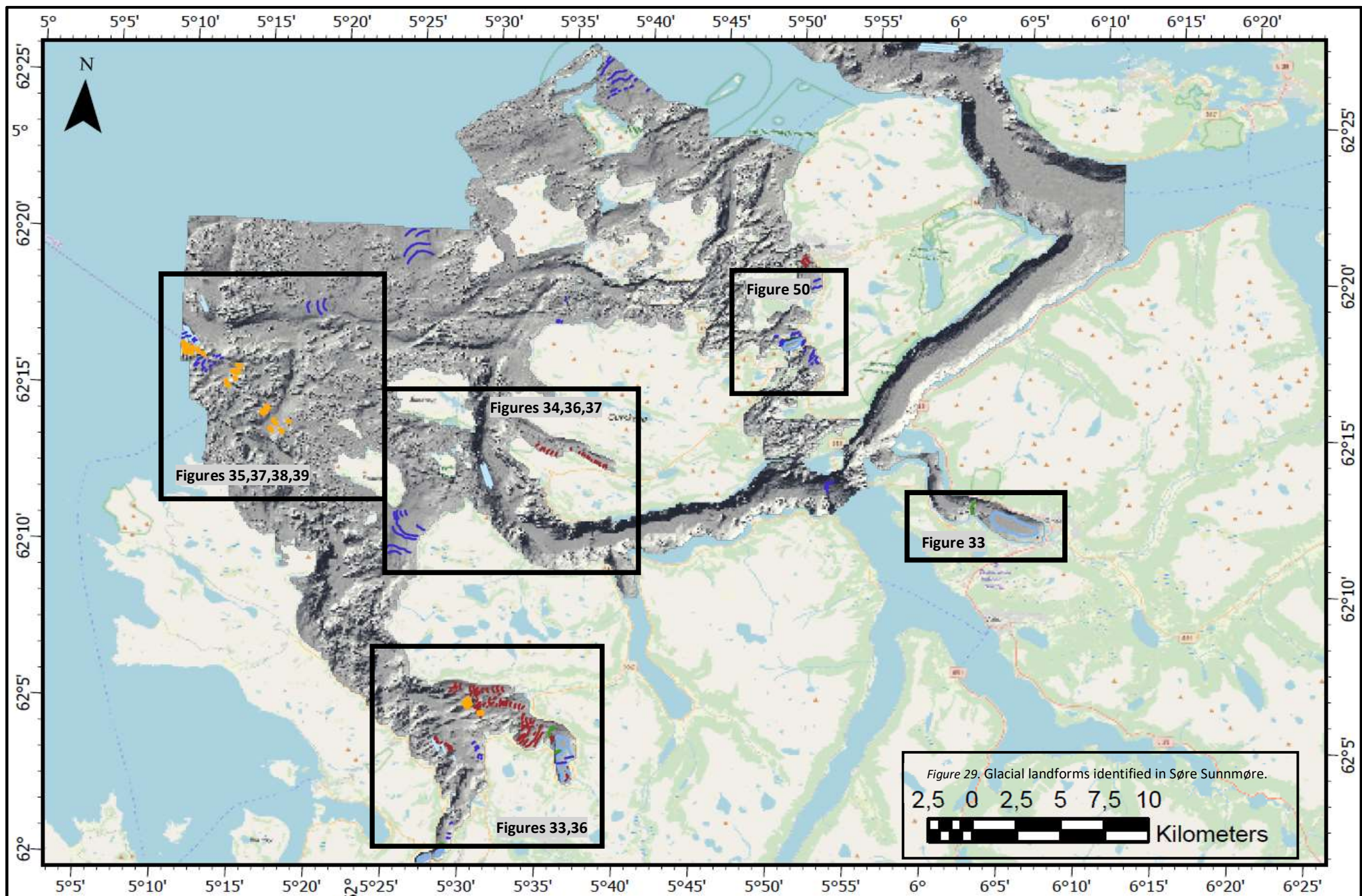


*Figure 28.* Legend showing colors used in ArcGIS for glacial landform identification.



Figures 35,37,38,39

Figures 34,36,37

Figure 50

Figure 33

Figures 33,36

Figure 29. Glacial landforms identified in Søre Sunnmøre.  
2,5 0 2,5 5 7,5 10 Kilometers

## 4.1 Submarine Glacial Landforms

### 4.1.1 Elongated Depressions– description

A network of elongated depressions can be found in the study area extending from the inner fjords, through the sounds between the outer coastal islands, and out on the continental shelf. These elongated depressions are generally rather flat and significantly deeper than their surroundings, although irregularities and cross-cutting ridges can be found within the depressions. The depths of these elongated depressions range from 250m to 450m.

The deepest elongated depression is also the most continuous elongated depression in the study area which runs through Sulafjord along the southeastern boundary of the bathymetric data (Figure 30). Water depths beyond the banks of this depression range from 0m to 150m, and from 400m to 450m within the depression. The bottom of most elongated depressions consists of very fine sediment, primarily muds (clays and silts), and contains only low percentages of sand content as shown by the Seabed Sediments of Søre Sunnmøre map (Elvenes, 2019). The elongated depressions are also seen to intersect with one another at a wide range of angles. There exist some long stretches of uninterrupted elongated depressions which can be over 35km long. Other segments of the elongated depressions are much shorter, between 1-5km long, and are segmented by zones of raised bedrock knolls. Banks are generally well defined and consistent along the entire length of the depression. Just outside the boundary of these elongated depressions the terrain becomes quite steep as it rises up to terrestrial environments or to elevated bedrock areas.

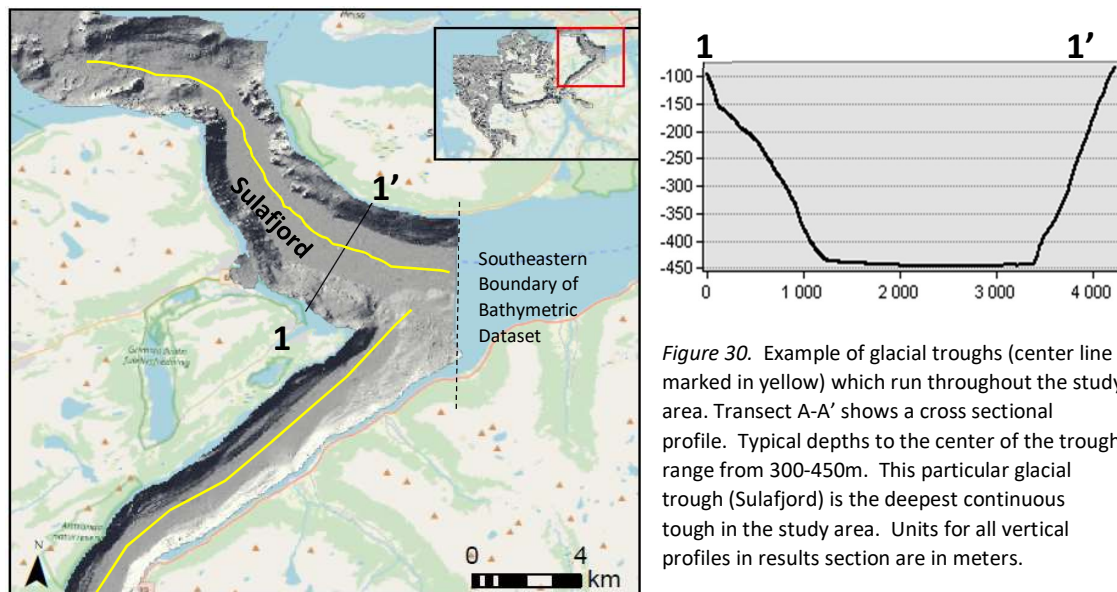


Figure 30. Example of glacial troughs (center line marked in yellow) which run throughout the study area. Transect A-A' shows a cross sectional profile. Typical depths to the center of the trough range from 300-450m. This particular glacial trough (Sulafjord) is the deepest continuous trough in the study area. Units for all vertical profiles in results section are in meters.

### 4.1.2 Infilled Glacial Troughs - interpretation

Elongated depressions are interpreted as glacial troughs that have been eroded by grounded ice streams during multiple glaciations (Vorren, 2003). Generally speaking, glaciers will tend to spread out evenly in all directions. However, if they are confined by structural controls such as topography or previously cut fluvial valleys, they will then begin to cut downward and erode the valley floor rather than spreading outward (Morland, 1987). The erosional processes necessary to form a glacial trough take tens of thousands of years and implies multiple glaciations (Waddington, 2000). Glacial troughs, which initially have V-shaped profile, are transformed into U-shaped valleys as they become infilled by sediment, mostly from suspension settling (Lyså et al., 2010) (Figure 31).

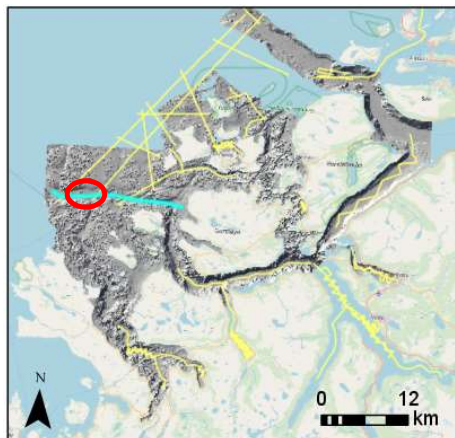
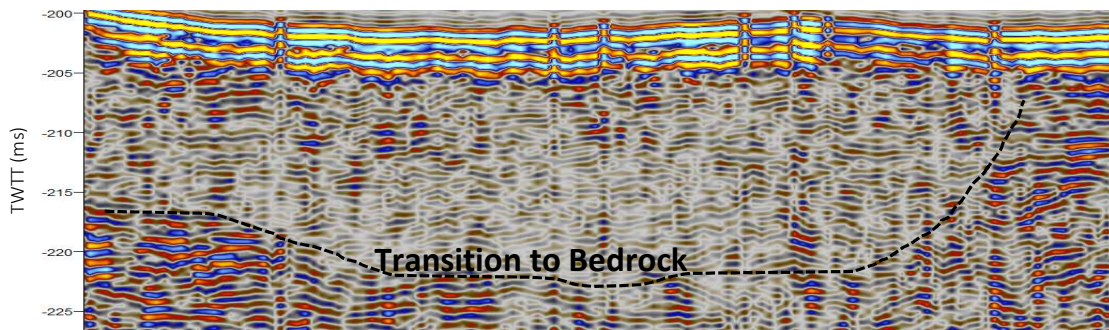


Figure 31. 3km section (highlighted by red circle on map) of seismic line 1508011\_SPARKER (highlighted in blue on map) which runs parallel to a glacial trough. Seismic data shows multiple layers of planar sediment beds, likely deposited through suspension settling. Soft sediment covers a Two Way Travel Time (TWTT) of 20ms. Using an assumed seismic velocity of 1500 m/s, which is typical for soft sediment (Bina, 2003), the beds here correspond to a thickness of roughly **15m of infill** using the formula  $TWTT/2 (s) * Velocity (m/s) = Depth (m)$ .



The longest glacial trough in Søre Sunnmøre which continues from Sulafjord out onto the continental is well-studied biologically diverse Marine Protected Area containing coral reefs known as Breisunddjuppet. Breisunddjuppet is one of Norway's longest and deepest glacial troughs (Figure 32).

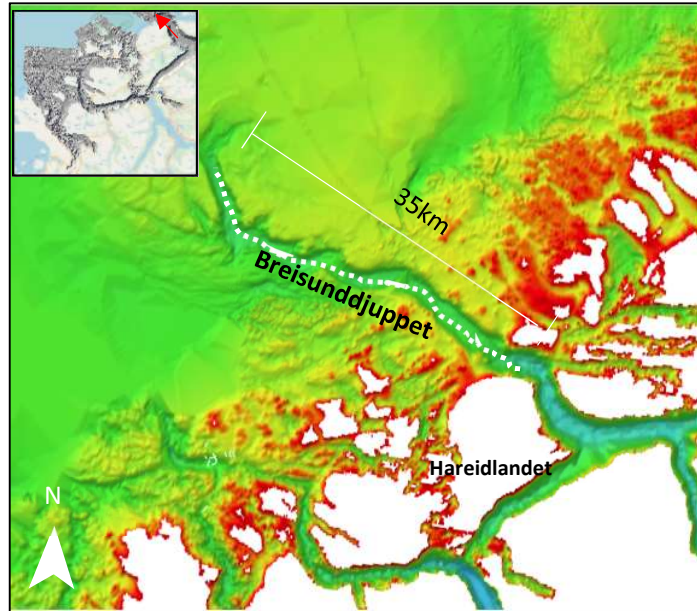


Figure 32. Breisunddjuppet as seen from bathymetry data borrowed from EMODnet. Dotted white line marks the center line of the glacial trough.

#### ***4.1.3 Deep Areas at Fjord Heads Bounded by Pronounced Ridges- description***

At the head of each of fjord, there is an oval shaped depression that is significantly deeper than the rest of the fjord (Figure 33). These depressions are also deeper than the thalweg (a line demarcating the deepest area in a body of water) along the rest of valley. Three fjords with these oval-shaped deep areas, or basins, are contained within the bathymetric data set. These basins are in general at least twice as deep as the sea within the adjacent glacial valley. Along the boundary of each basin, between 1-3km away from the head of the fjord, are pronounced ridges consisting of coarse sediment. In some cases, large boulders are visible in the bathymetric data associated with these ridges. In one location there exists two deep basins adjacent to one another separated by a large ridge (Figure 33a). In another location, there exists a partial ridge which does not extend all the way across the fjord (Figure 33b). If this ridge were to extend all the way across the fjord, two separate basins would exist in this location as well.

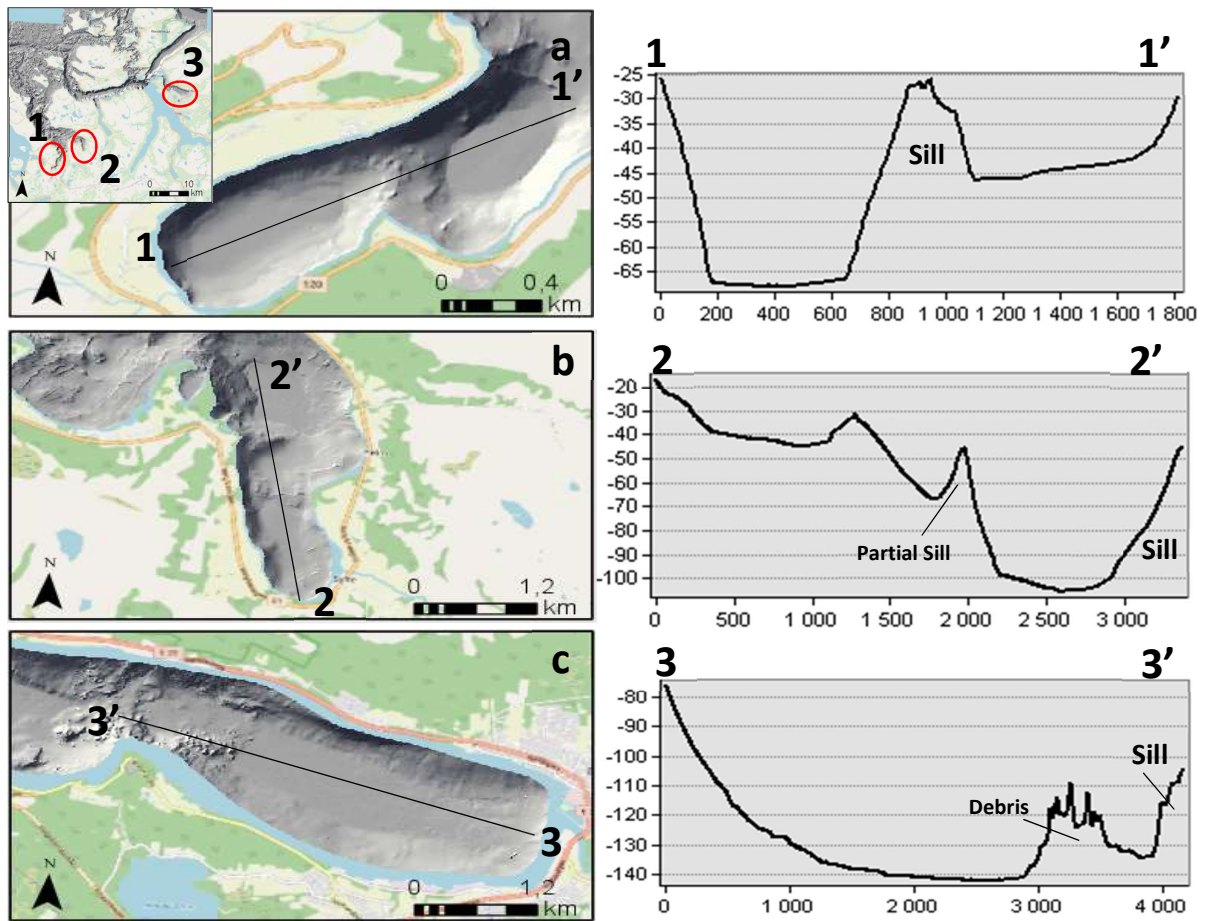


Figure 33. Overdeepened basins with sills at the heads of three fjords within the study area. Location of each fjord shown top left.

#### 4.1.4 Overdeepened Fjord Basins and Sills- interpretation

These basins and ridges have been interpreted as overdeepened fjord basins with sills.

Overdeepening is a common characteristic of fjord valleys which have been eroded by glaciers. This process occurs as the glacier erodes the head of the fjord through quarrying, abrasion and meltwater erosion, resulting in deepening far below a standard graded profile (Fiebig, 2014). The degree to which a glacier is able to overdeepen a fjord is largely controlled by topography, density of the glacial ice, and bedrock competence. Once a fjord is overdeepened, this can have significant impact on future glaciers' ability to advance as ice must be much thick enough to remain grounded and have the possibility to advance. Otherwise ice will simply calve into the fjord and not be allowed to advance any further (Fiebig, 2014).



The location, orientation, and grain size of the pronounced ridges at the boundary of each overdeepened basin have led to their interpretation as sills. Sills form when a stable or retreating glacier transitions from erosional processes to depositional processes and can be considered as special cases of a terminal moraine. The presence of a sill will significantly influence the flow of currents, tides, and the freshwater/saltwater exchange between the fresh fjord water and more saline sea water. Sills also act as pinning points which can slow the advance of a later glacial advance or allow a retreating glacier to stabilize (Favier et al., 2016).

#### ***4.1.5 Curved Transverse Ridges- description***

Curved transverse ridges can be found throughout the fjords and sounds of Søre Sunnmøre, and also on the continental shelf beyond the coastal islands (Figure 34). Generally speaking, the ridges form arcuate shapes which are concave toward the northwest away from the Norwegian coastline. Azimuth varies between the different sets of transverse ridges. Some ridges are continuous and form single arcs up to 1.5km long, while others are broken up into shorter segments between 10-100m long which belong to the same overall arcuate shape. The heights of these features range from 1-5m above the surrounding terrain. The inner side of the arc is typically slightly steeper than the outer side. Additionally, the ridges often appear proximal to other ridges, typically in sets of at least three. The ridges are also seen to occur proximal to other glacial features, such as adjacent to or within a glacial trough, or in association with glacial lineations. According to backscatter data, as well as the "Seabed sediments of Søre Sunnmøre" map (Elvenes, 2019), the sediment which makes up these ridges is also coarser than surrounding sediment.

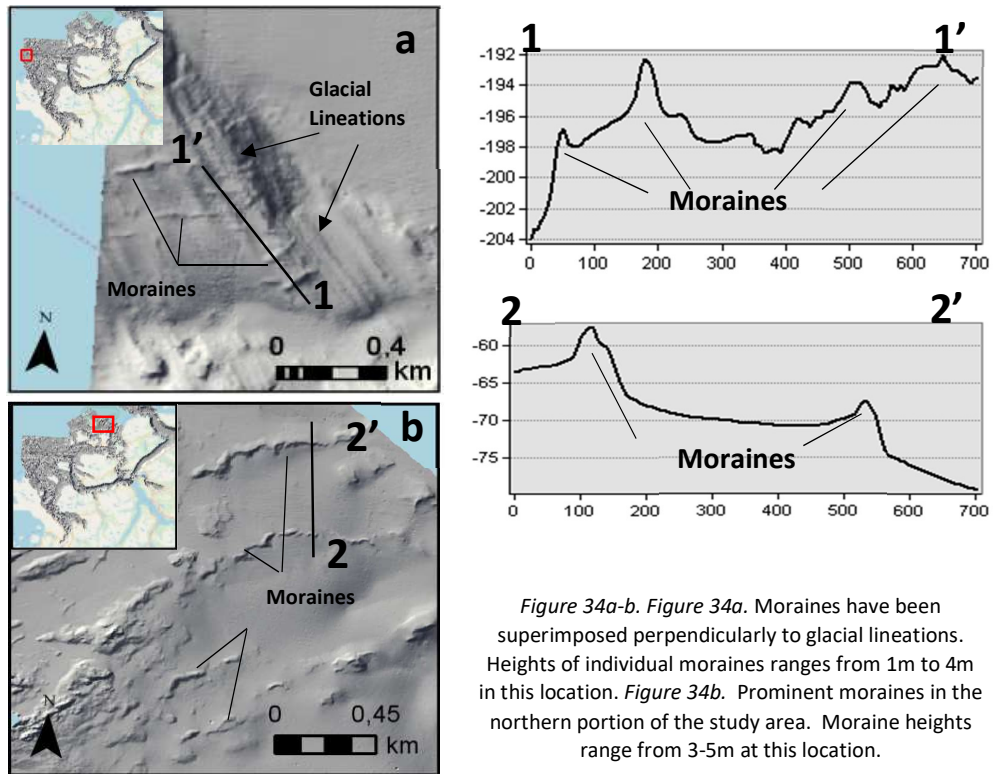


Figure 34a-b. Figure 34a. Moraines have been superimposed perpendicularly to glacial lineations. Heights of individual moraines ranges from 1m to 4m in this location. Figure 34b. Prominent moraines in the northern portion of the study area. Moraine heights range from 3-5m at this location.

One particular set of ridges is seen to trend southwest and meets with ridges oriented in the opposite direction. These opposing ridges are found in Haugsfjord between the island of Kvamsøy and mainland Norway (Figure 35).

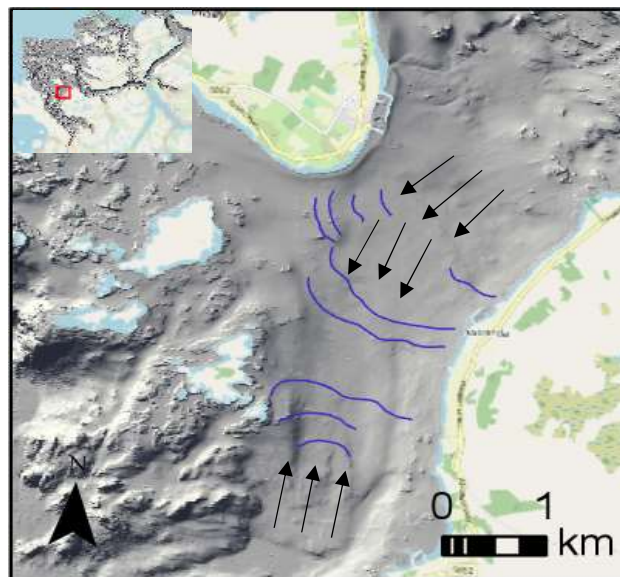


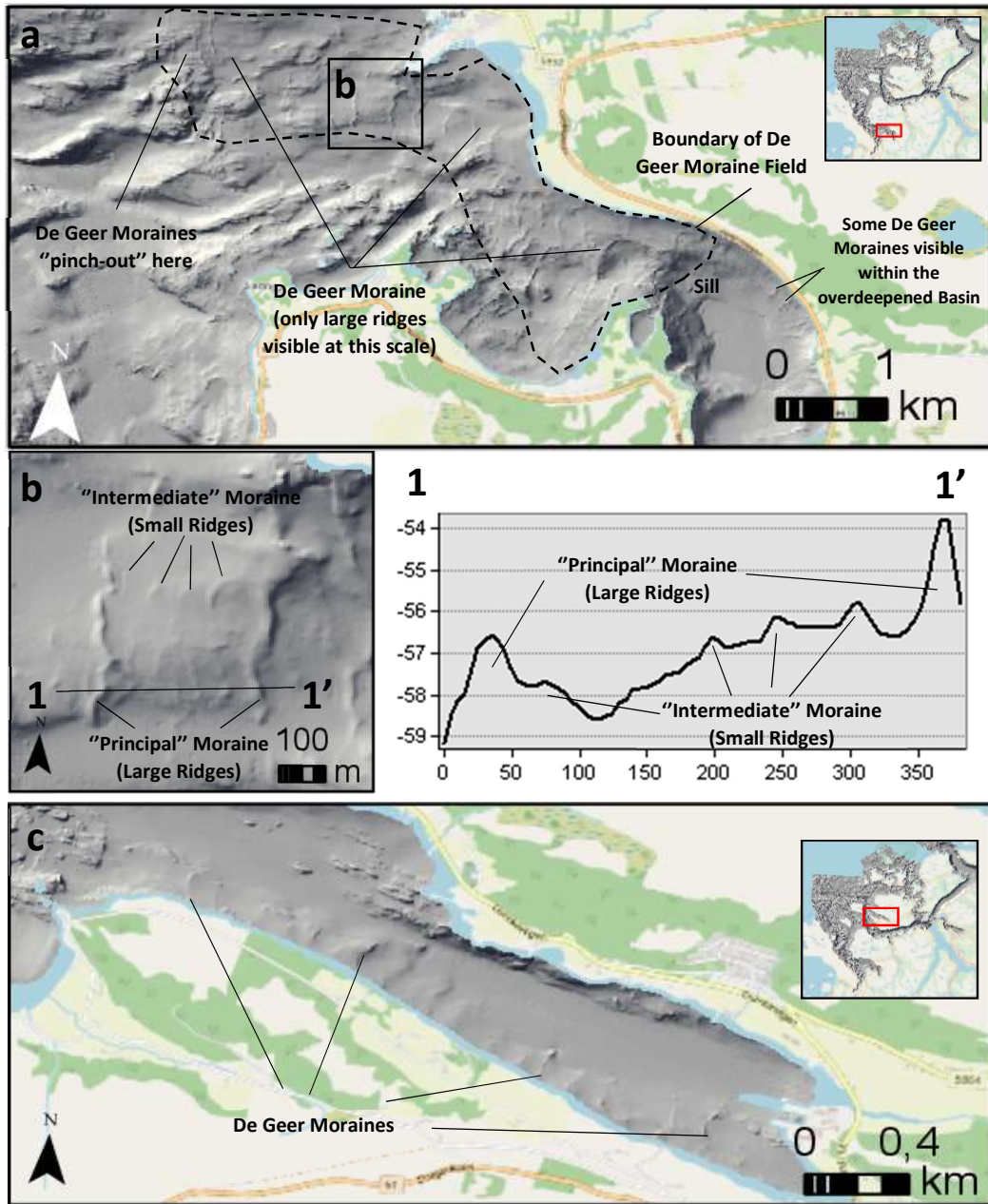
Figure 35. Two sets of transverse ridges meet with opposing orientations in Haugsfjord.

#### ***4.1.6 Moraine Banks- interpretation***

Based on the sediment composition and shape of these ridge features, they have been interpreted to be moraine banks (to be referred to as moraines). The characteristics of moraines in Søre Sunnmøre are in concurrence with previously identified moraines in nearby areas, such as the Bergen area studied by Mangerud (2019). The primary active process in the formation of these moraines is the glacier “pushing” material (both subglacial and proglacial sediment) in front of the glacial terminus or at its grounding line. The glacier will eventually deposit all of this material once the glacier has reached a standstill or begins to retreat (Van Der Wateren, 1995). In most cases, once a moraine has been deposited it can be inferred that no later glaciation has reached the area. This is because if there were to be another glacial advance, the moraine would be overrun and all of its material would be incorporated back into the glacier and pushed further along, forming a new moraine. Moraines are typically found proximal to other glacial features, for example moraines found along the western boundary of the study area which are superimposed over previously described glacial lineations (Figure 34a). In total 180 moraine ridges have been identified in Søre Sunnmøre.

#### ***4.1.7 Sequences of Multiple Regularly Spaced Ridges- description***

A characteristic feature of the study area are sequences of evenly spaced ridges that are parallel to one another and are similar in length, width, height, and arcuate shaping. The number of ridges in these sequences is much higher than in groups of previously described moraines. Such sequences are seen to occur mainly within two localities within the study area (Figure 36).



Figures 36a-c. 36a. De Geer moraines within Syltefjord. Notice the moraines are more prominent (i.e. better preserved) beyond the sill outside of the overdeepened basin. 36b. Example of typical De Geer moraine configuration in Syltefjord. Two "principal" moraines (2-3m in height) contain four "intermediate" moraines (0.5-1m in height) between them 36c. De Geer moraines in fiord along western Gurskøva.

Syltefjord contains a sequence of large ridges with smaller intermediate ridges between them. The number of small ridges visible between two large ridges can vary anywhere from zero to five. However, the larger ridges are still evenly spaced regardless of whether or not they have smaller intermediate ridges between them. The heights of the large ridges ranges from 3-4m compared with the smaller ridges measuring between 0.5-2m. The large ridges are generally continuous while the intermediate ridges are often partially obscured and appear less distinguishable and continuous.

There is a total of 18 large ridges and 45 small ridges. The average spacing between the large ridges is 220m. The ridges span over an area that is roughly 10km<sup>2</sup> and extends 9km from the head of the fjord. These ridges appear to be best preserved outside of the overdeepened fjord basin and past the sill, or farther in the direction of ice flow. However, some ridges are also faintly visible within the overdeepened fjord basin itself. Many of the ridges are segmented by elevated bedrock knolls, while others continue over such knolls uninterrupted. The ridges appear to “pinch-out” between the modern shoreline and a bedrock zone which lies roughly 500m from the shoreline (Figure 36a).

Sequential ridges also occur further north in the study area in an unnamed fjord inlet off the west coast of the island of Gurskøya. These ridges are most prominent along the southern edge of the fjord and appear to have been partially buried by fine to medium-grained sediment beyond the edge of the fjord. In total there are 19 individual ridges. Heights of ridges range between 1m to 4m. The average spacing between them is 180m. The ridges in Gurskøya appear to have been reworked more so than previously described ridges in Syltefjord, as they appear to be less consolidated and less prominent in bathymetry than ridges found in Syltefjord.

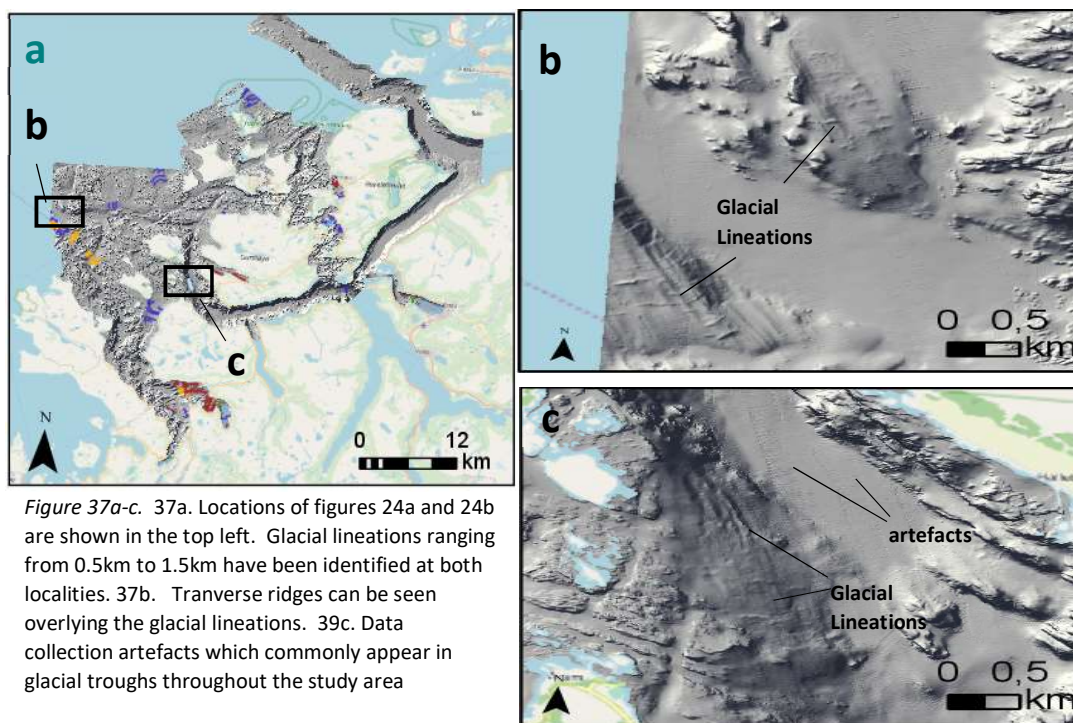
#### ***4.1.8 Feature Interpretation- De Geer Moraines***

Based on the size, shape, and even spacing of these ridges they have been interpreted to be De Geer moraines. This special case of recessional moraine occurs as sediment is successively deposited at regular intervals near the grounding line of a retreating glacier (Elvenes et al., 2016). However, some De Geer moraines can also form sub-glacially as material is pushed into up into basal crevasses proximal to the grounding line, but not necessarily directly at the grounding line (Larsen et al., 1991). The regular spacing between individual moraines means that the timing of deposition of each moraine within the succession is controlled by a regularly occurring cyclical variation in temperature, most often driven by seasonal variation (Bouvier et al., 2015).

#### ***4.1.9 Streamlined Linear Ridge Bedforms- description***

In two different locations there appear sets of elongated, streamlined ridge bedforms. Within each set the bedforms are parallel to one another and are sub-parallel to the direction of the adjacent glacial trough (Figure 37). The westernmost set is bisected by a glacial trough. The lengths of individual ridges range between 0.5km and 1.5km. However, in the westernmost set they appear to extend beyond the boundary of the bathymetric data, making the total length indeterminable. Typical widths of individual ridges is between 30-40m. Elongation ratios (elongation=length/width) therefore range from a minimum of 12 to a maximum of 65. Spacing between the ridges is generally

consistent and ranges from 50-60m. Azimuth angles for both sets of bedforms is between 320° and 330°.



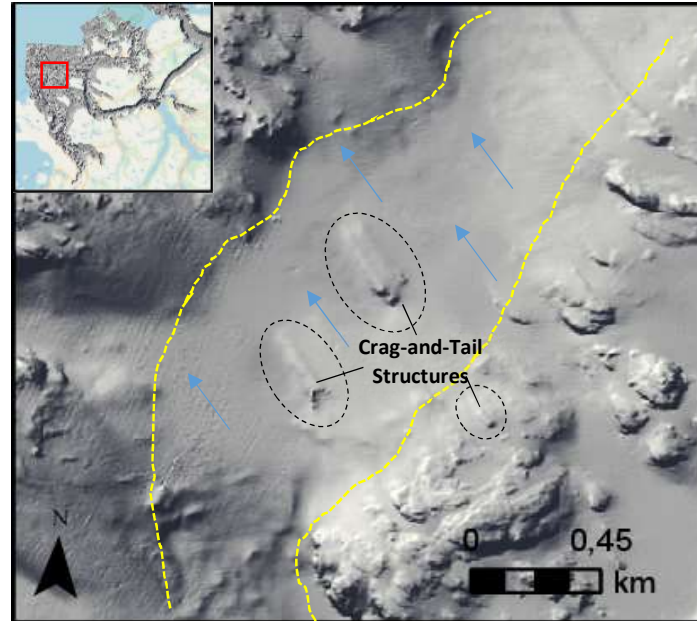
#### 4.1.10 Glacial Lineations- interpretation

Based on their orientation, sizing, spacing, and elongation, it is reasonable to interpret these bedforms as glacial lineations. Backscatter data for the areas containing each set of glacial lineations suggests the presence of easily deformed soft sandy mud. The primary processes active in their formation was likely soft sediment deformation within the subglacial environment where ice was in direct contact with the substrate (Fredin et al., 2013). Due to the consistency in characteristics between the two sets of lineations, it is reasonable to infer that both sets of glacial lineations were formed within a relatively short time from one another, likely during the same glacial advance.

Glacial lineations are to be expected in previously glaciated environments. Although the glacial lineations found here meet elongation ratio requirements to be considered mega-scale glacial lineations (MSGLs) of at least 10:1, they do not meet the overall length and width dimension requirements and should therefore be referred to as glacial lineations. Glacial lineations are direct indicators of ice flow direction and often form during advance when the glacier has its greatest landscape-shaping and erosive potential (Hjelstuen et al., 2009). Glacial lineations are generally formed under conditions associated with quickly moving ice (Bennett, 2001).

#### 4.1.11 Streamlined Knoll Features- description

Along the western boundary of the study area there can be found intermittent groupings of small-scale features which measure between 20-60m long and 2-10m wide that consist of a steep incline on one side of the feature and a more gently dipping leeward side on the other (Figure 38). These features generally trend to the northwest and are oriented obliquely to the direction of the glacial troughs in which they are located.



Figures 38. NW oriented crag-and-tail features (black dashed circles) found within a glacial trough (yellow dotted line). The glacial trough is oriented NNE. Interpreted direction of ice sheet movement is shown (blue

#### 4.1.12 Crag-and-Tail Structures- interpretation

Based on the sizes and mass distributions of these features they have been interpreted as crag-and-tail structures which develop as glaciers erode substrates of unequal competency and hardness (Nitsche et al., 2016). Erosional forces are focused on a “crag” on the stoss (“front”) side. Craggs are typically a knob of bedrock or other hard material. This erosion leads to a steep slope facing in the “up-ice” direction. Cavities formed on the lee (“back”) side of the bedrock knoll, or crag, protect less consolidated material from erosion. However, ice flow will gradually streamline this weaker material on the lee side into a tapered “tail”. This results in the tail pointing in the “down-ice” direction during glacial advance, making crag-and-tail features direct indicators of former ice-flow directions (MacLean et al., 2016).

#### 4.1.13 Elongated Jagged Ridges- description

At many locations throughout the study area, particularly within glacial troughs, there can be found jagged elongated ridges which are between 0.2-1.5km long and roughly 20-50m in height. In most cases there is one main ridge with several smaller knolls running parallel to the main ridge (Figure 39).

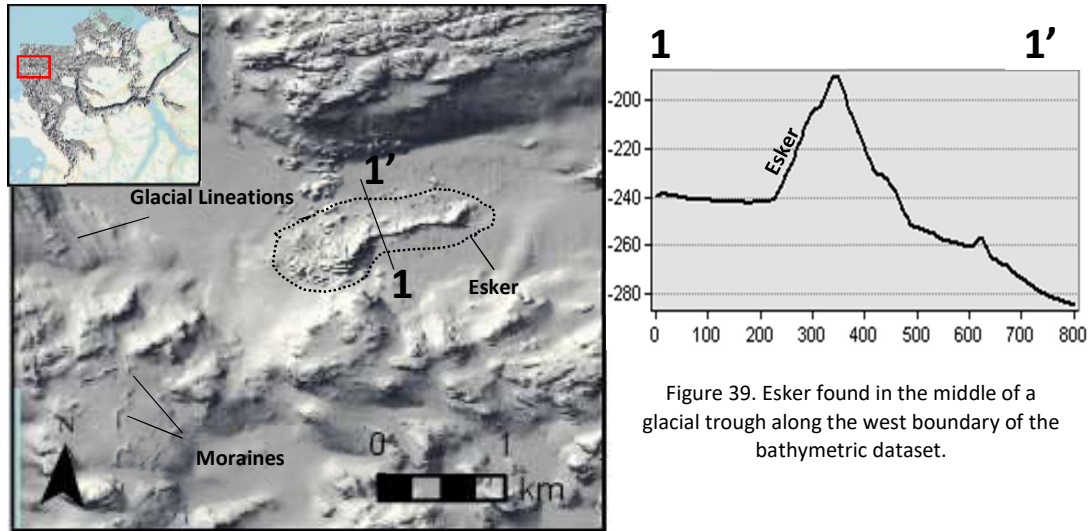


Figure 39. Esker found in the middle of a glacial trough along the west boundary of the bathymetric dataset.

#### 4.1.14 Eskers- interpretation

Based on their shape and location, these features have been interpreted as eskers. Eskers are deposits of coarse-grained material formed by glacial meltwater flowing through tunnels beneath the ice (Perkins et al., 2013). Eskers typically form transgressively and obliquely relative to the ice margin. Eskers in Norway often reflect the pattern of deglaciation during the late Weischelian (Fredin, 2013).

#### 4.1.15 Smoothed bedrock- description

Many bedrock dominated zones contain smoothed knolls and ridges with distinct orientations.

#### 4.1.16 Glacially smoothed bedrock- interpretation

In most cases, the long axis of smoothed bedrock ridges and knolls is parallel or sub-parallel to the primary direction of ice flow (NW) away from the coastline. This has led to their interpretation as glacially smoothed bedrock (Figure 40).



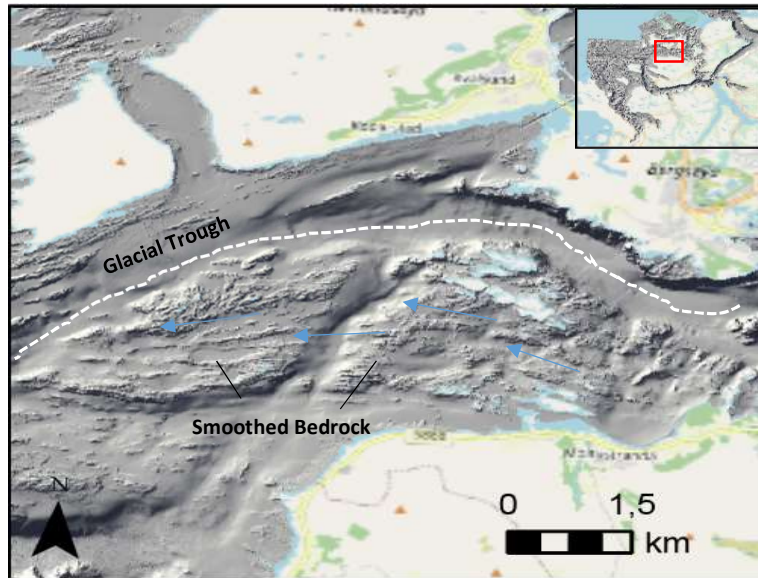


Figure 40. Bedrock ridges smoothed by ice flow. Ice-flow direction shown with blue arrows. Nearby glacial trough marked by dotted white line.

One unique case found between the islands Gurskøy and Haried exhibits a kind of “herring bone” pattern in its orientation (Figure 41). This suggests that not all distinctly oriented smoothed bedrock zones were shaped by ice-flow, as it is unlikely the ice sheet would flow perpendicular to its former direction. Bedrock in this area is likely foliated as such due to tectonic forces (Young, 2017).

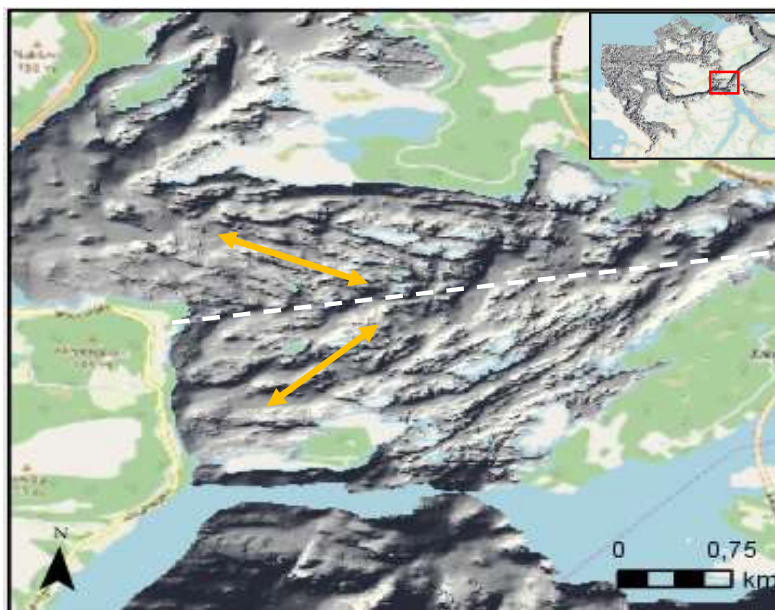


Figure 41. “Herring bone” pattern of bedrock foliation between Gurskøy and Hareid.

## 4.2 Non-Glacial/Postglacial Landforms and Deposits

### 4.2.1 Fan-shaped Deposits- description

Along the southwest bank of Vartdalsfjorden there can be found four separate fan-shaped deposits emanating from onshore. These deposits are raised 15-20m above the surrounding seafloor, extend between 0.5-1km away from the shoreline, and are 0.8-1.2km wide at their widest point. The deposits form in association with terrestrial fluvial systems at the point in which they enter the sea (Figure 42).

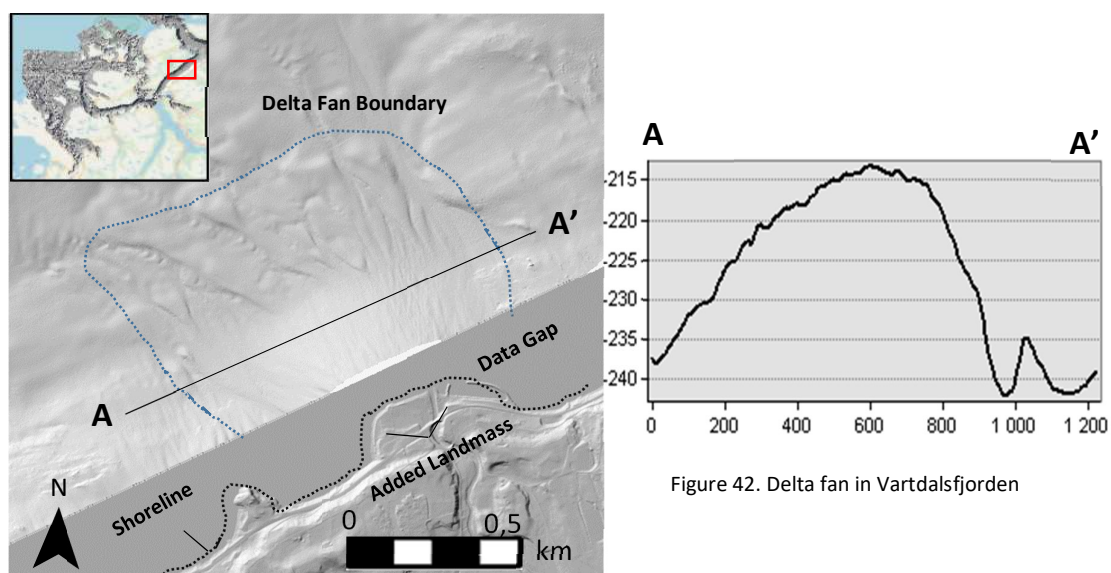


Figure 42. Delta fan in Vartdalsfjorden

### 4.2.2 Delta Fan Deposits- interpretation

Based on the shape of the deposits and their proximity to terrestrial fluvial systems, these deposits have been interpreted as delta fans. Delta fans form as the river carries sediment into a slow moving body of water and the rate of sediment deposition is higher than the rate at which sea currents can remove the sediment (Battacharya and Giosan, 2003). Thus the presence of these deposits implies a relatively calm sea. Delta fans have breached the water surface in most cases and have added landmass onto the shoreline. Based on the symmetrical shape of the deposits these can be considered to be fluvial dominated deltas (Battacharya and Giosan, 2003).

### 4.2.3 Irregular Depression- description

In the northern portion of the bathymetric data set, there is an irregularly shaped depression that is between 0.5-1m deeper than the adjacent seafloor. The depression has a width of roughly 300m at

its widest point and has two offshoot “fangs” which are each roughly 300m long. The surface sediment in the area consists of sandy mud, muddy sand, and muddy sand with gravel (Elvenes, 2019). The depression occurs directly to the south of a prominent moraine and the surrounding terrain has relatively low bathymetric relief (Figure 43).

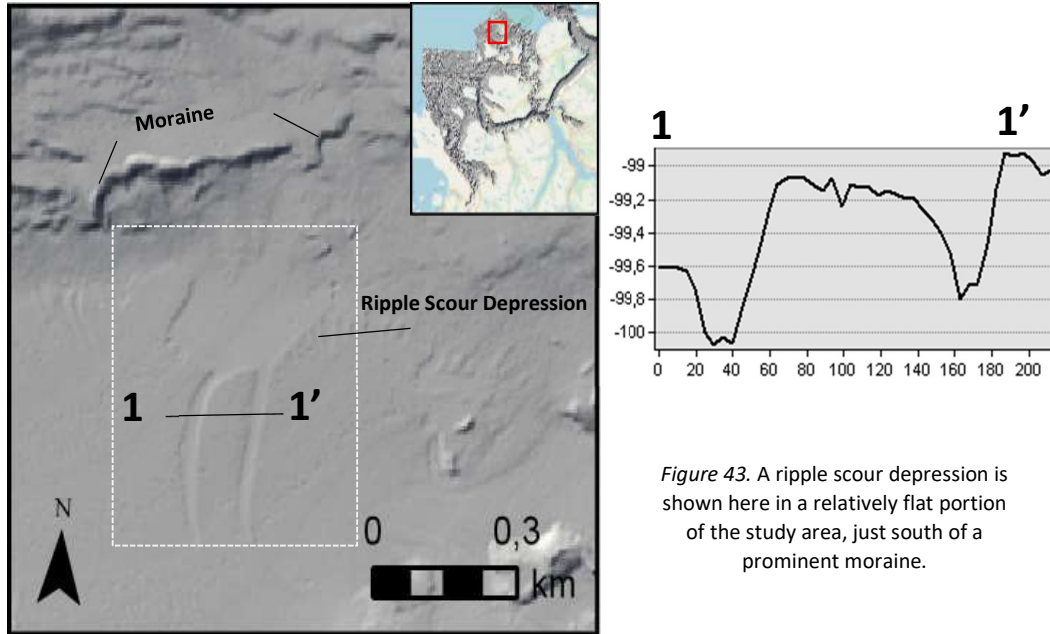


Figure 43. A ripple scour depression is shown here in a relatively flat portion of the study area, just south of a prominent moraine.

The floor of the depression is covered by rippled gravel which contains shells and sand as seen in video V1408011 (Figure 44). The crests of ripples are sub-parallel to the main axis of the depression orientation with featureless sands in between the different appendages of the depression.



Figure 44. Screenshot taken from V1408011 (4:23) showing rippled gravel with intermixed shells and sand along the floor of the depression.

#### 4.2.4 Ripple Scour Depression- interpretation

Based on the shape of the depression and the variable grain sizes associated with the feature, this has been interpreted to be a ripple scour depression (RSD) (Figure 44). Similar features have been described by Bellec et al. (2010) on the continental shelf off the coast of Norland and Troms counties in Northern Norway. RSD's form in areas where the slope gradient is low and sediments have evolved from distal, fine-grained glacial deposits into postglacial muddy sediments (Davis et al., 2013). While there is still speculation regarding the mechanisms involved in the formation of RSD's, it is likely that winnowing of surficial sediment during storm events results in the removal of sediment. Currents are also redirected by local topographic features, such as bedrock knolls. This multi-lateral current results in the irregular shapes commonly exhibited by RSD's (Cacchione, 1984).

#### 4.2.5 Boulder Fields- description

In Ørsta fjord there is a coarse-grained deposit containing mostly large boulders which spans across the entire fjord. Hundreds of individual boulders can be identified on the bathymetric data. The pattern of distribution of boulders follows a generally arcuate pattern which is widest (roughly 1.5 km wide) from east to west. The deposit appears to be overlaying a glacial sill (Figure 45).

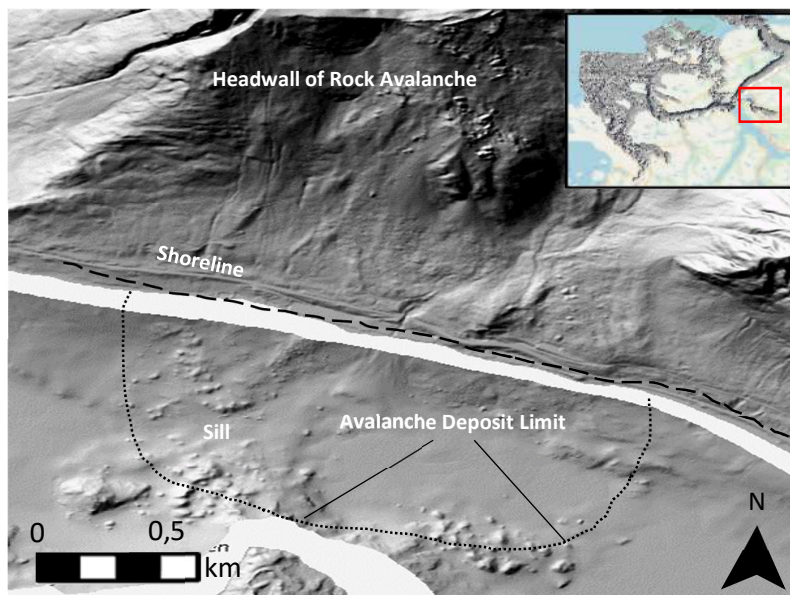


Figure 45. Skorgeua rock avalanche deposit in Ørsta fjord spanning the entire width of the fjord. Terrestrial area (North of shoreline) taken from LiDAR survey <<NDH Volda-Ørsta 2017>>.

On the northern bank of Rovdefjord between the island of Gurskøya and mainland Norway, there exists a conical shaped deposit of coarse-grained sediment, including several distinguishable boulders (Figure 46). The highest point of the conical deposit is approximately 12m above the adjacent area and the deposit is approximately 600m wide at its widest point. The submarine

deposit is clearly associated with a terrestrial mass wasting zone which is visible within the LiDAR dataset <<Vanylven-Sande 2012>>.

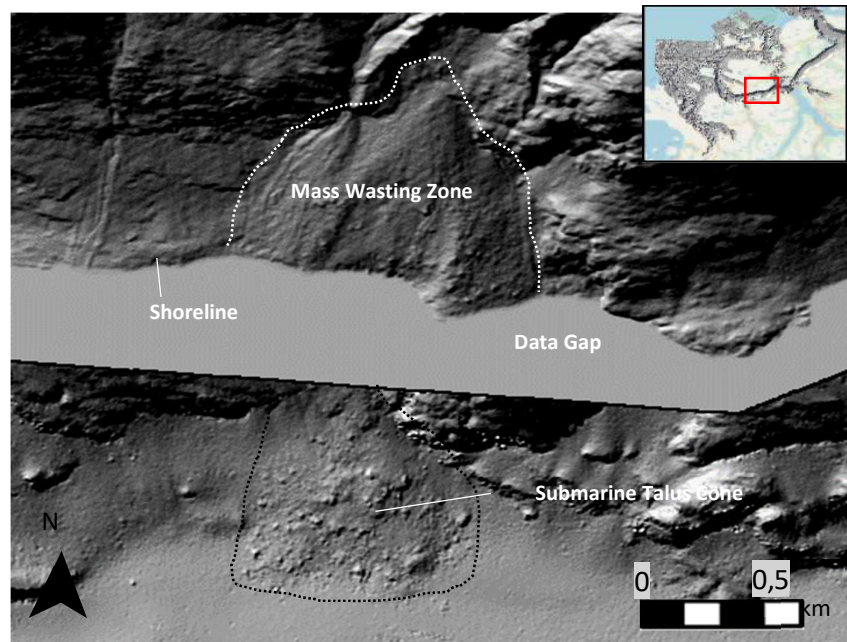


Figure 46. Talus cone deposit formed in Rovdefjord. Material from the fjord wall appears to have been funneled into its current shape by bedrock features on either side of the talus cone.

#### **4.2.6 Rock Avalanches- interpretation**

The boulder deposit found in Ørstafjord (Figure 45) is the result of a rock avalanche (Norwegian: fjellskred) which occurred in Skorgeua roughly 9-8 ka BP (Blikra, 2003). Blocks along the seafloor represent the sub-marine runout of the rock avalanche.

Based on the size, shape, and sediment composition of the deposit in Rovdefjord (Figure 46) it has been interpreted as a talus cone resulting from rock avalanching. When steep faces such as a fjord wall are subjected to weathering and erosional processes, this can result in large blocks of otherwise competent bedrock to become detached. The material becomes scree or talus which can accumulate at the base of the steep face. Over time talus accumulations begin to form a conical shape consisting of fine-grained material at its top and coarse-grained material at its bottom, otherwise known as a talus cone (Murton et al., 2006).

#### **4.2.7 Depressions- description**

Several depressions of slightly varying size and shape can be identified in the study area. These depressions have a headwall which typically occurs in areas of moderate to high relief and the rest of the feature is within a low relief area (Figure 47). Their width can range from 0.1-1km, however the

precise extent of the depression is difficult to measure accurately using available data, as they typically appear only faintly. The majority of each feature is depressed 2-3m below the adjacent seafloor.

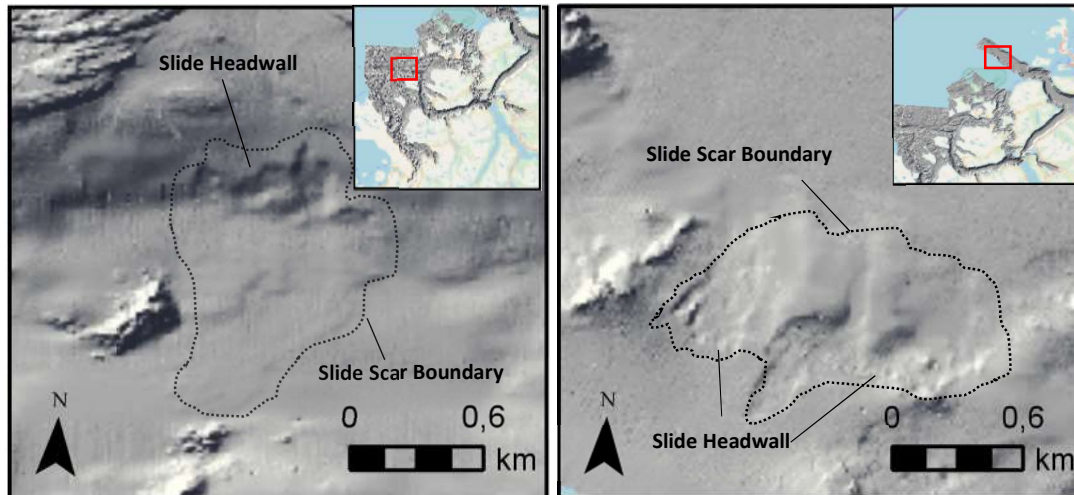


Figure 47. Slide scars are present in numerous locations throughout the study area, both in high relief and low relief environments.

#### **4.2.8 Submarine Slide Scars- interpretation**

Based on the location and shape of these features, they have been identified to be submarine slide scars which reflect mass wasting and sediment reworking processes. Submarine slides occur as downward stresses, most importantly gravity, exceed the shear strength of the slope and material begins to slide downward along a plane of weakness (Hampton et al., 1996). The extent of depositions resulting from landslides is not possible to identify in the bathymetric data because of their faint boundaries, likely due to post-slide sediment reworking.

#### **4.2.9 Lobe-Shaped Deposits- description**

Along the northeastern boundary of Syltefjord, there are two parallel deposits composed of stacked lobes which extend roughly 500m away from the shore and are associated with two gullies in a high relief terrestrial environment (Figure 48). The deposits are raised 2-3m above the adjacent seafloor.

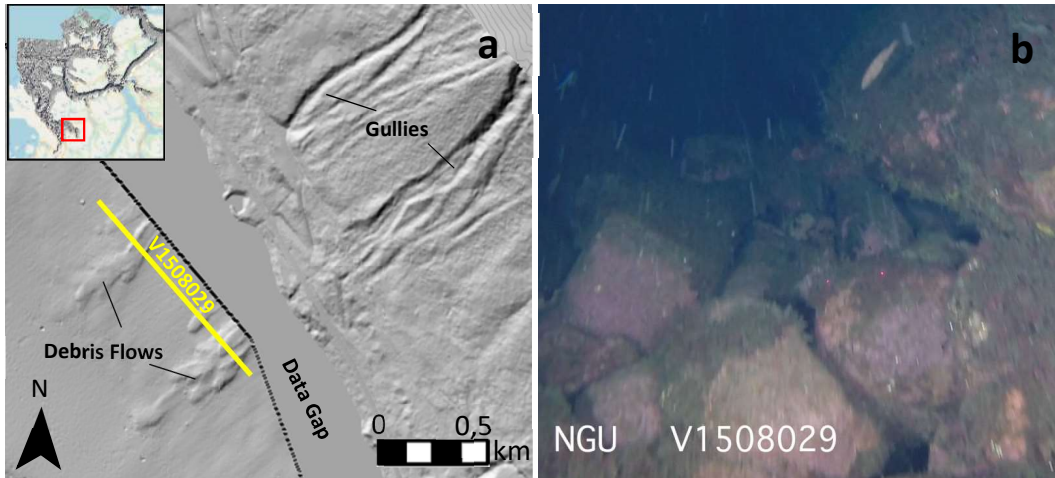


Figure 48ab. 48a Debris flow in Syltefjord. LiDAR data and bathymetric data show two distinct gullies and their associated lobes of a debris flow. 48b. Snapshot of video transect V1508029 (taken at 12:20) shows boulders within the debris flow deposit.

#### **4.2.10 Stacked Debris Flows- interpretation**

The shapes of the deposits and their association with the two gullies points to the occurrence of stacked debris flows which originated on land and flowed down into the fjord on multiple occasions. Debris flows are rather common occurrences in Norway due to the thick deposits of glacial till, colluvium, and weathered bedrock overlaying areas of high topographic relief which are also subjected to erosional forces (Stalsberg et al., 2012). Video V1508029 taken by NGU in 2015 spans both lobes of the debris flow. Coarse-grained debris, mostly boulders, can be seen from 2:33 to 4:55 and again from 11:20 to 12:35 (Figure 48b).

#### **4.2.11 Multiple Circular Depressions within Glacial Trough- description**

Multiple circular depressions (17 in total) exist along the seafloor within the glacial trough of Vartdalsfjorden. Individual depressions are 20-30m in width and 0.5-1m in depth. The zone containing these depressions is roughly 1.5km in length (Figure 49).

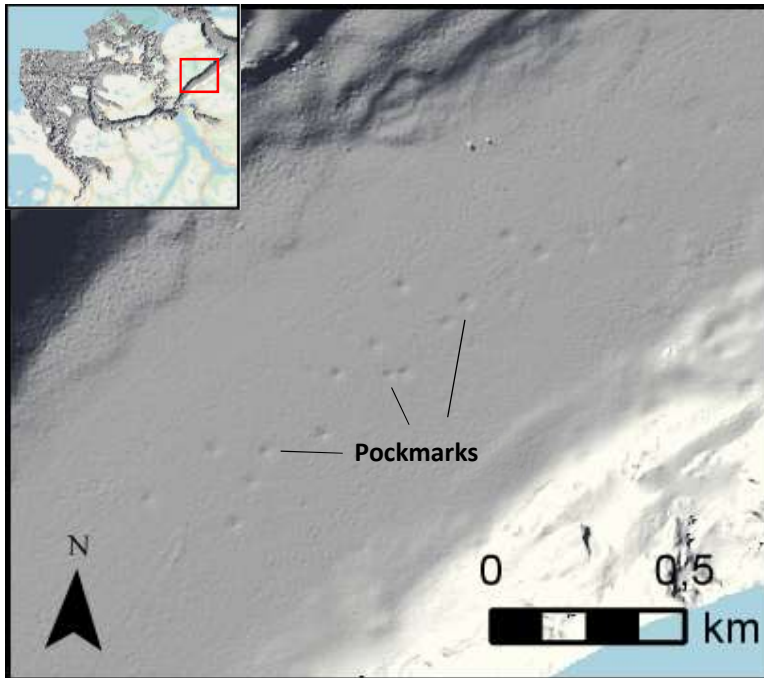


Figure 49. Group of pockmarks found within the glacial trough running along Vartdalsfjorden.

#### **4.2.12 Pockmarks- interpretation**

Due to their dimensions and linear distribution these circular depressions have been interpreted to be pockmarks formed by the seepage of thermogenic gas and porewater migration in sediment underlying the surface (Forwick et al., 2009). Faulting in this location is likely as Vartalsfjorden is perpendicular to the main ice sheet flow direction, resulting in maximum erosion and grinding of bedrock. Faults can act as conduits to allow for the seepage of thermogenic gas. Porewater migration is encouraged by tectonic forces. The preservation of pockmarks implies a generally low level of bottom-current activity in this area. The pockmarks have likely been formed relatively recently as they otherwise would've been smoothed or filled in by suspension settling or water currents (Forwick et al., 2009).

#### **4.2.13 Circular Depression- description**

Within the narrow sound between the islands of Gurskøya and Hareid there exists a symmetrical circular depression that is 170m in diameter and 6m deep at its center. The depression occurs in the middle of a basin which is 50m deeper than the seabed just to north. Prominent moraine ridges appear in succession to the east, west, and north of the depression (Figure 50).



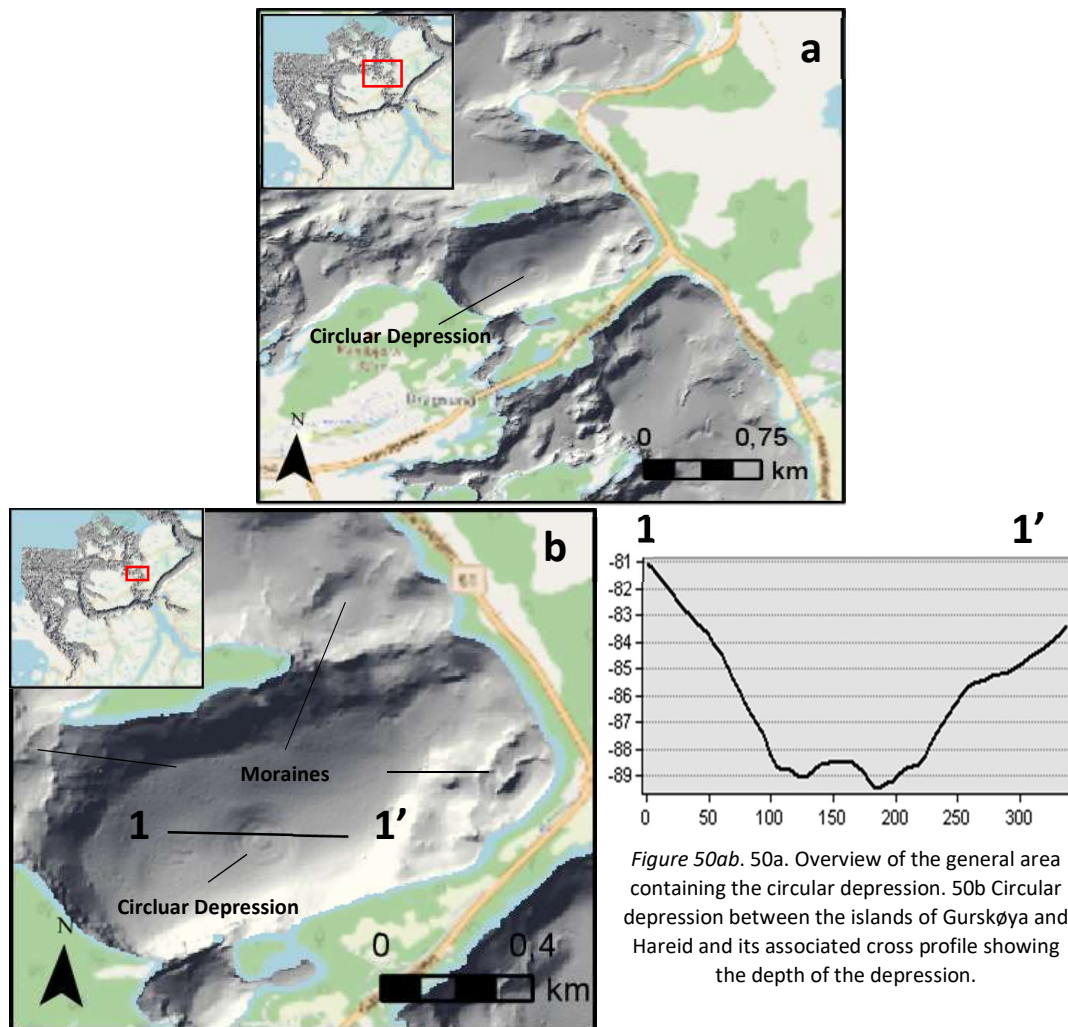


Figure 50ab. 50a. Overview of the general area containing the circular depression. 50b Circular depression between the islands of Gurskøya and Hareid and its associated cross profile showing the depth of the depression.

#### 4.2.14 Unknown- interpretation

It is unclear what process or mechanism led to the creation of this circular depression. It is doubtful that it is simply an artefact of data collection. It could possibly have resulted from an impact of a large object such as a falling boulder, however due to the features central location within the basin it is unlikely for a falling boulder to have reached so far inward. Another potential cause could be the impact of a falling chunk of ice during a calving event, which is again doubtful as the keel of the falling ice would not only create a single circular impact as seen here. The depression could possibly be a kettle hole, which resulted from a block of ice left behind by a retreating glacier which was then buried by sediment and later melted resulting in the depression. This is unlikely as such blocks of ice are not typically deposited in deep basins. The roundness and symmetry suggest the possibility that this is an impact crater from a falling meteorite. The lack of a raised rim surrounding the depression

would be the primary argument against this, however it is a small basin and sediment along the seafloor can easily be disturbed and reworked, potentially erasing the raised rim around the depression.

#### **4.2.15 Feature Description- Smoothed ridges**

At the mouth of Voldsfjorden in the southeast portion of the study area there is a collection of large smoothed ridges (Figure 51). Each ridge is between 4-5m in height, 80-100m in width, and roughly 0.5km in length. The four distinguishable ridges undulate with the same orientation and frequency. Areas of almost vertical bedrock are found on either side of the ridges.

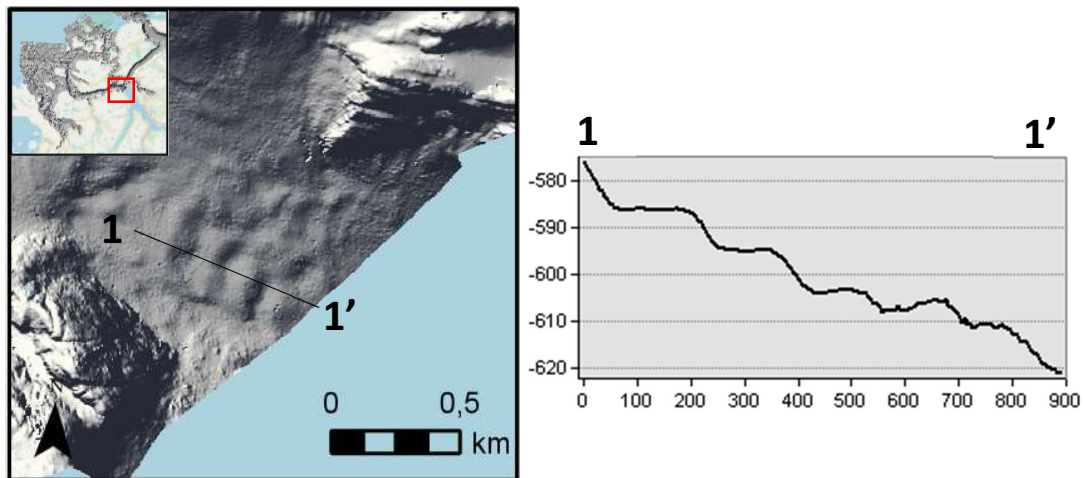


Figure 51. Large-scale smoothed ridge features found at the mouth of Voldsfjorden.

#### **4.2.16 Feature Interpretation- Unknown**

These features occur in the deepest portion of the study area (between 580m and 620m deep). They potentially represent morainic material which has been smoothed out as a result of soft sediment draping or bottom currents. Another potential explanation for the feature is that seabed currents at the mouth of Voldsfjorden have caused the lateral migration of seafloor sediment, creating what are known as sediment waves (Howe et al., 1994). The feature is also similar to thrust moraines formed by re-advancing glaciers as described by Forwick & Vorren (2010). Forwick & Vorren (2010) utilized seismic data to support their identification of thrust moraines, however seismic data is not currently available for this portion of Voldsfjorden.

# 5 Discussion

## 5.1 Glacial Trough Network

Landforms and deposits present in Søre Sunnmøre suggest that glaciers interacted through a complex network of tributaries and troughs during the late Weichselian glaciation. Glaciers originated as plateau and cirque glaciers which flowed through fjords and sounds influenced by structural elements of Caledonian age (Young, 2017). Glacial troughs intersect at a wide range of angles, for example those between Gurskøya and Sandsøya which intersect at a right angle (Figure 52) implying perpendicular ice flows.

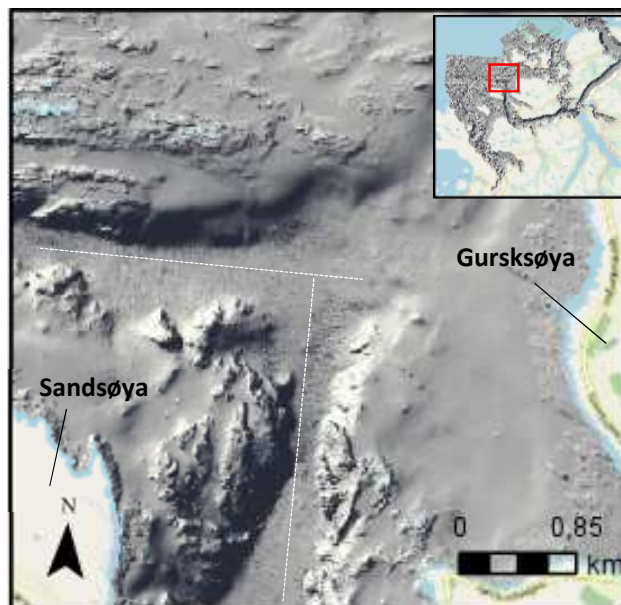


Figure 52. Glacial troughs intersecting at a right angle between Gurskøya and Sandsøya. Trough axes marked with dotted white line.

Many portions of the strandflat exhibit minimal topographic relief and little to no bedrock along the surface of the seafloor. In areas like this, ice was allowed to spread freely. Glacial lineations suggest fast flowing, grounded ice flows associated with the growth and decay cycles of the Fennoscandian Ice Sheet.

## 5.2 Extent of Glaciation and Topographic Constraints

A conceptual model for dividing different phases of glacial movement was presented by Landvik et al. (2014) based on empirical evidence from modern glaciers on Svalbard. Fluctuations between these

phases can occur frequently throughout glacial periods. The three phases, or flow styles, are as follows:

1. Maximum flow style- The ice sheet covers a large areal extent and has sufficient thickness (kilometers scale) and volume to flow completely independently of underlying topography. Ice flow reaches the continental shelf and will deposit large terminal moraines far beyond the coastal limit.
2. Transitional flow style- The ice sheet is no longer thick enough to flow independently of underlying topography and begins to conform to underlying structural elements. Ice flow is mostly limited to fjords and sounds and does not reach the continental shelf.
3. Local flow style- Movement of glaciers is completely controlled by local variations in topography. Relatively little ice is transported and ice flow is mostly limited to terrestrial environments and inner fjords. Local stage extent is often the most recent mode of glacial movement before final deglaciation, therefore landforms created by local flow style are often those which are best preserved.

Unconstrained ice sheet flow during maximum flow style and topographically constrained ice flows during transitional and local phases in coastal Søre Sunnmøre are made apparent by various landforms. Indicators of maximum flow style include features such as glacial lineations, crag-and-tail structures, and smoothed bedrocks zones, all of which are orientated obliquely to nearby glacial troughs and structural elements. Topographically constrained ice flows are evidenced by features such as glacial troughs and moraines bounded by the banks of glacial troughs. Interpretations of modes of ice flow based on physical evidence are presented below (Figure 53).

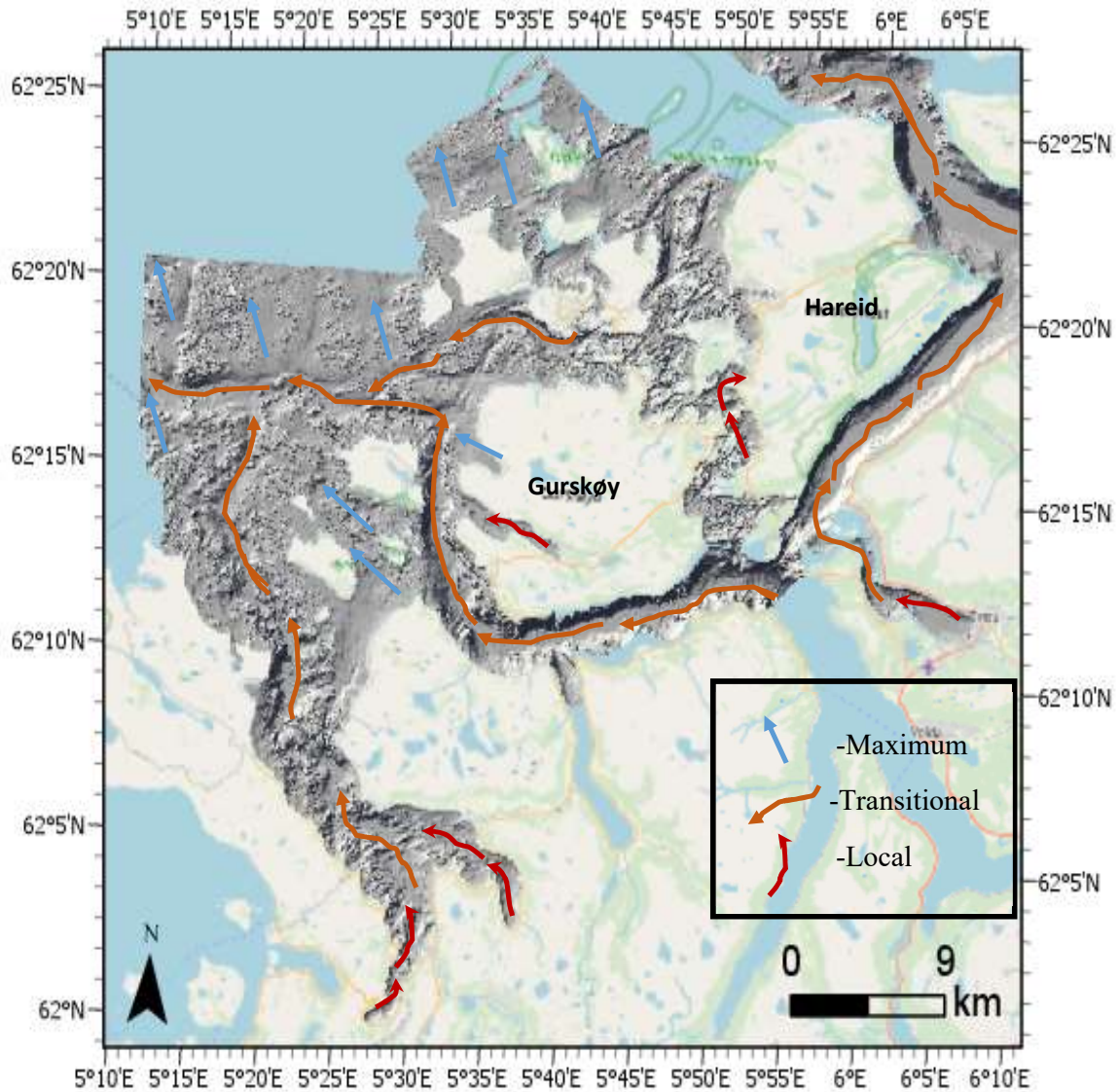


Figure 53. Flow dynamics based on landforms visible within the various datasets. Notice maximum flow style shifts from an ENE-WSW orientation in inland Søre Sunnmøre to a more NE-SW orientation in the outer coastal islands.

### 5.2.1 Maximum Flow Style Conditions of the Late Weichselian

The majority of glacial landforms and deposits currently present in Søre Sunnmøre were created by the growth and decay cycles of the Fennoscandian Ice Sheet during the late Weichselian glaciation. The Fennoscandian Ice Sheet is believed to have reached its furthest western extent between 25-24 ka BP, although the ice margin remained well beyond the Norwegian coast until roughly 16 ka BP (Olsen et al., 2013). A low degree of topographic relief in the portions of the study area furthest from the coast allowed for free flowing and spreading of ice in all directions. The presence of glacial lineations implies fast flowing ice conditions (Ottesen, 2006).

Mangerud (2019) reconstructed dynamics of the Fennoscandian Ice Sheet by analyzing glacial striae and ice marginal deltas which revealed that ice sheets were able to cross over several-hundred meter deep fjords without altering their course. Evidence of this maximum flow-style regime of glacial locomotion can be found in Søre Sunnmøre in areas such as the northwestern portion of the “Batymetri Søre Sunnmøre 2017” (Figure 54). Indicators of maximum flow style include smoothed bedrock, glacial lineations, and crag-and-tail features, all of which show orientations that are inconsistent with other surrounding structural elements.

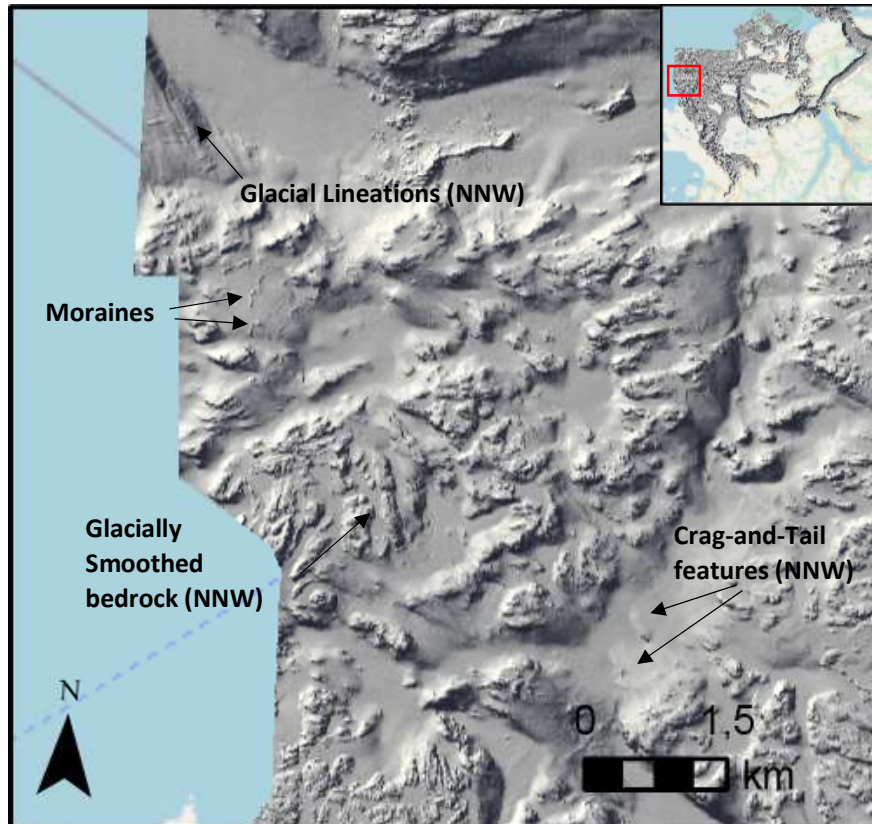


Figure 54. Glacially smoothed bedrock, glacial lineations, and crag-and-tail features serve as evidence of maximum flow style as they are oriented (NNW) obliquely to nearby glacial troughs.

### 5.3 Thermal Regimes

Variations of a glacier’s thermal regime can occur repeatedly over a short periods of time and can even vary from fjord to fjord between glaciers which stem from the same ice sheet. The potential for the frequent changing of thermal regime further convolutes the already complex process of glacial dynamic reconstruction.

For example, logic dictates that the outermost moraines, i.e. those farthest away from the coast, would be the oldest moraines because any sub-sequential ice advance would carry away morainic material deposited during the previous glaciation. However, other scenarios must be considered when determining relative ages of the moraines. If a glacier becomes cold-based, it will likely no longer have sufficient erosional power to carry away morainic material. If either sea level change or ice thickening cause a migration of the glacier's grounding line, new moraines could potentially be deposited beyond existing moraines, meaning the outermost moraine would therefore be younger than moraines closer to the coast (Benn and Evans, 1998; Mangerud and Landvik, 2007).

Deglaciation currently occurring on Svalbard shows that decaying glaciers often transition to cold-based glaciers as ice thickness decreases (Sevestre et al., 2015). If glaciers in Søre Sunnmøre were mostly cold-based at the end of the Weichselian glaciation it would be expected that relatively few moraines were deposited during this time, as depositional processes are typically less active in cold-based glaciers than in warm-based glaciers (Lorrain et al., 1999). If this were the case, it is possible that some moraines were deposited prior to the LGM. Cold-based glaciers during deglaciation could also account for the relatively low number of moraines in the outer portion of the study area when compared with areas further inland. Terminal moraines deposited during maximum glacial conditions are not shown by available datasets, as the ice margin was at or near the Norwegian Channel, beyond dataset boundaries.

## **5.4 Younger Dryas**

Younger Dryas climatic conditions in Søre Sunnmøre allowed for the formation of cirque glaciers in high elevation alpine environments, but such conditions did not last long enough for cirque glaciers to advance to low-lying areas (Mangerud et al., 2010). The high density of cirque moraines in Søre Sunnmøre (Section 2.4.3, Figure 15) indicates that the most recent glaciation was limited to high alpine areas (Mangerud, 1979, 1991; Reite, 1983; Aarseth et al., 1997). A master's thesis recently completed by Krohn-Nydal (2019) of NTNU identified several cirque moraines of Younger Dryas age within Søre Sunnmøre (Figure 55).

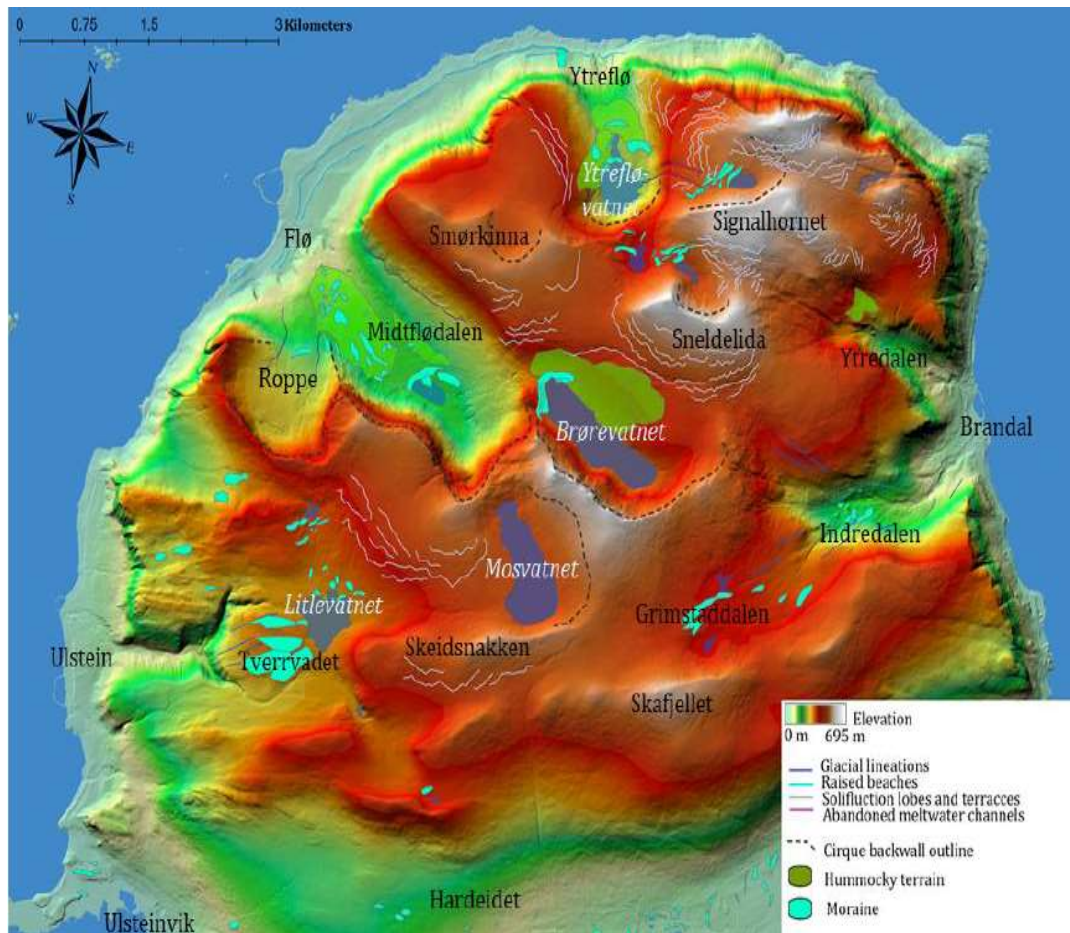


Figure 55. Cirque features including moraines of northern Hareidlandet (From Krohn-Nydal, 2019)

Not all cirques in the study area contain moraines. Therefore, the possibility that some glaciers extended down into valleys and other low-lying coastal areas must be considered. Most groups of submarine moraines, such as the De Geer moraines of Syltefjord (Section 4.1.7, Figure 36) extend for several kilometers beyond the head of the fjord in a continuous fashion. The lateral extent of such moraine fields is likely much further than a potential Younger Dryas re-advance would have allowed. Reite (1983) suggests that cirque moraines could've been deposited following the Younger Dryas, but there is little evidence that suggests a cooling period sufficiently long or cold enough for cirque moraines to have been deposited during the Holocene.

Another factor which could have prevented glaciers from reaching fjord valleys during the Younger Dryas is the overdeepening of fjord basins which prevented later glacial advances from stabilizing or becoming grounded as ice continued to calve into the fjord. This scenario is most likely in fjords adjacent to cirques which were glaciated but do not contain moraines. Evidence from sediment cores taken from wave cut caves revealed cave entrances to be unobstructed during the Younger Dryas (Larsen et al., 1987).



### 5.4.1 Younger Dryas Re-advances in other areas of Southwest Norway

Other portions of the Norwegian coast such as the Bergen area did become fully re-glaciated during the Younger Dryas (Hughes et al., 2016; Mangerud, 1980) (Section 2.4.3, Figure 16). Due to the dissected topography and generally discontinuous alpine areas which were above the ELA in Søre Sunnmøre during the Younger Dryas, there was likely insufficient snow accumulation and insufficient time for glaciers to form and advance down into valleys. However, less dissected topographies in the Bergen area offered less resistance to the advancing ice sheet compared to Søre Sunnmøre.

Mangerud (1980) highlights this difference in the modes of the Younger Dryas re-advance between the Bergen area and Nordfjord-Sunnmøre (Figure 56).

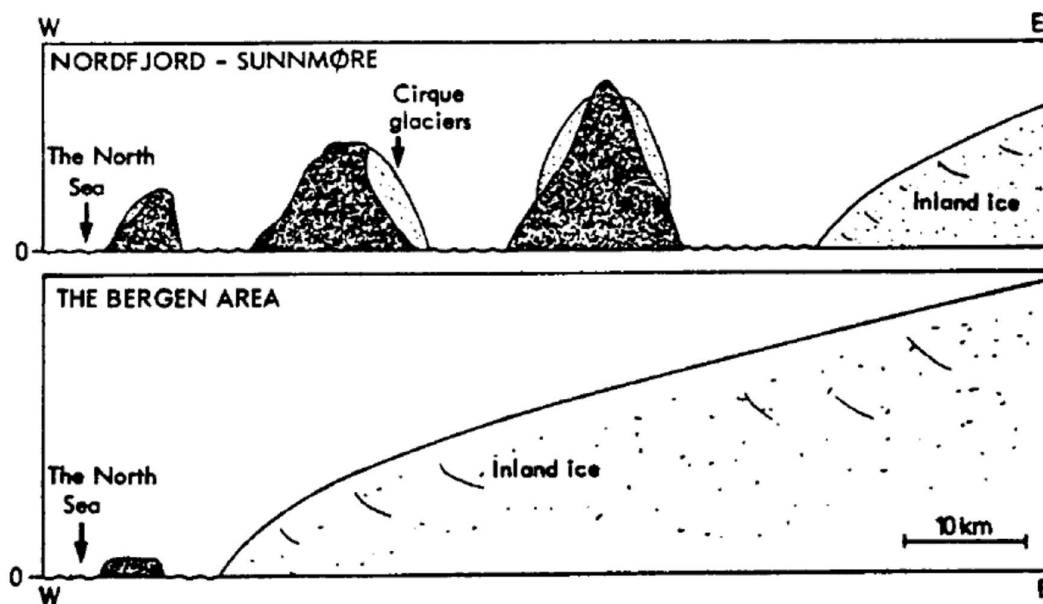


Figure 56. Showing the different modes of re-glaciation experienced in Nordfjord-Sunnmøre compared with the more southerly Bergen area during the YD cooling period (From Mangerud, 1980).

## 5.5 Final Deglaciation

### 5.5.1 Deposition of Moraines

Varying orientations of moraines are indicative of a complex history of stepwise deglaciation which included frequent standstills and/or minor re-advances. The rate and mode of retreat during deglaciation can vary due to factors such as fjord geometry and topographic relief which affect the characteristics of the resulting moraine (Mangerud et al., 2019). Areas which have potential pinning points such as sills or elevated bedrock knolls can allow the glacier to periodically stabilize, thus impeding deglaciation. Moraines found in relatively flat areas with no pinning points, particularly on the continental shelf, show a relatively symmetric arcuate form. Moraines in areas adjacent to or

among bedrock knolls tend to exhibit more irregular, discontinuous, and asymmetrical shapes (Figure 57).

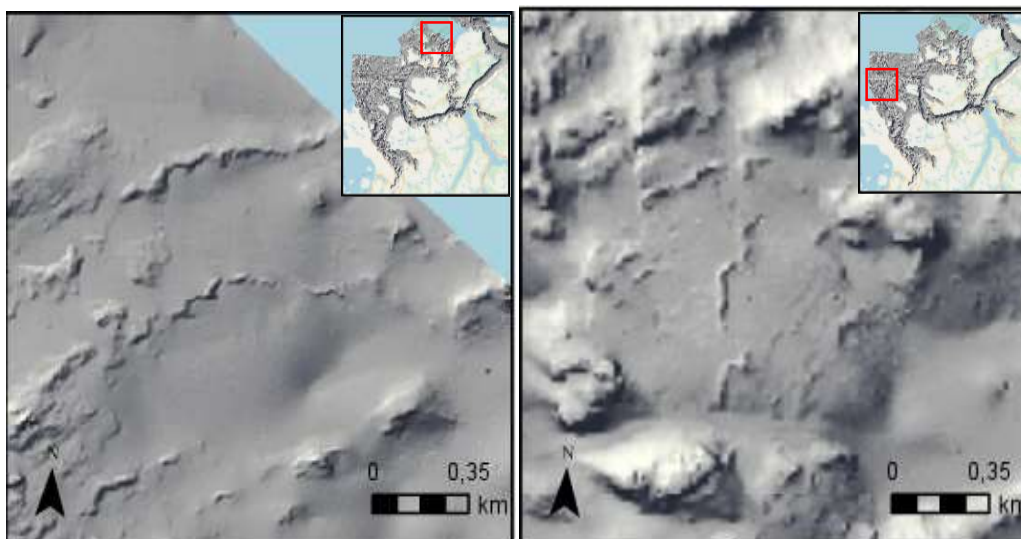


*Figure 57.* The image on the left shows an example of moraines found in a relatively flat lying portion of the study area on the continental shelf. Moraines here are more parallel and arcuate than moraines shown in the image on the right, which shows non-parallel, non-arcuate moraines among a cluster of bedrock knolls.

### **5.5.2 Implications of De Geer Moraines**

Final deglaciation resulted in the deposition of recessional moraines which are oriented parallel to one another with approximately equal lateral spacing between them, otherwise known as De Geer moraines (Section 4.1.7, Figure 36). De Geer moraines indicate a successional pattern of ice retreat, likely related to annual weather cycles (Larsen et al., 1991). In the Søre Sunnmøre area, De Geer moraines are primarily found in tributary fjords off shooting from the main fjords. They occur far beyond the margin of any potential Younger Dryas re-advance, thus they are likely associated with retreat at the end of the last glacial (Surovell et al., 2009).

The presence of De Geer moraines indicates that deglaciation occurred in a consistent stepwise fashion. Individual ridges in a succession of De Geer moraines often form during the winter season as minor re-advances in the ice sheet margin form push moraines (Larsen et al., 1991). However, individual ridges can also be formed as sediment is transported to the ice margin during temporary standstills of grounding line retreat which can occur in either the winter or summer season. This implies that the formation of De Geer moraines is not necessarily dictated solely by annual weather cycles (Linden & Møller, 2005). In Syltefjord, De Geer moraines exhibit both large “principal”

moraines and smaller “intermediate” moraines. It is possible that principal moraines were formed annually as push moraines during the winter months, and that intermediate ridges between them occurred during periodic standstills in grounding line migration. Not all principal moraines contain intermediate ridges between them, implying the possibility that grounding line standstills did not occur every year.

### **5.5.3 Rate of Retreat**

Retreat of the Fennoscandian Ice Sheet occurred at variable rates throughout Søre Sunnmøre. “Pinning points” such as sills or large bedrock knolls could have allowed the glacier to temporarily stabilize, thus resulting in temporary standstills which slowed the rate of retreat (Favier et al., 2016).

Deglaciation likely occurred most rapidly within glacial troughs. As sea level rises, glaciers will attempt to adjust by raising the ELA until stability is achieved. Raising of the ELA combined with the lack of addition of new ice being added to the glacier front will result in rapid retreat as the glacier continues to seek stability (Dowdeswell et al., 2008). The depth of glacial troughs makes them more susceptible to sea level rise-induced glacial retreat compared to shallower marine areas.

Additionally, a lack of pinning points in the low relief strandflat meant that the glacier retreated unhindered as it could not temporarily stabilize on a pinning point.

Principal moraines in the De Geer moraine field of Syltefjord have an average distance of 220m between each ridge, suggesting a net retreat of 220m/year during the deglaciation of Syltefjord (Section 4.1.7, Figure 36a). By contrast, ridges in the De Geer field along the coast of western Gurskøya have a smaller average spacing between them of 180m, suggesting a retreat rate of 180m/year (Section 4.1.7, Figure 36c). The location of Gurskøya in relation to the further inland Syltefjord implies that deglaciation accelerated as the ice sheet moved inland. However, this acceleration in retreat rate could also be explained by the discrepancy in depth between the two fjords, as retreat tends to be faster in deeper fjords (Mangerud et al., 2019). Depths of Syltefjord in the De Geer field are between 70-90m while the depths of the unnamed fjord on Gurskøy are between 40-60m. The likely late Weichselian age of these De Geer moraines suggests that they have been subjected to at least 15 ka years of reworking due to bottom currents. This is likely the cause of the smoothed profile of the De Geer moraine ridges, particularly the De Geer moraines found near Gurskøya.

Another process which may have catalyzed retreat of the ice sheet, particularly on the strandflat and continental shelf beyond the coastal islands, is the influx of warmer water coming from the Atlantic

Ocean heated by the Gulf Stream. Historically this has been a common influencing factor on the rate of ice retreat in both Norway and Svalbard (Hanssen-Bauer et al., 2019). Warmer Atlantic waters could have reached under the ice sheet causing accelerated melting and calving of the retreating glacier. However, Atlantic waters would not as easily have reached the inner portions of coastal Søre Sunnmøre as the topography became more complex and bedrock knolls and sills prevented the mixing of Atlantic Ocean water with cooler fresher water of the inner fjords.

#### ***5.5.4 Timing of Deglaciation***

Existing literature pertaining to the timing of final deglaciation in Søre Sunnmøre is not entirely in agreement. Earlier research suggests that the Norwegian Channel became ice free at roughly 15 ka BP but that coastal Søre Sunnmøre was not ice free until sometime between 14-12.6 ka BP (Mangerud, 1977; Andersen, 1979; Anundsen, 1985; Andersen et al., 1987; Paus, 1990). More recent research, such as the analyzation of pollen within sediment cores or carbon dating of plant fragments (Hughes et al., 2016) suggests that low-lying coastal areas in Søre Sunnmøre were mostly ice free by 15 ka BP and completely ice free by 14.5 ka BP.

Additionally, there is currently no existing literature which discusses the timing discrepancy between the deglaciation of low-lying areas and the deglaciation of high elevations alpine areas. Depending on the rate of retreat of the Fennoscandian Ice Sheet, low-lying areas in Søre Sunnmøre could have become ice free as early as 16 ka BP (Hughes et al., 2016). Assuming the Younger Dryas (12.9-11.7 ka BP) resulted in the re-glaciation of high elevation areas, it is possible that complete deglaciation of Søre Sunnmøre including alpine areas could have been a very lengthy process spanning up to 6 ka since the ice sheet margin first reached the coast following the LGM until the last cirque glacier melted following the Younger Dryas.

Using the updated DATED-1 database (Hughes et al., 2016), final deglaciation of Søre Sunnmøre has been dated between 15-14.5 ka BP (Figure 58). The extent of the ice sheet at 16 ka BP (green polygon) was much greater near Søre Sunnmøre and other areas to the north than it was in more southern areas. This is likely due to the divergence of the Norwegian Channel away from the coast, which means there is a wider continental shelf to accommodate the ice sheet in Søre Sunnmøre and further north.

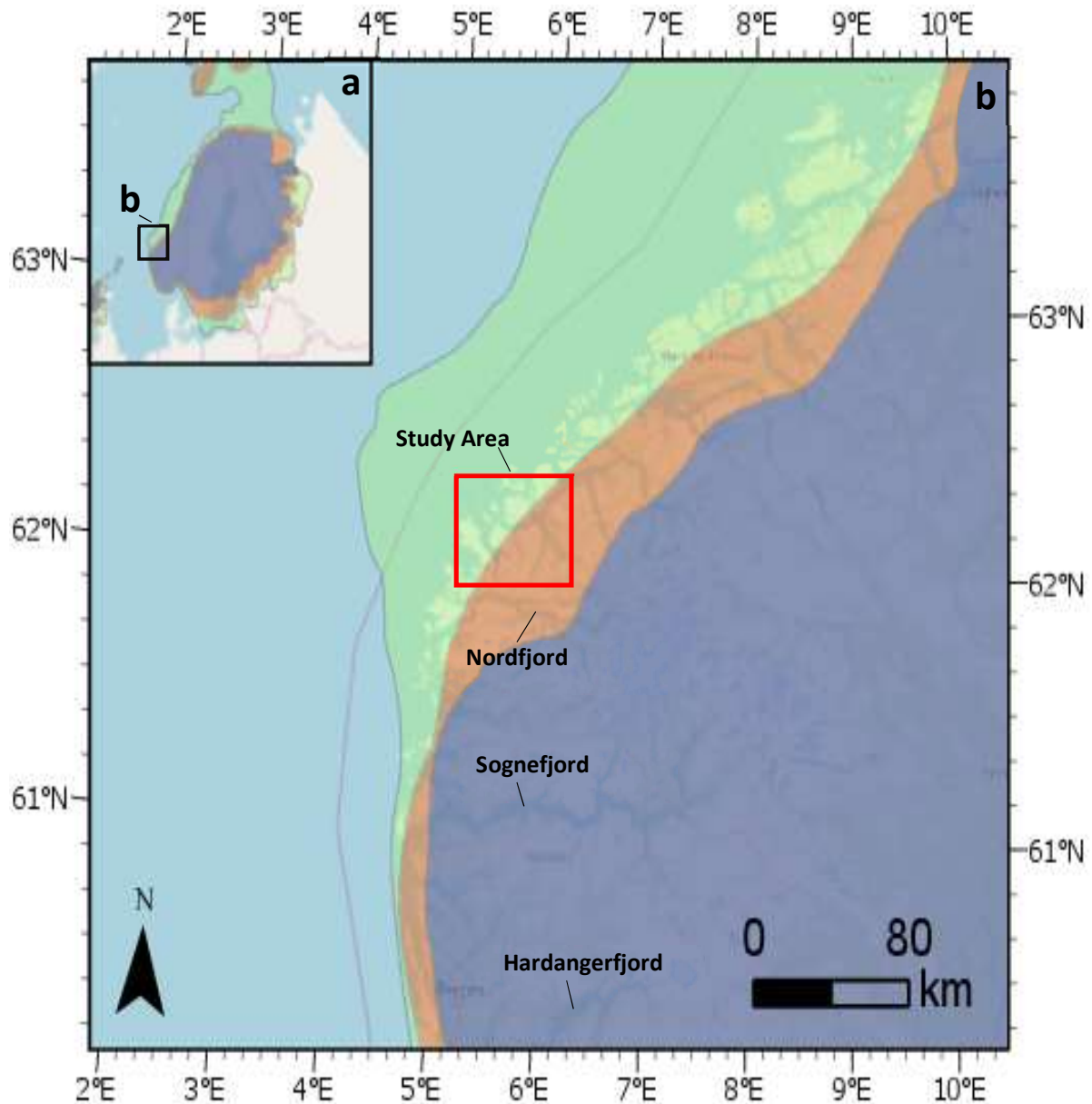


Figure 58ab. Ice margin reconstructions taken at 16 ka BP (green), 15 ka BP (orange), and 14 ka BP (blue). Complete coverage shown in top left. Notice the greater extent of the ice sheet at 16 ka BP near the study area (red box) but earlier deglaciation than south of the study area (Polygons from DATED-1; Hughes et al., 2016).

### 5.5.6 Deglaciation Comparison with other Regions of Southwestern Norway

An in-depth analysis of the deglaciation of the Fennoscandian Ice Sheet in the late Weichselian was conducted by Mangerud et al. (2019) between Hardangerfjord and Sognefjord, which lie approximate 150km and 100km respectively south of Søre Sunnmøre (Figure 58). The authors used thousands of field measurements of glacial striae and a high-resolution LiDar Digital Elevation Model (DEM) in order to constrain the rate and timing of deglaciation. As the ice sheet retreated the

heterogeneous and complex fjord topography, combined with fast ice-margin retreat, caused the ice sheet to dissect and become isolated on separate islands and peninsulas. Once a body of ice becomes isolated, it will melt much faster than if it were still connected to a larger ice sheet, thus accelerating the process of deglaciation (Mangerud et al., 2019). Fjord topographies and geometries exhibit a similar complexity in Søre Sunnmøre than they do in Hardangerfjord and Sognefjord. It is therefore likely that this led to the isolation of ice bodies in Søre Sunnmøre. Cooling during the Younger Dryas did result in the complete re-glaciation of both Hardangerfjord and Sognefjord (Section 2.4.3, Figure 16). Therefore, final deglaciation occurred 11.6 ka BP in those areas compared to the earlier deglaciation of (15-14.5 ka BP) Søre Sunnmøre's fjords and other low-lying areas.

Mangerud et al. (2019) suggests that deep fjords (400-500m deep at their midpoint) experienced an average retreat rate of 160m/year, while the deepest fjords in the area (>600m deep) experienced ice retreat as fast as 240-340m/year. Ice retreated slower in shallow fjords (200-300m deep) with typical rates of retreat falling between 60-80m/year. Depths of fjords in Søre Sunnmøre are on average deeper than those examined by Mangerud et al. (2019), suggesting a more rapid deglaciation in Søre Sunnmøre.

Another factor potentially contributing to an earlier and faster deglaciation of Søre Sunnmøre compared with more southern areas is the geographical distribution of precipitation. It has been suggested by Reite (1983) that Søre Sunnmøre's intermittent alpine areas meant that there is less surface area above the snowline, thus limiting the accumulation of snow. This means that less glacial ice was formed in Søre Sunnmøre compared to more continuous mountains ranges further to the south.

## **5.6 Formation and Preservation Potential of Landforms**

Landforms have been formed and erased throughout geologic time. When identifying landforms, whether terrestrial or submarine, it is important to consider both formation potential and preservation potential. When interpreting bathymetric or LiDAR data, it is important to keep in mind that the data is only a snapshot of how landforms appeared at the moment the data was collected.

One of the most important controlling factors pertaining to the formation potential of landform is the availability of sediment, as well as the sediment type. Sediment supply and its deformability (how easily the sediment can be molded into a landform) are both critical elements determining a landform's formation potential (Brynjolfsson et al., 2014).

Once a landform is created, its vulnerability to erosion, sediment reworking, and burial are all critical factors in determining whether or not the landform will survive, otherwise stated its preservation potential (Ewertowski, 2016). Submarine landforms are subjected to water currents and other erosional agents, however landforms in submarine environments generally have a higher preservation potential than landforms in terrestrial environments (Dowdeswell et al., 2016).

In Søre Sunnmøre moraines appear to be better preserved when surrounded by areas of raised bedrock which shield them from bottom currents. Moraines which are found in flatter areas or within glacial troughs generally appear more subtly and more rounded in their cross-sectional profiles. Additionally, glaciers reached the continental shelf with less frequency than they have reached areas further inland. Consequently, landforms beyond the coast will have a higher preservation potential than landforms further inland as they are less likely to be erased by moving ice (Elverhøi et al., 1995).

## 5.7 Ages of Landforms

In order to obtain absolute ages for submarine glacial landforms it would be necessary to directly date organic matter taken from sediment samples of the landforms themselves. Absolute ages have been established by recent research in areas to the north and south of Søre Sunnmøre such as those provided by Mangerud et al.'s (2019) study of the Bergen area. However, these areas are too far away from Søre Sunnmøre for direct extrapolation.

Given the datasets used in this thesis, relative ages based on cross-cutting and sub/super-positional relationships (Figure 59) are of greater relevance. However, an attempt to provide absolute ages can be made using ice margin reconstructions (Hughes et al., 2016), as well as recent dating efforts from areas between Nordfjord to the south and the city of Ålesund to the north (Koren et al., 2008; Mangerud et al., 2010; Mangerud and Bondevik et al., 2006). Proposed absolute ages for submarine glacial landforms in the study area and the stage of glaciation in which they were most likely formed are provided below as Table 3. Minimum ages for landforms assumed to have been formed during maximum glacial conditions is 16 ka BP, as this is the latest time possible when ice could have covered low-lying coastal regions of Søre Sunnmøre (Hughes et al., 2016).

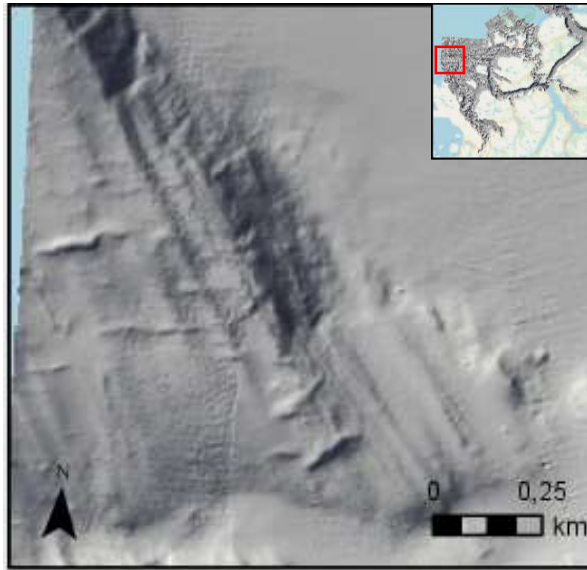


Figure 59. Relative ages can be determined for many landforms in the study area such as by the suprapositional relationship of these moraines and the underlying glacial lineations. Glacial lineations were formed during a late Weichselian advance of the Fennoscandian Ice Sheet. The superimposed moraines were deposited later as the ice sheet retreated.

Table 3. Suggested absolute ages of submarine glacial landforms in Søre Sunnmøre and their corresponding stages of glaciation. <sup>14</sup>C dates are taken from samples used in the DATED-1 database (Hughes et al., 2016).

Glacial Landform	Location	Proposed Absolute Age	Stage of Glaciation
Glacial lineations	Northwestern edge of dataset (Figure 34)	28-26 ka BP	Ice sheet advance
Crag-and-tail features	Concentrated along western boundary of bathymetric data, West of Kvamsøya (Figure 38)	28-26 ka BP	Ice sheet advance
Outermost moraines	Outer-edge of bathymetric data, directly West of Skorpa (Figure 34b)	20-16 ka BP	Ice sheet retreat near end of the last glacial
Sills	Near the heads of Vanylvsfjord, Syltefjord, and Ørstafjord (Figure 33)	16-15 ka BP	Ice sheet retreat near end of the last glacial
De Geer moraines	Syltefjord and unnamed fjord on Gusrkøy (Figure 36)	15-14.5 ka BP	Ice sheet retreat near end of the last glacial
Smoothed moraine ridges	At the mouth of Voldsfjorden (Figure 51)	16 ka BP-present	Ice sheet retreat near end of the last glacial followed by sediment reworking



## 5.8 Postglacial Sedimentation Processes

Evidence of sedimentation processes that have been occurring since final deglaciation and throughout the Holocene can be identified using available datasets. As is true with most fjord and coastal areas of Norway, the majority (>90%) of sediment comprising fjord infill was deposited during deglaciation, while relatively little (<10%) was deposited once the ice sheet had fully retreated (Aarseth, 1997).

As confirmed by the Seabed Sediments of Søre Sunnmøre map (Elvenes et al., 2019), deglaciation processes in Søre Sunnmøre acted as an effective sediment sorting agent. Sorting resulted in the deposition of fine-grained silts and clays within glacial troughs and the deposition of coarse-grained sands and gravels near fjord heads and high relief bedrock zones (Aarseth, 1997).

### 5.8.1 Fjord Infill

Suspension settling has resulted in the infilling of fjord valleys and burial of glacial landforms. Seismic profiling and gravity cores were collected from Nordfjord (Lyså et al., 2010), which lies only 20 km south of the study area (Figure 60). Data revealed important information regarding postglacial sedimentary processes and it is reasonable to conclude that similar processes have occurred in Søre Sunnmøre.

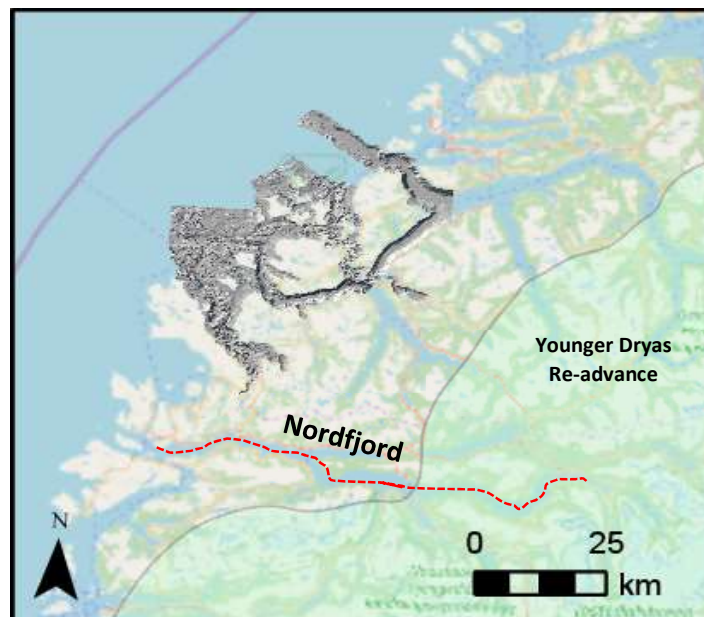


Figure 60. Figure showing the location of Nordfjord (the main fjord is marked here with a dotted red line) and its proximity to the primary study area (bathymetric data). The maximum possible extent of the Younger Dryas ice margin (12 ka BP) is shown by the light green polygon (Hughes et al., 2016). Notice that the head of Nordfjord is much further inland than fjords in Søre Sunnmøre which are more proximal to the outer edge of the coast.

The majority of infill sediment was deposited during and immediately after the last deglaciation (Aarseth, 1997). Fjord infill in Nordfjord is as much as 360m thick in its thickest portion (Lyså et al, 2010). Sediment has been primarily deposited in overdeepened sediment basins near the head of Nordfjord. Lyså et al (2010) determined that coastal erosion processes, such as wave action which carries sediment out onto the continental shelf, cause the thickness of sediment infill to decrease as fjords approach the coast. The head of Nordfjord is located approximately 25km further inland than the heads of Vanylvenfjord, Syltefjord, and Ørstafjord in Søre Sunnmøre. Due to coastal Søre Sunnmøre's greater exposure to coastal erosion processes, it follows that the thickness of fjord infill in the study area should be considerably less than 360m. As seismic data suggests (Section 4.1.2, Figure 31) fjord infill beyond the coast is approximately 15m thick in glacial troughs beyond the coastal limit of Søre Sunnmøre and is mostly likely thicker in more inland areas. Ice margin reconstructions (Hughes et al., 2016) show the Younger Dryas re-advance completely covering the easternmost portions of Nordfjord (Figure 60), thus implying a different narrative of deglaciation and postglacial sedimentation than has occurred in coastal Søre Sunnmøre.

Corner (2006) performed an in-depth analysis of mechanisms active during fjord-valley infilling processes. Deposition, emergence, incision, and terracing are processes that have been constantly occurring both during and following the last deglaciation (Figure 61). The main controls of fjord-valley infill systems are sediment supply during glacial retreat and directly following glacial retreat.

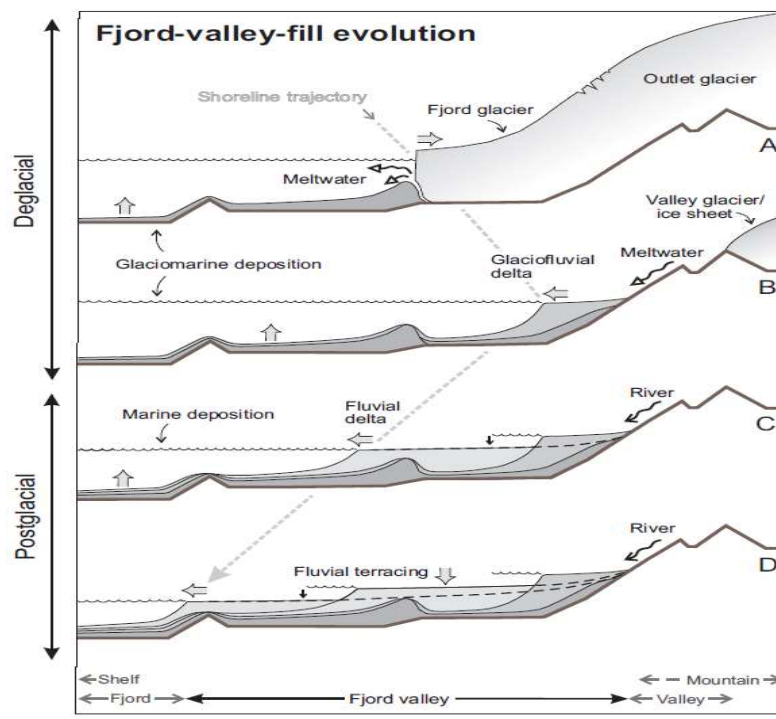


Figure 61. Norwegian fjord-valley fill processes which are applicable to Søre Sunnmøre. Processes are divided into two stages, deglacial and postglacial (From Corner, 2006).

Other important controls include the depth of fjord basins and sea-level variations driven by glacio-isostatic rebound (Corner, 2006).

Modern sediment supply comes primarily from fluvial systems and suspension settling. However, the amount of sediment supplied by fluvial systems is quite small when compared to the amount of sediment deposited during and immediately after the last deglaciation (Aarseth, 1997).

## 5.9 Bottom Currents

Many glacial landforms have been smoothed, rounded, and obscured. This is partly due to bottom currents active along the seafloor reworking glacially deposited sediment. Velocities and directions of bottom currents are subject to frequent change (Elvenes et al., 2019). This makes it difficult to determine the prevailing current flow strengths and directions based on landform characteristics which are apparent in the available datasets. Zones of coarse-grained sediment on the seafloor have likely resulted from winnowing away of fine-grained sediments (Vorren, 1978).

The ripple scour depression (RSD) identified on the strandflat (Figure 44) can be an important indicator for characteristics of bottom current and sediment types present in the area. As suggested by Murray and Thielert (2004), RSDs are the result of complex interactions between waves, bottom and tidal currents, and poorly sorted bed material. Such features typically occur in moderately high-energy environments, outside of the surf zone and beyond the coastal limit. Currents associated with the formation of RSDs have an average velocity of 0.6 m/s (Bellec et al., 2010). Bed material consists of sediments ranging from poorly sorted winnowed glacial deposits (gravelly sand to boulders) to postglacial fine-grained muddy sediment. This sharp contrast in grain size is thought to be integral to the formation of RSDs. The lack of fine-grained sediment within the depression itself is indicative that formation of the RSD is still an active process (Bellec et al., 2010).

## 5.10 Postglacial Mass Wasting

Forwick and Vorren (2011), and references therein, highlight potential trigger mechanisms for slope failures in glaciated environments which include; "(1) seismic activity due to postglacial isostatic rebound; (2) rapid progradation and deposition and/or increased sediment supply; (3) cyclic loading induced by surface waves and/or low tides; (4) increased pore pressure as consequence of relative sea-level fall and/or presence of gas".

Evidence of slope failures exists throughout Søre Sunnmøre such as rock avalanche deposits identified in Ørstafjord (Figure 45) and Rovdefjord (Figure 46). Submarine mass wasting events were likely most frequent immediately following deglaciation when glacio-isostatic rebound was most rapid (Lyså et al., 2010). Slide activity has continued to occur, but gradually decreased as conditions began to alternate with more stable marine conditions.

Numerous unstable rock slopes have been identified throughout Søre Sunnmøre, implying potential slope failures in the future (Oppikofer et al., 2014). The high degree of visibility of terrestrial gullies and submarine stacked debris flows identified in Syltefjord (Figure 48) imply that mass wasting processes are still active here. Fluvial systems feeding into Vartdalsfjorden (Figure 42) supply new sediment into the submarine environment, increasing the likelihood of slope failure. Pockmarks identified in Vartdalsfjorden (Figure 49) suggest increased pore pressure resulting from relative sea level fall as well as the presence of gas (Forwick and Vorren, 2011).

## **5.11 Further Studies**

In order to produce higher resolution ice margin reconstructions for the Søre Sunnmøre area, absolute ages need to be obtained through direct dating of organic material. All dating of organic material directly in the study area has been conducted in the 1990's, with the exception of work performed by Vorren et al. (2008). Thus the resolution of ice margin reconstructions and understanding of glacial dynamics would benefit greatly from an extensive and updated suite of sampling. Organic material which has been dated is either terrestrial material or originated from a marine environment but was collected in a terrestrial environment, leaving modern marine organic material undated. Additionally, several lakes within isolation and submerged basins remain unsampled.

Collection of video recordings and sediment samples of the large circular depression between the islands of Gurskøya and Hareid (Figure 50) is needed in order to properly describe the feature, which could potentially be the resulting crater of a meteorite impact.

Risk assessment maps for predicting future debris flows, rock avalanches, and other sudden mass wasting events which could potentially impact inhabited areas can be made using available datasets.

## 6 Summary and Conclusions

Multibeam echosounder (MBES) bathymetric data, backscatter data, and other datasets from coastal Søre Sunnmøre were analyzed in order to reconstruct glacial dynamics during the mid to late Weichselian glaciation and to describe sedimentary environments present through the Holocene.

- The majority of glacial landforms and deposits in coastal Søre Sunnmøre were created during the late Weichselian glaciation. Submarine landforms suggest that glaciers interacted through a complex network of tributaries and troughs. Glaciers originated as plateau and cirque glaciers and merged with the Fennoscandian Ice Sheet. Ice flowed through fjords and sounds oriented by structural elements of Caledonian age. Unconstrained ice flow during phases of maximum flow style is evidenced by glacial lineations, crag-and-tail structures, and smoothed bedrocks zones which are orientated obliquely to nearby glacial troughs and structural elements. Topographically constrained ice flow during phases of transitional and local flow style are made apparent by glacial troughs and bounded moraine fields.
- Younger Dryas climatic conditions allowed for the formation of cirque glaciers in high elevation alpine environments, but such conditions did not last long enough for glaciers to advance to low-lying areas. Alpine areas in Søre Sunnmøre are more dissected and less continuous than in other areas of southwestern Norway, resulting in less accumulation of snow above the ELA. Overdeepening of fjord basins prevented later glacial advances from stabilizing or becoming grounded as ice continued to calve into the fjord.
- Varying orientations of moraines are indicative of a complex deglaciation which included frequent standstills and minor readvances. The deposition of De Geer moraines indicates deglaciation occurred in a stepwise fashion. "Pinning points" such as sills or large bedrock knolls allowed retreating glaciers to temporarily stabilize and slowed deglaciation. It is possible that warm-based glaciers transitioned to cold-based glaciers during deglaciation due to decreasing ice thickness. Deglaciation occurred most rapidly within glacial troughs which are most susceptible to sea level rise-induced glacial retreat. Influx of warm water coming from the Atlantic Ocean heated by the Gulf Stream may have catalyzed deglaciation. Bodies of ice became dissected and isolated on islands and peninsulas, causing ice to melt more rapidly. Deglaciation processes acted as an effective sediment sorting agent, resulting in the deposition of fine-grained silts and clays within glacial troughs and coarse-grained sands and

gravels near fjord heads and in high relief bedrock zones (Aarseth, 1997; Elvenes et al., 2019). Final deglaciation of low-lying areas in coastal Søre Sunnmøre was complete between 15-14.5 ka BP (Hughes et al., 2016). High elevation alpine areas became ice free following the Younger Dryas at approximately 11.7 ka BP (Mangerud et al., 2010).

- Glacial landforms have been smoothed, rounded, and obscured due to bottom currents active along the seafloor reworking glacially deposited sediment. A ripple scour depression indicates complex interactions between waves, bottom and tidal currents, and poorly sorted bed material. Modern sediment supply from fluvial systems and mass wasting processes is much less than the amount of sediment which was deposited during and immediately after final deglaciation. Evidence of slope failures are indicated by rock avalanche deposits and submarine slide scars. Mass wasting events were most frequent immediately following deglaciation when glacio-isostatic rebound was most rapid. Unstable rock slopes have been identified implying potential slope failures in the future.

## References

- Aarseth, I., Austbø, P.K., Risnes, H. "Seismic Stratigraphy of Younger Dryas Ice-Marginal Deposits in Western Norwegian Fjords." *Norsk Geologisk Tidsskrift*, vol. 77, 1997, pp. 65–85.
- Aarseth, I. "Western Norwegian Fjord Sediments: Age, Volume, Stratigraphy, and Role as Temporary Depository during Glacial Cycles." *Marine Geology*, vol. 143, no. 1-4, 1997, pp. 39–53., doi:10.1016/s0025-3227(97)00089-3.
- Aksnes, D.L., Aure, J., Johansen, P.O., Johnsen, G.H., Salvanes, A.G.V. "Multi-Decadal Warming of Atlantic Water and Associated Decline of Dissolved Oxygen in a Deep Fjord." *Estuarine, Coastal and Shelf Science*, vol. 228, 2019, p. 106392., doi:10.1016/j.ecss.2019.106392.
- Andersen, B.G. "The Deglaciation of Norway 15,000-10,000 B.P." *Boreas*, vol. 8, no. 2, 1987, pp. 79–87.
- Andersen, B.G. "The Deglaciation of Norway after 10,000 B.P." *Boreas*, vol. 9, no. 4, 1979, pp. 211–216., doi:10.1111/j.1502-3885.1980.tb00697.x.
- Anundsen, K. "Changes in Shore-Level and Ice-Front Position in Late Weichselian and Holocene, Southern Norway." *Norsk Geologisk Tidsskrift*, vol. 39, 1985, pp. 205–225.
- Augustinus, P.C. "Rock Mass Strength and the Stability of Some Glacial Valley Slopes." *International Journal of Rock Mechanics and Mining Sciences & Geomechanics Abstracts*, vol. 33, no. 1, 1996, doi:10.1016/0148-9062(96)87568-1.
- Ballantyne, C.K. "A General Model of Paraglacial Landscape Response." *The Holocene*, vol. 12, no. 3, 2002, pp. 371–376., doi:10.1191/0959683602h1553fa.
- Bellec, V.K., Bøe, R., Rise, L., Slagstad, D., Longva, O., Dolan, M. "Rippled Scour Depressions on Continental Shelf Bank Slopes off Nordland and Troms, Northern Norway." *Continental Shelf Research*, vol. 30, no. 9, 2010, pp. 1056–1069., doi:10.1016/j.csr.2010.02.006.
- Bellec, V.K., Bøe, R., Rise, L., Lepland, A., Thorsnes, T., Bjarnadottir, L.R. "Seabed Sediments (Grain Size) of Nordland VI, Offshore North Norway." *Journal of Maps*, vol. 13, no. 2, 2017, pp. 608–620., doi:10.1080/17445647.2017.1348307.
- Benn, D.I., Evans, D.J.A. "Glaciers and Glaciation ." *Arnold*, 1998, pp. 734–734.
- Benn, D.I., Evans, D.J.A. "Glaciers and Glaciation." *Boreas*, vol. 40, no. 3, 2011, pp. 555–555., doi:10.1111/j.1502-3885.2011.00212.x.
- Bennett, M.R. "The Morphology, Structural Evolution and Significance of Push Moraines." *Earth-Science Reviews*, vol. 53, no. 3-4, 2001, pp. 197–236., doi:10.1016/s0012-8252(00)00039-8.
- Beyer, A. "Seafloor Analysis Based on Multibeam Bathymetry and Backscatter Data = Meeresbodenanalyse Auf Der Basis Von Bathymetrie Und Akustischer Rückstreuung , Berichte Zur Polar- Und Meeresforschung." *Alfred Wegener Institute for Polar and Marine Research*, p. 100., doi:10.2312/BzPM\_0540\_2006.

- Beylich, A.A., Liernmann, S., Laute, K. "Fluvial Transport during Thermally and Pluvially Induced Peak Runoff Events in a Glacier-Fed Mountain Catchment in Western Norway." *Geografiska Annaler: Series A, Physical Geography*, vol. 92, no. 2, 2010, pp. 237–246., doi:10.1111/j.1468-0459.2010.00392.x.
- Bhattacharya, J.P., Giosan, L. "Wave-Influenced Deltas: Geomorphological Implications for Facies Reconstruction." *Sedimentology*, vol. 50, no. 1, 2003, pp. 187–210., doi:10.1046/j.1365-3091.2003.00545.x.
- Bina, C.R. "The Mantle and Core." *Treatise on Geochemistry*, 2003.
- Blikra, L.H. "Rock Avalanches, Gravitational Faulting and Its Potential Palaeoseismic Cause." *Neotectonics in Norway, Annual Technical Report*, 1999.
- Bondevik, S., Svendsen, J.I., Johnsen, G., Mangerud, J., Kaland, P.E. "The Storegga Tsunami along the Norwegian Coast, Its Age and Run Up." *Boreas*, vol. 26, no. 1, 1997, pp. 29–53., doi:10.1111/j.1502-3885.1997.tb00649.x.
- Boulton, G. S. "Push-Moraines and Glacier-Contact Fans in Marine and Terrestrial Environments." *Sedimentology*, vol. 33, no. 5, 1986, pp. 677–698., doi:10.1111/j.1365-3091.1986.tb01969.x.
- Boulton, G. S. "The Origin of Glacially Fluted Surfaces-Observations and Theory." *Journal of Glaciology*, vol. 17, no. 76, 1976, pp. 287–309., doi:10.1017/s0022143000013605.
- Boulton, G.S., Van Der Meer, J.J.M., Hart, J., Beets, D., Ruegg, G.H.J, Van Der Wateren, F.M., Jarvis, J. "Till and Moraine Emplacement in a Deforming Bed Surge — an Example from a Marine Environment." *Quaternary Science Reviews*, vol. 15, no. 10, 1996, pp. 961–987., doi:10.1016/0277-3791(95)00091-7.
- Bouvier, V., Johnsen, M.D., Pässe, T. "Distribution, Genesis and Annual-Origin of De Geer Moraines in Sweden: Insights Revealed by LiDAR." *Gff*, vol. 137, no. 4, 2015, pp. 319–333., doi:10.1080/11035897.2015.1089933.
- Burki, V., Hanse, L., Fredin, O., Andersen, T.A., Beylich, A.A., Jaboyedoff, M., Larsen, E., Tønnesen, J.F. "Little Ice Age Advance and Retreat Sediment Budgets for an Outlet Glacier in Western Norway." *Boreas*, 2010, doi:10.1111/j.1502-3885.2009.00133.x.
- Cacchione, D. "Rippled Scour Depressions on the Inner Continental Shelf Off Central California." *SEPM Journal of Sedimentary Research*, Vol. 54, 1984, doi:10.1306/212f85bc-2b24-11d7-8648000102c1865d.
- Carrivick, J.L., Heckmann, T. "Short-Term Geomorphological Evolution of Proglacial Systems." *Geomorphology*, vol. 287, 2017, pp. 3–28., doi:10.1016/j.geomorph.2017.01.037.
- Catt, J.A., Gibbard, P.L., Lowe, J.J., McCarroll, D., Scourse, J.D., Walker, M.J.C. "Quaternary: Ice Sheets and Their Legacy." *The Geology of England and Wales*, 2006, pp. 429–467., doi:10.1144/goewp.17.
- Cofaigh, Colm Ó, et al. "Reconstruction of Ice-Sheet Changes in the Antarctic Peninsula since the Last Glacial Maximum." *Quaternary Science Reviews*, vol. 100, 2014, pp. 87–110., doi:10.1016/j.quascirev.2014.06.023.



- Cohen, K.M., Hoek, W.Z., Stouthammer, E. "Valley Evolution of the Lower Rhine in LGM, Lateglacial, and Early Holocene." *Abstract International Conference on Fluvial Sedimentology*, 2013.
- Corner, G.D. "A Transgressive-Regressive Model of Fjord-Valley Fill: Stratigraphy, Facies and Depositional Controls." *Incised Valleys in Time and Space*, 2006, pp. 161–178., doi:10.2110/pec.06.85.0161.
- Dahlgren, T.K.I., and Vorren, T.O. "Sedimentary Environment and Glacial History during the Last 40 Ka of the Vøring Continental Margin, Mid-Norway." *Marine Geology*, vol. 193, no. 1-2, 2003, pp. 93–127., doi:10.1016/s0025-3227(02)00617-5.
- Davis, A.C.D., et al. "Distribution and Abundance of Rippled Scour Depressions along the California Coast." *Continental Shelf Research*, vol. 69, 2013, pp. 88–100., doi:10.1016/j.csr.2013.09.010.
- Dolan, M.F.J., Bellec, V., Elvenes, S., Lepland, A. "Interpretation of Green Laser and Aerial Photograph Data for Seabed Sediment Mapping in Shallow Areas, Søre Sunnmøre." *Geological Survey of Norway*, 2018.
- Dowdeswell, J. A., Benham, T.J., Strozzi, T., Hagen, J.O. "Iceberg Calving Flux and Mass Balance of the Austfonna Ice Cap on Nordaustlandet, Svalbard." *Journal of Geophysical Research*, vol. 113, no. F3, 2008, doi:10.1029/2007jf000905.
- Dowdeswell, J. A., et al. *Atlas of Submarine Glacial Landforms: Modern, Quaternary and Ancient*. The Geological Society, 2016.
- Easterbrook, D.J. *Surface Processes and Landforms*. Prentice Hall, 1999.
- Eilertsen, R., Corner, G., Aasheim, O. "Deglaciation Chronology and Glaciomarine Successions in the Malangen–Målselv Area, Northern Norway." *Boreas*, vol. 34, no. 3, 2005, pp. 233–251., doi:10.1080/03009480510013051.
- Elvenes, S., Bøe, R., Rise, L. "Post-Glacial Sand Drifts Burying De Geer Moraines on the Continental Shelf off North Norway." *Geological Society, London, Memoirs*, vol. 46, no. 1, 2016, pp. 261–262., doi:10.1144/m46.25.
- Elvenes, S., Bøe, R., Lepland, A., Dolan, M. "Seabed Sediments of Søre Sunnmøre, Norway." *Journal of Maps*, vol. 15, no. 2, 2019, pp. 686–696., doi:10.1080/17445647.2019.1659865.
- Elverhøi, A., et al. "Late Quaternary Sediment Yield from the High Arctic Svalbard Area." *The Journal of Geology*, vol. 103, no. 1, 1995, pp. 1–17., doi:10.1086/629718.
- Engelkemeir, R., Khan, S. "Near-Surface Geophysical Studies of Houston Faults." *The Leading Edge*, vol. 26, no. 8, 2007, pp. 1004–1008., doi:10.1190/1.2769557.
- Ewertowski, M. "Preservation Potential of Subtle Glacial Landforms Based on Detailed Mapping of Recently Exposed Proglacial Areas: Application of Unmanned Aerial Vehicle (UAV) and Structure-from-Motion (SfM)." *EGU General Assembly*, 2016.
- Favier, L., et al. "Dynamic Influence of Pinning Points on Marine Ice-Sheet Stability: a Numerical Study in Dronning Maud Land, East Antarctica." *The Cryosphere*, 2016, doi:10.5194/tc-2016-144-ac1.

- Ferrini, V.L., Flood, R.D. "The Effects of Fine-Scale Surface Roughness and Grain Size on 300 KHz Multibeam Backscatter Intensity in Sandy Marine Sedimentary Environments." *Marine Geology*, vol. 228, no. 1-4, 2006, pp. 153–172., doi:10.1016/j.margeo.2005.11.010.
- Fiebig, M., et al. "Some Remarks about a New Last Glacial Record from the Western Salzach Foreland Glacier Basin (Southern Germany)." *Quaternary International*, vol. 328-329, 2014, pp. 107–119., doi:10.1016/j.quaint.2013.12.048.
- Forwick, M., Vorren, T.O. "Stratigraphy and Deglaciation of the Isfjorden Area, Spitsbergen ." *Norwegian Journal of Geology*, vol. 90, 2010, pp. 163–179.
- Forwick, M., Vorren, T.O. "Submarine Mass Wasting in Isfjorden, Spitsbergen." *Submarine Mass Movements and Their Consequences. Advances in Natural and Technological Hazards Research.*, vol. 31, 2011, pp. 711–722., doi:10.1007/978-94-007-2162-3\_63.
- Forwick, M., Baeten, N.J., Vorren, T.O. "Pockmarks in Spitsbergen Fjords." *Norwegian Journal of Geology*, vol. 89, 2009, pp. 65–77.
- Fredin, O., et al. "Glacial Landforms and Quaternary Landscape Development in Norway." *Geological Survey of Norway*, vol. 13, 2013, pp. 5–25.
- Fredin, O.. "Glacial Inception and Quaternary Mountain Glaciations in Fennoscandia." *Quaternary International*, vol. 95-96, 2002, pp. 99–112., doi:10.1016/s1040-6182(02)00031-9.
- Gehrels, W.R., et al. "Rapid Sea-Level Rise in the North Atlantic Ocean since the First Half of the Nineteenth Century." *The Holocene*, vol. 16, no. 7, 2006, pp. 949–965., doi:10.1177/0959683606h1986rp.
- Giskeødegaard, O. " Akustiske Undersøkelser Av Sedimentene i Noen Fjorder På Nordvestlandet." *University of Bergen, Department of Geology*, 1983.
- Hampton, M.A., et al. "Submarine Landslides." *Reviews of Geophysics*, vol. 34, no. 1, 1996, pp. 33–59., doi:10.1029/95rg03287.
- Hansel, A.K. "End Moraines – the End of the Glacial Ride." *Illinois State Geological Survey*, 2003.
- Hanssen-Bauer, I., et al. "Climate in Svalbard 2100." NCCS Report, 2019.
- Hastie, T., et al. *The Elements of Statistical Learning: Data Mining, Inference, and Prediction*. Springer, 2017.
- Hjelstuen, B.O., et al. "Late Cenozoic Glacial History and Evolution of the Storegga Slide Area and Adjacent Slide Flank Regions, Norwegian Continental Margin." *Marine and Petroleum Geology*, 2005, pp. 57–69., doi:10.1016/b978-0-08-044694-3.50009-3.
- Hjelstuen, B.O., Hafliðason, H., Sejrup, H.P., Lyså, A. "Sedimentary Processes and Depositional Environments in Glaciated Fjord Systems — Evidence from Nordfjord, Norway." *Marine Geology*, vol. 258, no. 1-4, 2009, pp. 88–99., doi:10.1016/j.margeo.2008.11.010.
- Holdus, S. "Para-Amphibolite from Gurskøy and Sandsøy, Sunnmøre, West Norway." *University of Dundee, Department of Geology*, 1971.

- Howe, J. A., Stoker, M.S., Stow, D.A.V. "Late Cenozoic Sediment Drift Complex, Northeast Rockall Trough, North Atlantic." *Paleoceanography*, vol. 9, no. 6, 1994, pp. 989–999., doi:10.1029/94pa01440.
- Hughes, A.L.C., Gyllencreutz, R., Lohne, Ø.S., Mangerud, J., Svendsen, J.I. "The Last Eurasian Ice Sheets - a Chronological Database and Time-Slice Reconstruction, DATED-1." *Boreas*, vol. 45, no. 1, 2016, pp. 1–45., doi:10.1111/bor.12142.
- Knight, P.G. "Glaciers." *Glaciers*, Journal of Glaciology, 1999.
- Koren, J.H., Svendsen, J.I., Mangerud, J., Furnes, H. "The Dimna Ash — a 12.814Cka-Old Volcanic Ash in Western Norway." *Quaternary Science Reviews*, vol. 27, no. 1-2, 2008, pp. 85–94., doi:10.1016/j.quascirev.2007.04.021.
- Krohn-Nydal, A. O. "Mapping of Geological Lineaments and Glacial Geomorphology on the Southern Coast of Sunnmøre." *Norwegian University of Science and Technology*, 2019.
- Landvik, J.Y., Alexanderson, H., Henriken, M., Ingolfsson, O. "Landscape Imprints of Changing Glacial Regimes during Ice-Sheet Build-up and Decay: a Conceptual Model from Svalbard." *Quaternary Science Reviews*, vol. 92, 2014, pp. 258–268., doi:10.1016/j.quascirev.2013.11.023.
- Larsen, E., et al. "Cave Stratigraphy in Western Norway; Multiple Weichselian Glaciations and Interstadial Vertebrate Fauna." *Boreas*, vol. 16, no. 3, 1987, pp. 267–292., doi:10.1111/j.1502-3885.1987.tb00096.x.
- Larsen, E., Longva, O., Follestad, B.A. "Formation of De Geer Moraines and Implications for Deglaciation Dynamics." *Journal of Quaternary Science*, vol. 6, no. 4, 1991, pp. 263–277., doi:10.1002/jqs.3390060402.
- Lidmar-Bergström, K., Ollier, C.D., Sulebak, J.R. "Landforms and Uplift History of Southern Norway." *Global and Planetary Change*, vol. 24, no. 3-4, 2000, pp. 211–231., doi:10.1016/s0921-8181(00)00009-6.
- Lindén, M., Möller, P. "Marginal Formation of De Geer Moraines and Their Implications to the Dynamics of Grounding-Line Recession." *Journal of Quaternary Science*, vol. 20, no. 2, 2005, pp. 113–133., doi:10.1002/jqs.902.
- Lorrain, R. D., Fitzsimons, S.J., Vandergoes, M.J., Stievenard, M. "Ice Composition Evidence for the Formation of Basal Ice from Lake Water beneath a Cold-Based Antarctic Glacier." *Annals of Glaciology*, vol. 28, 1999, pp. 277–281., doi:10.3189/172756499781822011.
- Lyså, A., Hjelstuen, B.O., Larsen, E. "Fjord Infill in a High-Relief Area: Rapid Deposition Influenced by Deglaciation Dynamics, Glacio-Isostatic Rebound and Gravitational Activity." *Boreas*, vol. 39, no. 1, 2010, pp. 39–55., doi:10.1111/j.1502-3885.2009.00117.x.
- Løwe, A., Løwe, D. *North Atlantic Biota and Their History: a Symposium*. Pergamon, 1963.
- Maclean, B., et al. "Crag-and-Tail Features, Amundsen Gulf, Canadian Arctic Archipelago." *Geological Society, London, Memoirs*, vol. 46, no. 1, 2016, pp. 53–54., doi:10.1144/m46.84.

- Mangerud, J., Bondevik, S., Gulliksen, S., Hufthammer, A.K., Høisæter, T. "Marine 14C Reservoir Ages for 19th Century Whales and Molluscs from the North Atlantic." *Quaternary Science Reviews*, vol. 25, no. 23-24, 2006, pp. 3228–3245., doi:10.1016/j.quascirev.2006.03.010.
- Mangerud, J., Landvik, J.Y. "Younger Dryas Cirque Glaciers in Western Spitsbergen: Smaller than during the Little Ice Age." *Boreas*, vol. 36, no. 3, 2007, pp. 278–285., doi:10.1111/j.1502-3885.2007.tb01250.x.
- Mangerud, J., Gulliksen, S., Larsen, E. "14C-Dated Fluctuations of the Western Flank of the Scandinavian Ice Sheet 45-25 Kyr BP Compared with Bølling-Younger Dryas Fluctuations and Dansgaard-Oeschger Events in Greenland." *Boreas*, vol. 39, no. 2, 2010, pp. 328–342., doi:10.1111/j.1502-3885.2009.00127.x.
- Mangerud, J., Larsen, E., Longva, O., Sønstegeard, E. "Glacial History of Western Norway 15,000-10,000 B.P." *Boreas*, vol. 8, no. 2, 1979, pp. 179–187., doi:10.1111/j.1502-3885.1979.tb00798.x.
- Mangerud, J., Hughes, A.L.C., Sæle, T.H., Svendsen, J.I. "Ice-Flow Patterns and Precise Timing of Ice Sheet Retreat across a Dissected Fjord Landscape in Western Norway." *Quaternary Science Reviews*, vol. 214, 2019, pp. 139–163., doi:10.1016/j.quascirev.2019.04.032.
- Mangerud, J. "Ice-Front Variations of Different Parts of the Scandinavian Ice Sheet, 13,000–10,000 Years BP." *Pergamon Press*, 1980.
- Mangerud, J. "Late Weichselian Marine Sediments Containing Shells, Foraminifera, and Pollen, at Ågotnes, Western Norway." *Norsk Geologisk Tidsskrift*, vol. 57, 1977, pp. 23–54.
- Meier, M. F., Post, A. "Fast Tidewater Glaciers." *Journal of Geophysical Research*, vol. 92, no. B9, 1987, p. 9051., doi:10.1029/jb092ib09p09051.
- Morland, L. W. "Unconfined Ice-Shelf Flow." *Dynamics of the West Antarctic Ice Sheet Glaciology and Quaternary Geology*, 1987, pp. 99–116., doi:10.1007/978-94-009-3745-1\_6.
- Moustier, C.D., Kleinrock, M.C. "Bathymetric Artifacts in Sea Beam Data: How to Recognize Them and What Causes Them." *Journal of Geophysical Research: Solid Earth*, vol. 91, no. B3, 1986, pp. 3407–3424., doi:10.1029/jb091ib03p03407.
- Murray, B., and Thieler, R. "A New Hypothesis and Exploratory Model for the Formation of Large-Scale Inner-Shelf Sediment Sorting and 'Rippled Scour Depressions.'" *Continental Shelf Research*, vol. 24, no. 3, 2004, pp. 295–315., doi:10.1016/j.csr.2003.11.001.
- Murton, J. B., Peterson, R. Ozouf, J.C.. "Bedrock Fracture by Ice Segregation in Cold Regions." *Science*, vol. 314, no. 5802, 2006, pp. 1127–1129., doi:10.1126/science.1132127.
- Möller, P. "Rogen Moraine: an Example of Glacial Reshaping of Pre-Existing Landforms." *Quaternary Science Reviews*, vol. 25, no. 3-4, 2006, pp. 362–389., doi:10.1016/j.quascirev.2005.01.011.
- Nitsche, F. O., et al. "Crag-and-Tail Features on the Amundsen Sea Continental Shelf, West Antarctica." *Geological Society, London, Memoirs*, vol. 46, no. 1, 2016, pp. 199–200., doi:10.1144/m46.2.

- Nygård, A., Sejrup, H.P., Halifdason, H., Cecchi, M., Ottesen, D.. "Deglaciation History of the Southwestern Fennoscandian Ice Sheet between 15 and 13 14C Ka BP." *Boreas*, vol. 33, no. 1, 2004, pp. 1–17., doi:10.1080/03009480310006943.
- Olesen, O., et al. "Tropical Weathering In Norway, TWIN Final Report." *NGU Report*, 2012.
- Olsen, L., Sveian, H., Bergstrøm, B., Ottesen, D., Rise, L. "Quaternary Glaciations and Their Variations in Norway and on the Norwegian Continental Shelf." *Geological Survey of Norway*, 2013.
- Oppikofer, T., Saintot, A., Otterå, S., Hermanns, R.L., Ande, E., Dahle, H., Eiken, T.. "Investigations on Unstable Rock Slopes in Møre Og Romsdal – Status and Plans after Field Surveys in 2012." *Geological Survey of Norway*, 2014.
- Ottesen, D., Dowdeswell, J.A, Landvik, J.Y., Mienert, J. "Dynamics of the Late Weichselian Ice Sheet on Svalbard Inferred from High-Resolution Sea-Floor Morphology." *Boreas*, 2006.
- Ottesen, D., Dowdeswell, J.A., Rise, L. "Submarine Landforms and the Reconstruction of Fast-Flowing Ice Streams within a Large Quaternary Ice Sheet: The 2500-Km-Long Norwegian-Svalbard Margin (57°–80°N)." *Geological Society of America Bulletin*, vol. 117, no. 7, 2005, p. 1033., doi:10.1130/b25577.1.
- Patton, Henry, et al. "Deglaciation of the Eurasian Ice Sheet Complex." *Quaternary Science Reviews*, vol. 169, 2017, pp. 148–172., doi:10.1016/j.quascirev.2017.05.019.
- Paus, A. "Late Weichselian Vegetation, Climate, and Floral Migration at Sandvikvatn, North Rogaland, Southwestern Norway." *Boreas*, vol. 17, no. 1, 1990, pp. 113–139., doi:10.1111/j.1502-3885.1988.tb00128.x.
- Perkins, A.J., et al. "Genesis of an Esker-like Ridge over the Southern Fraser Plateau, British Columbia: Implications for Paleo-Ice Sheet Reconstruction Based on Geomorphic Inversion." *Geomorphology*, vol. 190, 2013, pp. 27–39., doi:10.1016/j.geomorph.2013.02.005.
- Rasmussen, S.O., et al. "A New Greenland Ice Core Chronology for the Last Glacial Termination." *Journal of Geophysical Research*, vol. 111, no. D6, 2006, doi:10.1029/2005jd006079.
- Reite, A.J. "Lokalglacijasjon På Sunnmøre (On the Mountain Glaciation of Sunnmøre, West Norway)." *University of Bergen, Department of Geology*, 1983.
- Rye, N., Nesje, A., Anda, E. "The Late Weichselian Ice Sheet in the Nordfjord – Sunnmøre Area and Deglaciation Chronology for Nordfjord, Western Norway." *Norsk Geografisk Tidsskrift - Norwegian Journal of Geography*, vol. 41, no. 1, 1987, pp. 23–43., doi:10.1080/00291958708552170.
- Sevestre, H., Benn, D.I., Hulton, N.R.J., Bælum, K. "Thermal Structure of Svalbard Glaciers and Implications for Thermal Switch Models of Glacier Surging." *Journal of Geophysical Research: Earth Surface*, vol. 120, no. 10, 2015, pp. 2220–2236., doi:10.1002/2015jf003517.
- Sitorus, F. "Seabed Morphology Mapping for Jack-up Drilling Rig Emplacement." *Bandung Institute for Technology*, 2015.
- Sollid, J.L., Sørbel, L.. "Notisartikkel – Short Article." *Norsk Geografisk Tidsskrift - Norwegian Journal of Geography*, vol. 36, no. 4, 1982, pp. 225–232., doi:10.1080/00291958208552084.

- Spagnolo, M., et al. "Size, Shape and Spatial Arrangement of Mega-Scale Glacial Lineations from a Large and Diverse Dataset." *Earth Surface Processes and Landforms*, 2014, doi:10.1002/esp.3532.
- Stalsberg, K., Fischer, L., Rubensdotter, L., Sletten, K. "Approaches to Shallow Landslide and Debris Flow—Assessments in Norway." *Geological Survey of Norway*, 2012.
- Surovell, T. A., et al. "An Independent Evaluation of the Younger Dryas Extraterrestrial Impact Hypothesis." *Proceedings of the National Academy of Sciences*, vol. 106, no. 43, 2009, pp. 18155–18158., doi:10.1073/pnas.0907857106.
- Svendsen, J.I., et al. "Late Quaternary Ice Sheet History of Northern Eurasia." *Quaternary Science Reviews*, vol. 23, no. 11-13, 2004, pp. 1229–1271., doi:10.1016/j.quascirev.2003.12.008.
- Svendsen, J.I., Mangerud, J. "Sea-Level Changes and Pollen Stratigraphy on the Outer Coast of Sunnmøre, Western Norway." *University of Bergen, Department of Geology*, 1990, pp. 111–134.
- Syvitski, J.P.M., Burrell, D.C., Skei, J.M. *Fjords: Processes and Products*. Springer, 1988.
- Theberge, A.E., Cherkis, N. "A Note on Fifty Years of Multi-Beam: The Early Years." *United States Naval Research Laboratory*, 2013.
- Valen, V., Larsen, E., Mangerud, J. "High-Resolution Paleomagnetic Correlation of Middle Weichselian Ice-Dammed Lake Sediments in Two Coastal Caves, Western Norway." *Boreas*, vol. 24, no. 2, 1995, pp. 141–153., doi:10.1111/j.1502-3885.1995.tb00634.x.
- Valen, V., Mangerud, J., Larsen, E., Hufthammer, A.K. "Sedimentology and Stratigraphy in the Cave Hamnsundhelleren, Western Norway." *Journal of Quaternary Science*, vol. 11, no. 3, 1996, pp. 185–201., doi:10.1002/(sici)1099-1417(199605/06)11:33.0.co;2-y.
- Van Der Wateren, D. "Structural Geology and Sedimentology of Push Moraines: Processes of Soft Sediment Deformation in a Glacial Environment and the Distribution of Glaciotectonic Styles." *Boreas*, 1995.
- Vorren, K.D. "Late and Middle Weichselian Stratigraphy of Andøya, North Norway." *Boreas*, vol. 7, no. 1, 1978, pp. 19–38., doi:10.1111/j.1502-3885.1978.tb00047.x.
- Vorren, T.O., 2003. Subaquatic landsystems: continental margins. In: Evans, D.J.A. (Ed.): *Glacial Landsystems*. Arnold Publishers, London, pp. 289-312
- Waller, R.I. "The Influence of Basal Processes on the Dynamic Behaviour of Cold-Based Glaciers." *Quaternary International*, vol. 86, no. 1, 2001, pp. 117–128., doi:10.1016/s1040-6182(01)00054-4.
- Yde, J.C., Paasche, Ø. "Reconstructing Climate Change: Not All Glaciers Suitable." *Eos, Transactions American Geophysical Union*, vol. 91, no. 21, 2010, p. 189., doi:10.1029/2010eo210001.
- Young, D. J. "Structure of the (Ultra) High-Pressure Western Gneiss Region, Norway: Imbrication during Caledonian Continental Margin Subduction." *GSA Bulletin*, vol. 130, no. 5-6, 2017, pp. 926–940., doi:10.1130/b31764.1.

